FIRE RETARDANCY, THERMAL STABILITYAND MECHANICAL PROPERTIES OF POLYMERIC BASED NANOCOMPOSITES

A Thesis by

ALI GHAZINEZAMI

Bachelor of Science, Tehran Azad University 2009

Submitted to the Department of Mechanical Engineering
and the faculty of the Graduate School of
Wichita State University
in partial fulfillment of
the requirements for the degree of
Master of Science

December 2013

FIRE RETARDANCY, THERMAL STABILITYAND MECHANICAL PROPERTIES OF POLYMERIC BASED NANOCOMPOSITES

The following faculty members have examined the final copy of this thesis for form and content, and recommend that it be accepted in partial fulfillment of the requirement for the degree of Master of Science with a major in Mechanical Engineering.

_____

Ramazan Asmatulu, Committee Chair

_____

Hamid M. Lankarani, Committee Member

_____

Esra Büyüktahtakın Toy, Committee Member

DEDICATION

To my loving parents, for their continuous love and support, and my beloved sisters Sanaz and Farnaz and my family for their support

ACKNOWLEDGEMENTS

Foremost, I would like to express my deepest gratitude to my advisor, Dr. Ramazan Asmatulu, for his excellent guidance, caring, patience, and providing me with an excellent atmosphere for doing research.

I would also like to express my sincere gratitude to my committee members, Dr. Hamid M. Lankarani, and Dr. Esra Büyüktahtakın Toy for their constructive comments, time and help.

Last but not least; I would like to give my heartfelt appreciation to my parents for their endless love, support and encouragement. The constant love and support of my sister, Farnaz, is sincerely acknowledged. I would like to be thankful to all my family and friends for their help.

ABSTRACT

Polymeric materials have a wide variety of applications in many manufacturing industries. However, because of the molecular structures and chemical compositions of polymeric materials, they have considerably low resistances against fire or heat. Although these materials are highly flammable, their flame retardancy can be improved significantly by incorporating the flame retardant nanomaterials. Nanoclay, nanotalc and graphene are some of the examples of the flame retardant nanomaterials. These are highly cost effective and environmentally friendly for these applications. These inclusions have a great potential to improve thermal, electrical, and mechanical properties of the new materials. This study is mainly focused on the effects of nanoparticle additions in the polyvinyl chloride (PVC) in terms of the flame retardancy. Five sets of nanocomposite materials were prepared using the solvent casting method at different weight percentages of the nanomaterials. The flame retardancy values of the resultant nanocomposite samples were determined using the ASTM UL 94 standard tests. The results of the experiment were also supported by the thermogravimetric analysis (TGA) and differential scanning calorimetry (DSC). Surface characterization of the resultant materials was carried out using scanning electron microscopy (SEM), while mechanical properties were determined through a tensile test method. Test results showed that the flame retardancy values of the new nanostructured materials were significantly enhanced in the presence of nanoscale inclusions, which may be useful for various industrial applications. This study may open up new possibilities of using many nanoscale inclusions in various polymers as flame retardant materials for different industrial applications.

TABLE OF CONTENTS

TABLE OF CONTENTS (continued)

Chapter Page

LIST OF FIGURES

LIST OF FIGURES (continued)

Figure Page

LIST OF FIGURES (continued)

Figure Page

LIST OF FIGURES (continued)

Figure Page

LIST OF FIGURES (continued)

Figure Page

LIST OF TABLES

CHAPTER 1

INTRODUCTION

1.1 Introduction

1.1.1 Fire

In 2006 only, there was $11.3 billion economic loss and 3334 life losses and 16400 injuries in the United States just because of the fire. The exact worldwide statistics of fire loss are not available now, but it can be assured that fire losses or damages occurred in every country on the earth last year. They either stayed constant or increased compared to the previous years. Fire is a fatal force of nature and is very destructive (Figure 1.1) [1,2].

Figure 1.1. Firefighters extinguish the fire [1].

Fire is a thermo-oxidative decomposition of materials. CO_2 and water are the consequence of the conversion of carbon and combustible materials when decomposition occurs. Humanity has controlled and conquered fire and turned it into something that we can make life easier. With the help of fire we have losses that come up with wealth, livelihood and life loss. It can be prevented by a variety of methods. For these reasons, engineers and scientists are putting effort to find new methods to prepare some fire protections, which are useful in daily life. By this

way there will be no more worries about the accidental fires or at least there will be a way to control or quick extinguish before it cause a disaster [2].

1.1.2 Combustibility

It is defined as an ability to resist ignition under a series of conditions. This phenomenon occurs in all carbon-based materials by converting into CO_2 and H_2O once they are exposed to flame/heat source. For polymers, the polymer combustion of the flame retardant materials can also reduce smoke emission [2].

1.1.3 Thermal Decomposition

Thermal decomposition means the decomposition of materials from their component once they exposed to the source of heat. It then causes depolymerization and the molecules breaks up into potential fuel molecules [2, 3].

1.1.4 Fire Retardancy/Flame Retardancy Definition

Fire Retardancy and Flame Retardancy are two different words which are used interchangeably. Typically, fire retardancy engages in higher risk than flame retardancy, but both words generally have the same meaning. This term refers to any type of materials which are used as additives to help polymers to retard a flame or controlling the rate of fire growth.

If the materials are not burnt, this does not mean it is fire retardant. It means that some materials have added to an initial material, thus by this method, the additive materials will help to slow down the rate, growth and the propagation of fire once it has been ignited. In some cases, fire retardant materials could act as a self-extinguishing material, once the external flame is removed. Also in some other cases the flame-retardant materials outcome will be the slow rate of fire growth [2, 3]. In a function of nature, the flame retardant system can act both physically and chemically. Physically means by either protective layer formation or cooling and chemically means of reaction either in the gas phase or condensed. They can come up with a different

process which involves polymer combustion such as pyrolysis, heating, ignition and thermal degradation propagation [4].

1.1.5 Physical Action

The flame retardant endothermic decomposition leads to a temperature reduction of heat consumption. This involves the cooling reaction of medium temperature to the temperature below the polymers combustion. Magnesium hydroxide (Talc) or Tri alumina is the example of this category which respectively liberates water vapor at temperatures of 300 and 200 °C. This type of endothermic reaction is noted to act as a heat sink. With the formation of inert gases at the decomposition of flame retardants, the combustible gases will dilute, which limits the ignition possibility. Some flame retardant additives lead to produce gaseous or a solid protective layer between the gaseous phase where combustion takes place and the phase of solid where the thermal degradation takes place. This protective layer restricts the transfer of combustible gases and oxygen. Consequently, the quantity of producing gases will be decreased. Physically, the fuel gases can be isolated from the oxygen, by avoiding the combustion process further [2, 4].

1.1.6 Chemical Action

Flame retardancy via chemical modification can take place either in the condensed or gaseous phase. During the combustion process, the free radicals can be stopped by the flame retardant additive incorporating the release of some specific radicals such as Br, F and Cl in the gas phase. In the condensed phase, the flame retardancy can increase the rate of rupture in polymer chains. This causes the polymers to drip and moves it away from the center of the location. Alternatively, the flame retardant materials can create vitreous or carbonized layer at the polymer surface by the chemical transformation of polymer chain degradation. The char layer acts as a physical insulator between the condensed phase and gas phase [2, 4].

There are two types of flame retardants:

1. Additive flame retardants: These types of flame retardants include the main matrix during the transformation process and do not react with polymers. They are categorized as mineral fillers, organic or hybrid compounds, which contains macromolecules [4].

2. Reactive flame retardants: Unlike the pervious type of flame retardant, these are introduced into polymers as monomers during the synthesis or in a process of post reaction through chemical grafting [4].

Generally, fire retardant materials reduce the flammability of the plastic materials with the help of their endothermic decomposition. It absorbs heat from the substrate and dilutes the oxygen in the surroundings by accompanying water vapor evolution. The other property of FR materials is their ability to suppress smoke production in case of fire occurrence [2-4].

1.1.2 Motivation

Polymer is an organic substance composed of molecules with large mass with the repeating structural units, or monomers, which are connected to each other by mainly covalent bondings. Since polymers are composed primarily of carbon and hydrogen, they are highly combustible [2]. The attractive force which holds the chains together is a key factor to determine the properties of polymers. By dispersing organic or inorganic nanoscale inclusions into polymers, their structure can be modified and the rearrangement of the atoms represents a new material with a new set of characteristics [5].

Poly (vinyl chloride) (PVC) is one of the most commonly used polymers in many industries, and has the third largest production among the all polymers. The biggest drawbacks of the commonly used polymer are their relatively poor fire retardancy because of the molecular structure and chemical composition [4, 5].

1.3 Research Objective

We hypothesized that flame retardancy of PVC can be significantly improved by incorporating some nanoscale inclusions in this type of polymer. By changing the arrangement of the atoms in a desirable way, a new material with improved fire retardancy properties can be produced. Carbon nanotubes, carbon nanofibers, carbon black, graphene, C60, nanoclay and nanotalc are some of the examples of these organic fillers which are highly efficient and environmentally-friendly. Moreover, these nanoparticles have the potential to provide enhancements in terms of electrical, mechanical, and thermal properties to the polymers. This study is mainly focused on the fabrications of PVC nanocomposite materials incorporated with nanoscale inclusions, and characterizations of these materials (mainly thermal and mechanical) [6].

Chapter 2

LITERATURE REVIEW

2.1 Nanotechnology

Nanotechnology is the study of materials within the size range of 1 and 100 nm. “Nano” is a unit of length and is equal to 10^{-9} m, while the width of a human hair is about 10^{5} nm. Nanomaterials can improve the properties of materials by changing their atomic arrangement and producing new materials with better features. This is the reason that makes “Nano” very popular among the variety researched field like engineering, biology, physics, etc. Nanomaterials can be classified into following categories: nanopolymers, nanocomposite, nanoceramics, metals, alloys and carbon-based nanomaterials [3, 4].

2.2 Composite

A composite is composed of at least two different components with different chemical and physical properties. This makes composite materials unique among all the materials. Now days, composites are used in a wide variety of applications due to their lightweight and high strength. They can be customized to have specific features in order to meet all the requirements and satisfy the demands for specific engineering applications. Most of the composites contain the bulk phase which is called matrix and dispersed phase which is called reinforcement. The role of matrix is accepting the load and transfers it to reinforcement [7].

2.3 Polymeric Composite

Polymeric materials, which are lightweight, are widely used in many applications due to unique features such as great ductility, which brings ease of production process. Polymeric material strength is not as high as ceramics and metals. Since the usage of commercial polymers is increasing, more modifications are needed in order to satisfy the demands. The properties of

polymeric materials can be improved with the help of the composite technology while maintaining their unique properties [8]. However by adding typical fillers such as clay, talc, graphene, etc., it usually requires a large amount of fillers in the main matrix to reach significant improvements in final products. This may result in some undesired features like brittleness of final product [9].

The final properties of composites (reinforced composites) depend on different parameters such as properties of the components, components dimension and interfacial interaction between the matrix and reinforcement. The improvement highly depends on the fillers properties and the adhesion force between the filler and matrix. The aspect ratio of fillers is also a very important factor since they are crucial for most properties in composite structures such as mechanical, electrical and thermal properties. Polymer based composites incorporated with the high aspect ratio of nanoinclusion fillers such as nanoclays, nanotalc and graphene are receiving more attention due to their well enhanced properties and multi-functionality. The combination of high aspect ratio, nano-particles fillers and dispersing them within the polymeric matrix leads to the distinct improvement in the properties of polymers even at low filler volume fraction [7].

2.4 Polymeric Nanocomposite

The term of nanocomposite is described as a composite material in which the dimension of one of the components is in the nanometer scale. Now days, nanocomposite demonstrates a new field in technology to humanity but it has been used for centuries by the nature. Bones and woods are the examples of the natural nanocomposites [10]. Many researches have been done to analyze the nanoscale structures based on studying the natural surroundings. Nanocomposite technology offers an impressive strategy to enhance the high functional and structural properties

of polymers. The very first report in this area of research belongs to Toyota in 1993 [7]. Based on this study the nylon-6 properties were improved with nanoclay incorporation. More studies have extended the nylon-6 properties with other nano fillers such as graphene and nanocrystalline metals within the polymeric based composites. Since the polymeric nanocomposite materials exhibit exceptional properties such as high strength, toughness, modulus and barrier, they have attracted great attention in wide variety of applications including academic and industry. Polymeric nanocomposite have also provided more great advantages such as low density and ease of process ability. Once the fillers dimension is decreased to the nanoscale, their properties will change significantly which is known as nano-effect [4, 7].

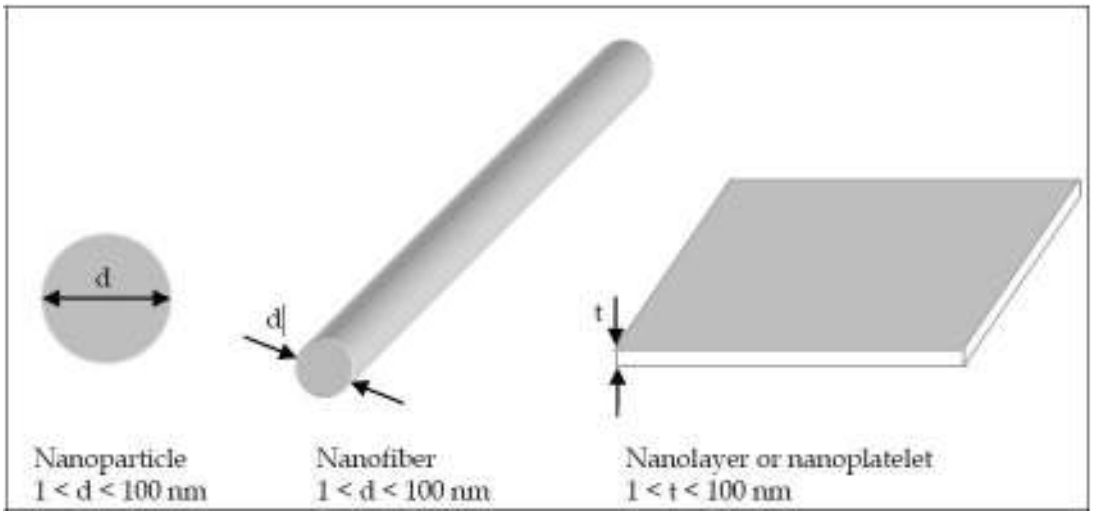

Figure 2.1. Scheme of various types of nanoinclusions [7].

The modelings of continuum mechanics reveal the enhanced properties of polymeric based nanocomposites and are affected by the important factors such as; nanofillers, content, and aspect ratio of filler to the matrix (Figure 2.1) [7].

2.5 Polymer Combustion

The massive usage of polymeric materials in our daily life is driven by their exceptional combination of all great properties. However polymers are known for their high flammability

and their burning is usually accompanied by producing smoke and toxic gases during the combustion process. Consequently, improving the fire retardancy of polymers is the major concern for extending their usage in more applications. Now days, safety requirements are becoming more and more important in terms of polymer reaction to fire and their performance during the fire. Halogenated additives used to be very common but due to their suspected adverse effects on the environment, they are banned to use [2]. The flammability of polymers and discovering the proper environment friendly fire retardants for polymers are the major challenges for researchers. The technical and scientific literature contains very efficient strategies to improve fire resistance of polymers but it all depends on the chemical structure, nature of polymers, their decomposition, the level of safety and also the performance of the final product. The understanding of flame retardant materials and their burning structure that take place during the combustion requires the superb collaboration between several scientific fields with different expertise such as heat transfer and physical chemistry. The main fire control process is divided into five steps: 1) The fundamental behavior of polymers during the combustion 2) The flame retardant properties 3) The standard test to describe the behavior of fire 4) The most representative flame retardant materials 5) Emerging synergistic effects of fire retardants fillers in main polymeric matrices. Since polymeric materials are mainly made of carbon and hydrogen, they are highly combustible [4]. The combustion reaction includes two main factors: 1. A combustible 2. A combustive. The oxygen in the air is usually considered as combustive. The process usually starts with increasing the temperature of the materials because of heat source, and it induces the scissions of polymer bonds and as the results the polymer fragment diffuses into the air and makes combustible gaseous which is known as a fuel. These gaseous mixtures start to ignite and reach the auto ignition temperature [2]. The gaseous mixtures or the fuel can

also ignite at low temperatures if they are exposed to the external source of heat. The duration of the combustion cycle depends on the amount of heat generated. The new decomposition creates and induces in solid phase if the amount of heat exceeds a certain limit. In this case more combustibles are expected and the combustion cycle keeps maintained. It is called a fire triangle (Figure 2.2) [2-4, 11].

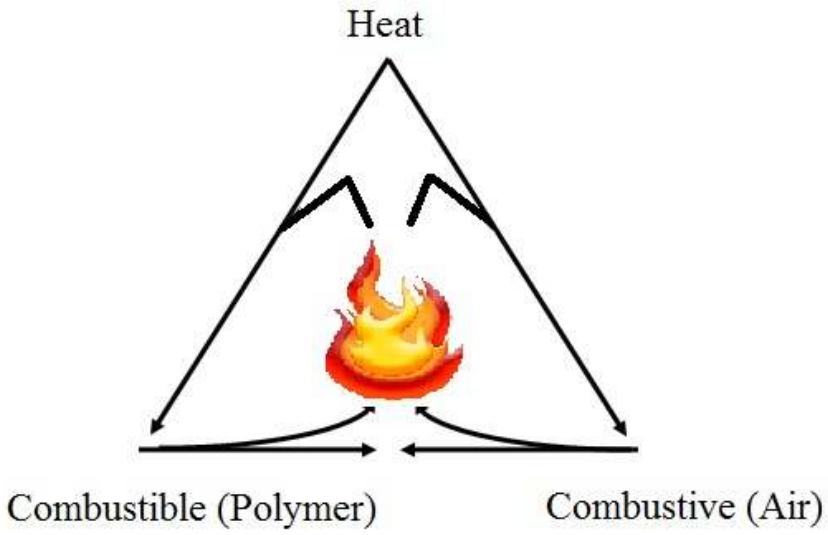

Figure 2.2. Fire Triangle [2].

This is a complex process and it involves several types of reactions and transport phenomena in the interfacial, solid and gaseous phases. Heating is a consequence of thermal energy contribution from an external heat source and the heat transfer occurs through conduction, convection or radiation. Hating also occurs by the chemical process contribution or the contribution of the combustion reaction exothermicity [4].

In polymers, the initial amount of energy required to start the combustion is the function of the materials' physical properties. For example, when semi crystalline thermoplastics are exposed to the heat source, they initially become soft resulting in melting of the polymers. The amount of energy stored by the polymer during the processes mentioned above depends on the degree of crystallinity, enthalpy of fusion and heat-storage capacity. Therefore, the temperature

growth rate depends on the temperature difference due to exothermicity of the reaction occurrence, heat flow, thermal and heat conductivity of semi crystalline thermoplastics. Amorphous materials such as most of thermosets and thermoplastics, because of the absence of a melting point, the heating step has directly led to decomposition. Polymer decomposition is an endothermic phenomenon, which needs to have sufficient energy input. This energy must be higher than the binding energy between the atoms to overcome the covalent bonding between the polymer atoms. The energy for C-C polymers is about 200 to 400 KJ/mol. Weak bondings and also the absence or presence of oxygen in gas and solid phase directly affect the decomposition mechanism. Thermal decomposition occurs due to combination of oxygen and heat. There are two types of degradation: 1. Non-oxidizing thermal degradation 2. Oxidizing thermal degradation [2-4]. Non-oxidizing thermal degradation is initiated because of the chain scissions under the effect of temperature. This scission depends on several factors such as, the chemical defects in chains of polymers, the presence of weak bonding along the chain and oxygen atoms in the chain. It can occur in different ways:

1. The Formation of free-radicals: at this stage the reaction does not stop since radicals start a chain reaction, which takes place under non-oxidizing and oxidizing.

2. The Migration of hydrogen atoms and by forming of two stable molecules. In the oxidizing thermal process, the polymers react with oxygen and produce low molecular weight materials. The polymer oxidation stability depends on C-H bond energy [4, 9]. According to some studies the degradation of polymers happens at combustion temperatures above 300°C through non-oxidizing thermal decomposition. Under this condition, the pyrolysis rate will be faster than the oxygen diffusion in solid phase. Because of the presence of low molecular weight compounds which was produced by thermal decomposition, the oxidation takes place in the gas

phase. The decomposition gases will mix with oxygen by both diffusion and convection into the closest layer to the surface, then ignite. This ignition can be caused by flash ignition (external flame) or self ignition when the temperature is high enough. Oxygen concentration is one of the most important parameters in the ignition. Polymer temperature increases by the combustions of gases. These gases supports the production of new gases and pyrolysis , thus combustion continues even without the presence of an external heat source [2, 12]. The physical factors and thermal transfer can affect the flame propagation. Convective transfer and conductive transfers are very important in the fire development when the flame height remains at a few tens of centimeter. In a more advanced phases, the propagation of flame on the surface contributes to a quick increase in radiative transfer. Maries and Calcraft were the first researchers to publish details about the presence of a microporous carbonized layer dominating the cellular porous underlayer, which was observed for several polymers [2]. The produced decomposition gasesous tend to be placed in underlayers cavities, and migrates toward the surface whereas the combustion occurs [4].

2.6 Flame Retardant Additives

2.6.1 Mineral Flame Retardants

All types of fillers influence the polymer reaction by reducing the combustibility of products, modifying thermal conductibility and changing the viscosity of products. Some of the materials are known as flame retardants because of their behavior at very high temperature. One of the most common flame retardant materials are metal hydroxides family, such as aluminum and magnesium hydroxide. Zinc borates and hydroxycarbonates are also classified as flame retardant materials. As temperature rises, the inorganic fillers decompose endothermically and absorb energy. Moreover, they release H_2O and CO_2 which are non flammable molecules and

they can dilute the combustible gases and create a vitreous or a protective ceramic layer [2, 4, 12].

2.6.1.1 Metal Hydroxides

Metal hydroxide is one the candidates that can be used as flame retardants. It needs to release water at a temperature close to the decomposition (endothermical) temperature of polymers. Magnesium di-hydroxide (MDH) and Aluminum Tri-hydroxide (ATH) are very commonly used mineral flame retardants. The aluminum tri-hydroxides endothermic decomposition takes place between 180 and 200°C which leads to release water. This reaction tends to take place in two stages. It correlates with two endothermic transition and has several effects on the polymers combustions. The effects include the cooling down polymer materials by absorbing more than 1050 kJ/kg of ATH,. Al_2O_3 creates an insulating coating, the released vapor of water dilutes the combustible gases and creates a protective layer. ATH usage also decreases the peak in HRR in the cone calorimeter test and reduces smoke production. Magnesium di-hydroxie acts very similar to $Al(OH)_3$ but its endothermic degradation takes place in higher temperature (above 300 °C) compare to ATH which makes it proper with respect to injection molding and extrusion processes. It has to be mentioned that the flame retardant action of magnesium di-hydroxide (MDH) is very effective up to 400°C. Magnesium di-hydroxide nanoparticles are also considered as flame retardant materials. They can be obtained by various methods, via a hydrothermal reaction using different solvents and precursors or by sol-gel technique [4, 12].

2.6.1.2 Hydroxycarbonates

All types of carbonates release CO_2 at very high temperatures except calcium and magnesium carbonates. They release CO_2 below 1000 °C. The release temperature for magnesium carbonates presenting the lowest release temperature among all carbonate which is 550 °C. Synthetic magnesium hydroxycarbonate (hydromagnesite) release carbon dioxide and water over a wider temperature range compare to magnesium di-hydroxide and tri-hydrate. Hydromagnesite has been used as a flame retardant in different compounds such as polypropylene and low density polyethylene(LDPE) / ethylene vinyl acetate copolymer (EVA) polymer blend [4, 13]. The magnesium di-hydroxide and aluminum tri-hydroxide water release temperature is around 340 °C and 200 °C respectively while the hydromagnesite release both carbon dioxide and water at a temperature between 200 to 550 °C. It means they show better efficiency as flame retardant than MDH and ATH [4].

2.6.1.3 Borates

Borate is one the member of inorganic additives family with flame retardant properties. Zinc borates are the most commonly used among this family. The B_2O_3 become soft at temperature 350 °C and flows above the 500 °. It causes the creation of a protective layer which protects the polymeric materials from oxygen and heat, therefore the combustible gaseous release will be reduced [3, 4].

2.6.2 Halogenated Flame Retardants

The halogenated flame retardant effectiveness depends on the halogen type. Iodine-based and fluorine compounds do not interfere with the combustion process of polymer, thus they are not used as flame retardant materials. Since fluorinated compounds are thermally more stable compared to most of the polymers , they do not release halogen radicals at the same or below the

polymer decomposition temperature. The iodinated compounds are less thermally stable than polymers so they release halogenated species during the polymer processing [2, 4].

2.6.2.1 Halogenated Flame Retardant Additives

Tetrabromobisphenol A (TBBPA) is one the most common halogenated flame retardants. It is mainly used as a flame retardant additives especially in epoxy resins for printed circuit boards. Penta and Octa bromodiphenylethers are mixture of different diphenylic ethers with various bromine atoms and they are characterized by very high molecular weight and acceptable thermal stability. They are mainly used in polymers, polyesters and nylons [3, 4].

2.6.2.2 Halogenated Monomers and Copolymers (Reactive Flame Retardants)

The main principal advantage of reactive copolymer and monomer flame retardants, compared to other type of flame retardant additives, is their good functionality in low concentrations. By incorporating these additives into polymer structure, they can increase the flame retardant capability, decrease the heterogeneous additive's damages to mechanical properties of materials and the flame retardant agents migration onto the surface of materials. The halogenated monomer effectiveness depends on the polymers composition and structure. The more halogen atoms in polymers, more fire retardants behavior is expected [2-4].

2.6.3 Phosphorus-based Flame Retardants

Phosphorus based products are including very wide range of materials such as phosphonates, phosphates and red phosphorus. They can be incorporated into the polymer structure during the synthesis or can be used as additives. They are known to be active in vapor or condensed. Phosphorus based materials are more effective if nitrogen or oxygen exists within the chains [4].

2.6.3.1 Red Phosphorus

Red phosphorus is one of the most concentrated sources of phosphorus for flame retardancy purposes. Using in small quantity for example less than 10%, could be very effective in many polymers such as polyamides, polyurethane and polyesters. Glass filled PA-6 which contains about 6-8 % red phosphorus is the good example which classified as V0 in the UL94 test. The very first report about the usage of red phosphorus as a flame retardant in polymers, dates back to 1965 [4]. Usually, the red phosphorus shows the flame retardant properties just in the presence of polymeric materials containing oxygen atoms such as polyurethanes, polyamides and polyesters. It is highly toxic during the melting process. Phosphine (highly toxic) could be released via reaction of red phosphorus with moisture as a result of poor thermo-stability. This issue can be solved by polymer encapsulation of red phosphorus, which can also improve its flame retardant properties [2, 12].

2.6.3.2 Inorganic Phosphates

Ammonium polyphosphate (APP) is one of the members of the inorganic phosphate family. It is a salt and made of polyphosphoric ammonia and acid. These materials are known to be non-volatile and stable compounds. The long-chain APPs start to decompose into polyphosphoric ammonia and acid at temperatures higher than 300 °C. For the short-chain, this temperature is above 150 °C. The APPs effectiveness depends on the incorporation level. At high concentration they become more efficient compared to low concentration [2].

2.6.3.3 Organic Phosphorus-based Compounds

Many of the organic phosphorus derivatives show flame retardant properties. Because of some limitations such as commercial importance, they need to be modified to be able to use in polymeric materials. These materials can act as reactive monomers/comonomers or as additives.

The reactive phosphorus flame retardant can incorporate directly into the polymer chain to obtain phosphorated polymer and reacts with polymers to create a grafted or branched phosphorated polymer [2, 14].

2.6.3.4 Intumescent Flame Retardant Systems

The intumescent flame retardant systems were developed to protect wood, fabrics and coatings when they are exposed to the source of heat. This concept is based on the creation of a carbonized layer on the polymer surface during thermal degradation. This layer reduces heat transfer between the surface of polymer and heat source. An acid source, a carbonizing agent and a blowing agent are three requirements to formulate of intumescent. One of the most common acid source compound is ammonium polyphosphate (APP). In polyoelfins, in order to generate the char, it is necessary to combine carbonized agent with APP. Pentaerythritol has been combined with APP, but tends to migrate toward the surface especially during the injection molding. In order to solve this issue, PA-6 can be a suitable candidate as carbonizing agent. In fact, a carbonized layer link to atoms of carbon which are formed during the combustion [15]. Bourbigot et al. highlighted that PA-6 organomodified nanoclay composite can be a good alternative for PA-6. Nanoparticles assistance can improve both fire retardant behavior and mechanical properties of the final products. The effectiveness of a system containing nanocomposite can also increase by the creation of a protective ceramic layer [16].

2.6.4 Silicon-based Flame Retardants

According to several reports, the addition of a low amount of silicon-based compounds such as silicas, silicones, organosilanes and silicates to polymers can improve fire retardancy of polymers [17, 18].

2.6.4.1 Silicone

Silicones has displayed high heat resistance and excellent thermal stability with the limited toxic gases release during the thermal decomposition. Silicones can act as flame retardant agents by direct blending within the polymeric matrix. Another study has investigated the effect of silicone on the flame retardant properties of polycarbonate (PC) and also various types of silicone as flame retardant in polycarbonates [2, 17].

2.6.4.2 Silica

Gilman studied the effect of silica gel on the polypropylene flammability properties. He also investigated the effect of three silica gels with different particle size, surface silanol and pore volume. Some other researches were based on two types of silica (silica gel and fused silica). In this case, the porous volume and surface area of the silica affected the flame retardant properties and also the thermal stability of the polymers by viscosity modification of the system in the molten state. Viscosity control is the main key to form the protective layer [2, 3, 17].

2.6.5 Nanoscale Particles

The dispersion of nanoscale particles within polymeric matrices are known to provide the great properties such mechanical, thermal and fire resistance. They are enabled to make a noticeable loading reduction rate as parallel as the interfacial area between the nanofiller and the polymer is extremely increased. Nanoparticles contribution to flame retardancy depends on their geometry and chemical structure [5].

2.6.5.1 Nanoclay

The layered silicates are natural minerals. They are made of the regular stacks of aluminum silicate layers with the high surface area and aspect ratio. Clay is one of the most common layered silicates which is used in polymer nanocomposites preparation. The availability

and affordable price are the biggest advantages of layered silicates. Clay is a piece of the soil particles. It has a very small particle size and is considered as nanomaterial. Various types of clays are available due to diversity of properties such as formula, swelling and exfoliation [5-7]. The best nominees in construction of polymer based nanocomposites are types of clays which can be exfoliated by poly/mono-mer chains and distributed as independent clay layers within the polymer matrix. These layers provide the enhancement in polymer properties, because they have a high aspect ratio and interactions with polymer matrix. Nanoclay belongs to nano-fillers group. The filler's nature and morphology influence the final properties of polymeric nanocomposite [7, 19]. Polymeric composite incorporated with clays have received great attention due to their unique properties which can never be achieved by micro size. Polymer properties can be improved without sacrificing the pure polymer features such as ease of process, light weight and mechanical properties [7].

Nanoclays are containing of tetrahedral and octahedral sheets. In the tetrahedral sheets, a silicon atom is surrounded by four oxygen atoms but in the octahedral sheets, a metal atom is surrounded by eight oxygen atoms. Sharing the oxygen atoms causes the adhesion of the octahedral and tetrahedral sheets. The unshared oxygen atom will appear in hydroxyl form. The adhesion of octahedral and tetrahedral sheets creates the first layer of clay. The van der Waals and electrostatic forces hold the layered structure together. They are relatively weak. The inter layer distance variation influenced by the layer charge density, hydration degree and cation radius of the inter layer. Since the inter layer forces are weak, clay swelling occurs in the solution due to the hydration of the present cation between the layers. The inter layer space will increase because of swellings. Since there are different types of clays, the charge density of the

clay layer is different. The unique exfoliation and intercalation behavior mineral clays makes them very powerful as a reinforced filler for polymers [2, 7, 11, 20].

The incorporation of a low amount of clay nanolayers within the polymer matrices forms a layer of protection during the combustion [4]. The molten viscosity of polymer layered silicate nanocomposite decreases when the temperature is increased. It comforts the clays migration to the surface. The heat transfer elevates organomodifers thermal decomposition and formation of protonic catalytic sites onto the surface of the clay, which can catalyze the creation of a stable char residue [21]. Therefore the growth of the clay on the material's surface can act as a protective barrier, limits the heat transfer and diffusion of oxygen into the materials. Furthermore, the migration of nanoclay is increased by the creation of the gas bubbles that initiated with decomposition of both polymer chains and ammonium organomodifiers. The transferred heat elevates the organomodifier thermal decomposition. The combination of the silicates layers and charred structure produces a ceramic char layered silicate nanocomposites on the surface of materials. The evolution of the structure of EVA-clay nanocomposite during the thermal decomposition under oxidation atmosphere was studied by Camino et. al. At lower temperature, the layer distance of clays decreased under air atmosphere and nitrogen. At higher temperature, the modification of nanocomposties structure depends on the atmosphere [4, 21].

The formation of char during the thermal degradation of polymer matrix is the important factor. It improves the flame retardancy of the nanocomposites. The incorporation of organomodified montmorillonite and sodium layered montmorillonite in polypropylene grafted maleic anhydride can form a layer of char in the existence of organomodified montmorillonite [21, 22]. Based on Wilkie et al., the polymer nanosclaed composite with good fire retardancy displays great intermolecular reactions. It is accepted that creation of nanocomposite whether

exfoliated or intercalated, provides very good flame retardancy to the materials. For instance, the peak of heat release rate was decreased by 25% for EVA containing 5% Na-MMt compared to 50% for the EVA contained 5% cloisite 30B nanocomposites [4]. The other study suggests, the dispersion of the nanoclays within a polymer matrix may have a significant influence on flammability [22]. Organomodifier such as ammonium salt can improve the nanoclays dispersion. The increase of nanoclay within polymer can affect the heat release rate curves and leads to a quick decrease of the heat release. However, the ignition time tends to decrease but there is no change in the total heat release rate. In case of PA-6 containing the nanoclay particles, the melt viscosity increases and it is because of the presence of nanoclays which slow down the melt state formation [2-4, 22].

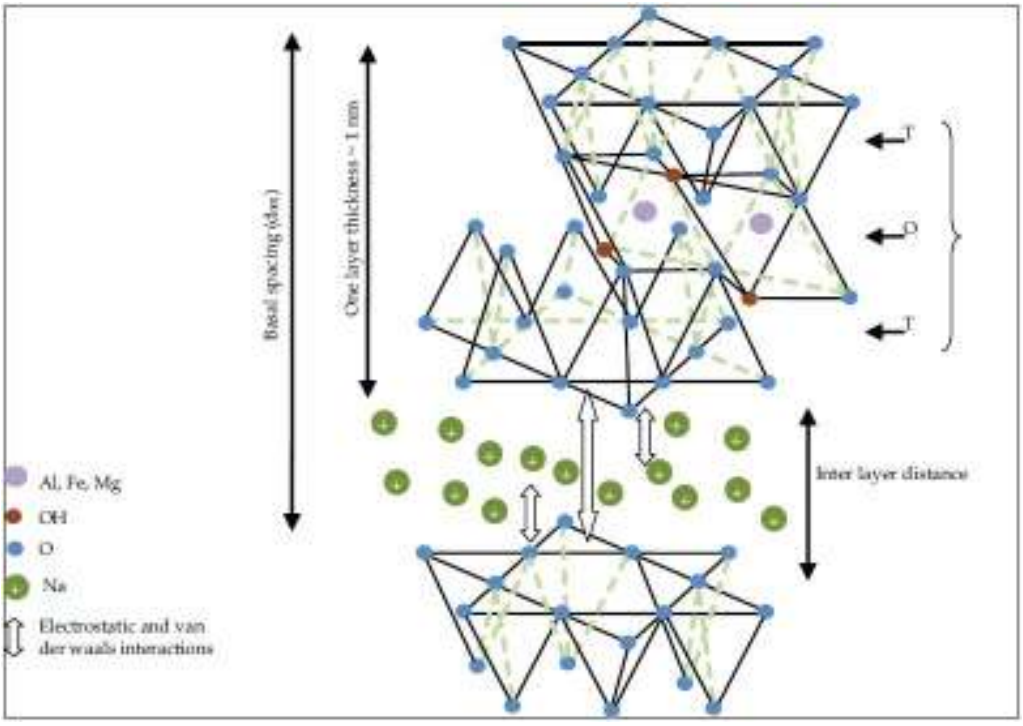

Figure 2.3. The schematic of the clay structure [7].

Figure 2.3 shows the schematic of the clay structure with 1 nm in thickness and 30 nm to several microns in lateral. These dimensions are determined by the methods of preparation and

source of clays. Clay aspect ratio is dominated by both clay lateral dimension and the dispersion ability into detached layers. It has an important role in polymer/clay interfacial and interactions. Based on the level of exfoliation and intercalation of nanoparticles within the polymers, the different type of polymeric nanocomposites can be produced [7, 20, 23]. Nanoclays have a higher aspect ratio compared to regular fillers like glass fiber. According to this feature, they can provide a dramatic enhancement in the mechanical properties of nanocomposite even at lower additions [11, 24]. According to another approach, polymer chains adhesives into the rigid clay mono layers and exhibits the high modulus. By considering the huge interfacial area in well dispersed nanostructure composite, the noticeable enhancement in the modulus is expected. The better transformation of stress can be achieved by any enhancement in the polymeric nanocomposites interfacial contact. According to some studies, the significant increase in mechanical properties of nanocomposites was observed by improving the interfacial adhesion between polymer chain and clay. It should be mentioned that plasticitization which occurs due to higher loadings, has the unfavorable effects on the modulus of nanocomposites [25-28]. Using the modified organic clays as fillers can increase stiffness and modulus of nanocomposites since more exfoliation/intercalation can be achieved [23]. It is not a simple technique to have the complete exfoliation due to the presence of different types of platelet with various thickness in the polymer matrix. According to studies, the incomplete exfoliating effect has formulated on the properties of nanocomposites [29]. Based on the other studies, the tensile modulus increases by increasing the volume fraction of fillers in nanocomposites. However, several studies reported the reduction of tensile strength by adding the clay minerals to polymer based materials [7, 18, 30, 31]. Elongation at break for polymeric based nanocomposite depends to the interfacial interactions of polymer and clay layers. Some studies have reported, both increase and decrease

of elongation at break point for polymeric based clay nanocomposites [18, 24]. According to some studies, the transition temperature (T_g) of polymer/clay nanocomposites improved by the addition of nanoscaled clays [7, 23, 27, 32].

2.6.5.2 Nanotalc

Talc is naturally occurring hydrated magnesium sheet silicate [20]. The elementary sheets are composed of a magnesium-hydroxyl/magnesium octahedral, sandwiched between the layers of silicon-oxygen tetrahedral. Talcs are naturally lamellar. They are chemically inert, water-repellent and organophilic to a great extent. At temperatures above 900 °C, talc gently loses their hydroxyl groups. At temperatures above 1050 °C the recrystallization into various forms of enstatite will occur. Similarly to clays, talc categorized in phyllosilicates group, but compared to montmorillonite, saponite and hectorite, they cannot be exfoliated by the use of cationic surfactant because of the metallic cations absence between the layers.

Talc has been used as filler (as reinforcement) in silicon elastomer. They can be used as insulation of electrical equipments, as sealants and as encapsulants where the flame retardancy is the main concern. Tkaczyk et al. from general electric used 20 wt% of nanotalc to produce silicon nanocomposite which is useful in insulation of electrical wires. It is found that using the talc in nanosclae and mixing it with silane can provide lower conductivity than untreated surface, and also better mechanical properties were provided. George et al , used talc as filler in the silicon rubber preparation process. This invention can be useful in different applications like fire blanket production [17, 20].

Talc is a hydrated magnesium silicate. There are different types of talc and each ore body has their own properties and geology. They were formed many years ago. Talcs are lamellar, but their platelet size differs from on deposit. Small crystals are known as microcrystalline talc and

larger crystals are known as macrocrystalline talc. Talc can be in different colors such as white, gray, blue, pink, green and black [33].

Talc can be used as fire resistance and electrical insulator. In terms of fire retardancy of polymeric materials, they can: 1. Reduce the combustibility of the compound, by dilution of the fuel 2. Create a barrier to transfer the mass which limits the oxygen diffusion to combustibles and delays the gaseous diffusion and reduce the combustion rate. 3. Contribute to the creation of the char phase that formed during the combustion. It acts as an efficient barrier (heat transfer) to improve the flame retardancy of products. 4. Contribute to lower smoke creation if used with the other types of flame retardants which promotes the char formation [34].

2.6.5.3 Graphene and Carbon Nanotubes

The study of graphene is one of the most recent topics in materials science. Graphene has very good prospects for various applications in a number of different fields. It has been a quick rise of interest in the study of the properties and structure of graphene following the very first report in 2004 of the isolation and preparation of a single layer of graphene in Manchester.

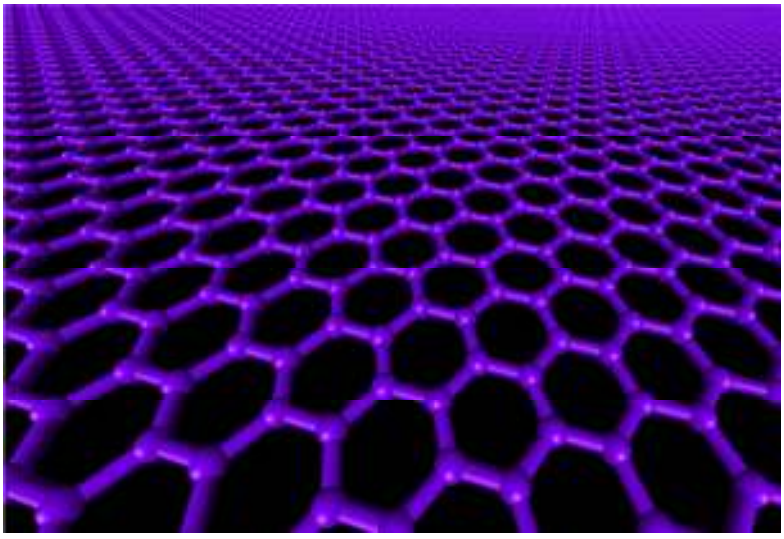

Figure. 2.4. A molecular model of Graphene [39].

Graphene is the most basic building block of all carbon's graphitic forms. It has a honeycomb structure and from the atomic aspect it consists of a single layer of sp^2 . Graphene is one the most popular nanoparticles in nanocomposites filed (Figure 2.4) [35-38].

The expanded graphite was developed more than 100 years as filler for the polymeric resins. More recently, there has been a lot of researches on preparation of the thinner forms of graphite which is known as graphite nanoplatelets. The addition of graphite nanoplatelets to polymers has been found to lead a significant improvements in electrical and mechanical properties [35, 39, 40]. According to other studies, carbon based nanoparticles was used in particular carbon nanotubes to combine several properties such as electrical conductivity, mechanical strength and thermal stability. This great potential arises from the exceptional properties of the nanotubes. This is because of the structure of graphene. Although significant achievement has been made in usage of carbon nanotubes as reinforcement of a polymer matrix, there are some issues such as nanotubes tendency to agglomerate during the process and high cost of production. Raquel et al,. reviewed the graphene filled polymer nanocomposites including the process of producing the graphene/polymer nanocomposite and also resultant properties and their application [3, 39, 41, 42].

Carbon nanotubes exhibit extraordinary properties that can be used in various applications ranging from macroscale down to the nanoscale. Because of their high aspect ratio, carbon nanotubes pervade to create a network at low loading in the polymer matrix and lead to significant improvement of several functional properties such as rheological, flame retardant and mechanical properties [43, 44]. There are two types of CNTs, small diameter single-walled nanotubes (the diameter is about 1 ~ 2 nm) and larger-diameter multi-walled nanotubes (the

diameter is about 10~100 nm) [4, 45] . Figure 2.5 shows the single wall nanotube (SWNT) and multi-wall nanotube [46].

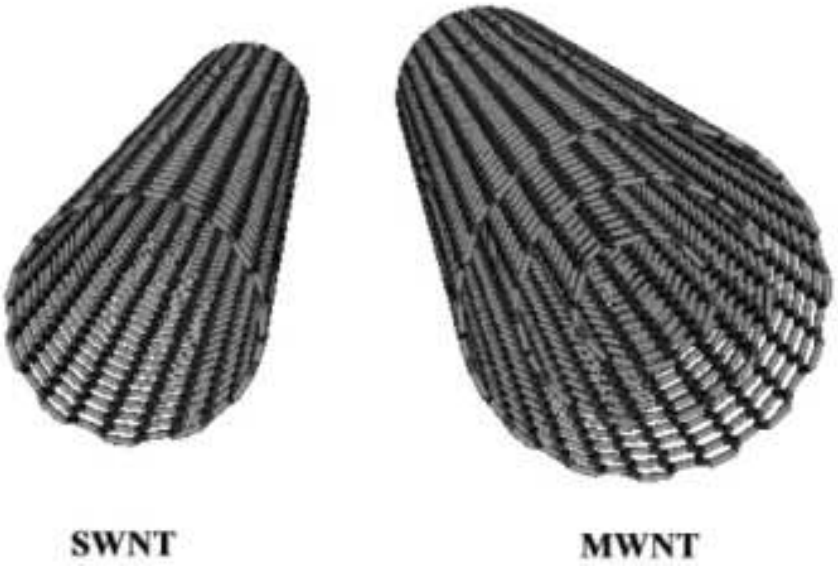

Figure 2.5. Single wall nanotube (SWNT) and multiwall nanotube [46]

CNTs can act as flame retardant materials and also are a good alternative for clay and mineral materials like talc. According to reports, the incorporation of CNTs at a low loading rate (less than 3 wt%) has improved the flammability a wide range of polymeric materials such as ethylene vinyl acetate copolymer, poly(styrene), poly(methyl methacrylate), low density poly(ethylene), poly(propylene) [4, 44, 47]. The effect of the nanotubes dispersion on the flame retardant properties of PMMA nanocomposites was studied by Kashiwagi et al. and it was shown that the incorporation of just 0.5 wt% of single-walled nanotube well dispersed in PMMA led to a significant decrease in the heat release rate, liberated over longer time range compared to unfilled PMMA [45, 48]. However, the thermal behavior of PMMA nanocomposite which contain of poorly dispersed single-walled nanotube proved to show very similar behavior to neat PMMA, with no remarkable reduction in the heat release rate. The flammability of the PMMA containing nanocomposites affected by the nanotube loading rate. For example, the addition of

0.1 wt% of SWNT did not reduce the heat release rate (HRR) of the PMMA while by incorporation of 0.5 wt% of SWNT more than 50% reduction in HRR was achieved. Based on the reports, the flame retardant properties of PP containing multi-walled nanotube appear to be governed by two physical processes: 1. The network layers (MWNT) act as a shield and they can re-emit the radiation back into the gas phase, and decrease the rate of polymer degradation. 2. The existence of carbon nanotubes increases the polymer thermal conductivity. As a result, the time ignition and the peak HRR of the PP containing MWNT will increase. Dubios et al., has studied the effect of the MNWT mean size on the flammability of EVA . By incorporation of 3 wt% MWNT within EVA (ethylene-vinyl acetate) copolymer and a remarkable increase in ignition time was obtained when it was submitted to cone calorimeter test [4, 36, 47, 49].

Several studies have evaluated the effect of chemical modified graphene on thermal stability, melting temperature, glass transition and polymer crystallinity of the nanocomposites. Most of the polymers degrade at very low temperatures which limits their usage for high temperature applications, as compared to metals or ceramics. The degradation polymer behavior is evaluated in three parameters: 1. The onset temperature 2. The degradation temperature 3. The degradation rate. The onset temperature refers to a temperature that system starts to degrade. The degradation temperature considered as a temperature that the maximum rate of degradation occurs. The degradation rate is observed in the derivative weight loss as temperature curve's function. Non crystalline materials, such as polymer exhibit a second order of phase transition, which is called the glass transition temperature (T_g). At this temperature materials start changing from a brittle crystalline solid phase to the elastic solid phase. There are several reports that show an increase of glass transition temperature in a thermally exfoliated graphene oxide and poly(methyl methacrylate) [37, 41, 50].

2.7 Preparation Methods and Mechanical Properties

The solution intercalation is one the most common methods to prepare the nanocomposites. In this technique, the polymer dissolves in a proper solvent and the nanoparticles disperses in the same solution. After this step the nanoscale particles swell in the solvent and the polymer chain intercalate between the layers. The solvent will be vaporized and the intercalated nanocomposite will be remained. The diffusion of the polymer chains within the nanoparticles layer occur during the solvent evaporation process. Since this method requires solvent, it is maybe not the best option for industrial purposes. In most of industrial applications, emulsion polymerization is the most proper method for the nanocomposite preparation [7]. The main aim of adding the nanoparticles to polymers is improving the properties of polymers and producing the polymeric based nanocomposites for desired applications. The nanocompiste with demanded properties are mainly produced to overcome the polymers drawback while maintaining the advantages of primary polymer matrix [7, 8, 16].

Additive fillers improve the properties of nanocomposites [51]. The sufficient interactions between the filler and matrix supports the added rigid fillers to matrix to transfer the major applied load to the matrix under stress. The larger interfacial interaction between the matrix and filler and higher filler ratio can increase the reinforcement effect and modulus in nanocomposite composition respectively. The main goal of the most of research on carbon nanotubes/polymer nanocomposites is to achieve remarkable mechanical properties, thermal stability or electrical conductivity. The possibility of making both functional and structural system is more applicable for graphene filled nanocomposites due to improved interfacial adhesion, larger specific area and outstanding properties [52, 53]. According to more recent reports, the mechanical properties of graphene sheets were measured and below results were

obtained: fracture strength of 130 GPa, Young's modulus of 1.0 TPa . Based on the studies which was focused on the mechanical properties of polymeric nanocomposites filled graphene confessed an increase in modulus as a function of loading [38, 42, 53-56]. Graphene has a low intrinsic modulus, therefore the most distinct improvement was observed in elastomeric matrices. The majority of the studies gave no detailed information on the nanocomposites strength except some reports. They reported an increase of 75% with 0.7 wt% unreduced graphene oxide in poly(vinyl alcohol) (PVA) and also graphite nanoplatelets and thermally expanded graphene reduced the propagation of cracks in epoxy polymers [41].

2.8 Laboratory Fire Testing

The flammability of polymeric materials can be determined by their flame spread rate, ignition and heat release. Depending on the application of polymers, some of the flammability criteria need to be measured by the appropriate test. These tests are available in different scale to be used in academic or industrial laboratories for either testing the manufactured products or monitoring the materials during the flame test. Troitzsch has reviewed different types of flammability tests and their standards [4].

2.8.1 Limited Oxygen Index

Limited oxygen index (LOI) test was proposed in 1966 by Martin and Fenimore. It was used to depict the relative flammability of polymeric materials [12]. Then it was standardized in the United States, ASTM D2863, and in France, NF T 51-071. This test is now known as ISO 4589 as an international standard. The LOI value is calculated by the oxygen concentration in the mixture of oxygen and nitrogen that either preserves the material's flame combustion for 3 minutes or expends a length of 5 cm of the sample [2]. The sample must be placed in vertical

position and the flame must be applied on top of the sample. The below formula express the LOI calculation:

$$LOI = 100\frac{[O_2]}{[O_2][N_2]} \quad [12]$$

Based on ISO 4589 (International Standard), the sample size must be 80 x 10 x 4 mm^3 and must be placed vertically at the glass chimney center. As air contains the 21 % of Oxygen, the materials with an IOL above 21 are considered as self extinguishing whereas those materials with an LOI below 21 are considered as combustible. The higher number of IOL means the better flame retardant property. Now days, due to the developments of the standards, the other tests are more common, but this method remains as the important technique to monitor and control the quality of plastics in industry [4, 12]. Figure 2.6 shows the schematic of LOI unit.

Figure. 2.6. Schematic of the LOI chamber [57].

2.8.2 UL 94 Test

The UL94 test has been approved by the underwriters laboratories. It is approved as a reliable test for plastics flammability where they used as parts in appliances and devices. It

includes different types of flammability tests such as horizontal test for bulk materials, vertical test in small and large scale and radiant panel flame spread test [6, 16, 20, 22, 23].

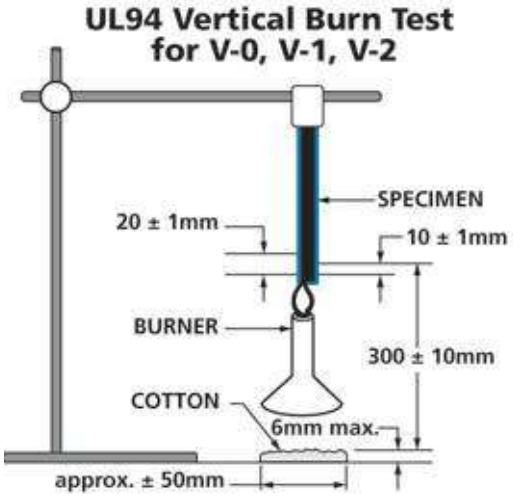

Figure 2.7. Schematic of UL94 Test [58].

It is a very common method to measure the ignition ability of vertical bulk materials when they expose to flame. Figure 2.7 shows the schematic of the ASTM UL 94 Vertical test. The vertical test is classified in three ratings. The V-0, V-1 and V-2 are the ratings of the vertical test. Figure 2.8 shows the UL 94 Chamber [4, 13].

Figure 2.8. UL 94 Chamber [59]

The flame must be applied to the bottom of the specimen and the top of the flame must be placed at 10 mm from the bottom of specimens edge. The flame applies for the first 10 seconds and then removed. T_1 is the after flame time, this is the time which required for the flame to be extinguished. After extinction, the other 10 second will apply, which is called after flame time t_2, with t_3 (after glow) is the required time for the fire glow to be disappeared. It is very important to maintain the distance between the burner and the specimen. If the drops fall, the burner must be either isolated from the flame or must have the angle of 45°. During the test, the burning drops causes ignition of a cotton located below the sample. 5 sets of specimens must be prepared and tested. According to standard criteria, the specimen classified as V_0, V_1, V_2 (Table 2.1) [4, 14, 24].

Table 2.1. UL 94 ASTM classification [2].

UL94 Classification	
V_0	t1 and t2 < 10 seconds for each specimen t1 + t2 < 50 seconds for the 5 specimens t2 + t3 < 30 seconds for each specimen No afterglow or after flame up to the holding clamp No burning drops are allowed.
V_1	t1 and t2 < 30 seconds for each specimen t1 + t2 < 250 seconds for the 5 specimens t2 + t3 < 60 seconds for each specimen No afterglow or after flame up to the holding clamp No burning drops are allowed
V_2	t1 and t2 < 30 seconds for each specimen t1 + t2 < 250 seconds for the 5 specimens t2 + t3 < 60 seconds for each specimen No afterglow or after flame up to the holding clamp Burning drops are allowed

2.8.3 Cone Calorimeter

Cone calorimeter is one the most effective test to discuss about polymer thermal behavior. The cone calorimeter principals are simple. It is based on the measurement of the decrease amount of oxygen concentration in the combustion gases when the specimen is subjected to a given heat flux (Figure 2.9). It is standardized in the United States, ASTM E 1354 and in the international standard is known as ISO 5660. The sample must follow the standard size (100 X 100 X 4 mm3). It must be placed on load cells to evaluate the mass loss evolution when the experiment is running. An electric spark can trigger the combustion. The measurement of the oxygen concentration and gas flow are used to calculate the heat released quantity per unit of surface area and time. Heat release rate (HRR) is expressed in kW/m^2. The cone calorimeter test measures the combustion time, extinction time (TOF), time to ignition characterization (TTI), mass loss during the combustion, total smoke released and quantity of CO_2 and CO [2, 4, 22, 60].

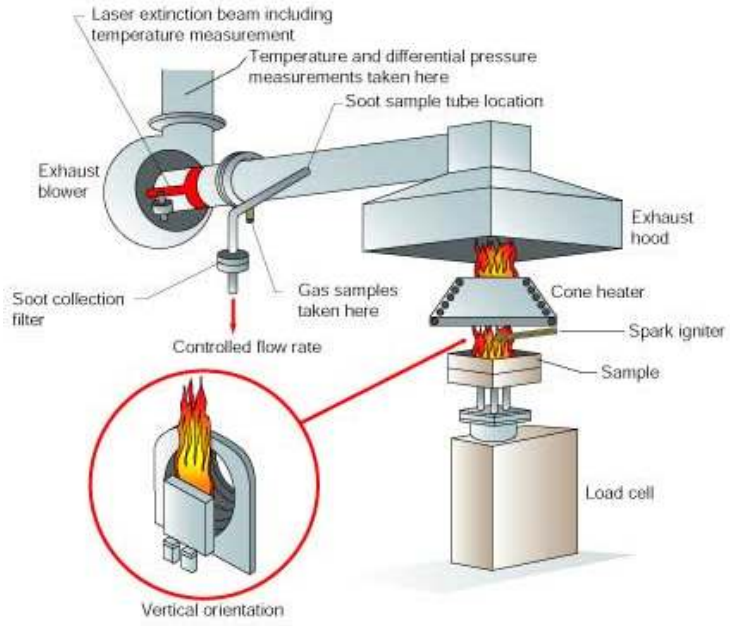

Figure 2.9. Cone Calorimeter [61].

2.8.4 Notes About Fire Tests

The inflammation resistance and ignition-ability of polymers are characterized by the LOI test. It is important to note that dripping and melting of polymeric materials during the LOI test may lead to some inaccurate values like very high LOI values. The dripped polymer can take the fire away from the specimen's surface and extinguish the fire [4]. The vertical UL 94 test is widely used both in academic studies and industry. However, the obtained results remain limited due to unrefined character. Some of the users in the academic domain recommend three applications of fire for 5 seconds rather than using two successful applications of the burner for 10 seconds to gain better difference between the compositions understudies. There is no doubt, the cone calorimeter test provides more information on fire characteristics. The heat release rate is certainly very useful parameter to evaluate the polymeric material's fire properties [16].

CHAPTER 3

EXPERIMENTAL

To investigate the effect of nanoparticles in polymer based matrix nanocomposites, the below experiments were conducted, 1. UL 94 test 2. Scanning electronic microscope 3. TGA 4. DSC 5. Tensile Test.

3.1 Materials

3.1.1 PVC and DMAC

Poly (vinyl chloride) $[-CH_2CH\ (Cl)\ -]_n$, the white and brittle powder, were purchased from Sigma-Aldrich was used as the main matrix (Figure 3.1.a). N,N-Dimethylacetmide (DMAC), purchased from Fisher Scientific was used as a solvent which is a colorless liquid and contained 0.005 % water (Figure 3.1.b).

Figure 3.1. a) PVC, b) DMAC.

3.1.2 Nanoclay

Cloisite 30B was provided by Southern Products, Inc, Texas for the study purposes. It is powdery and white in color, and the typical dry particle size is less than 10 μm (Figure 3. 2. a).

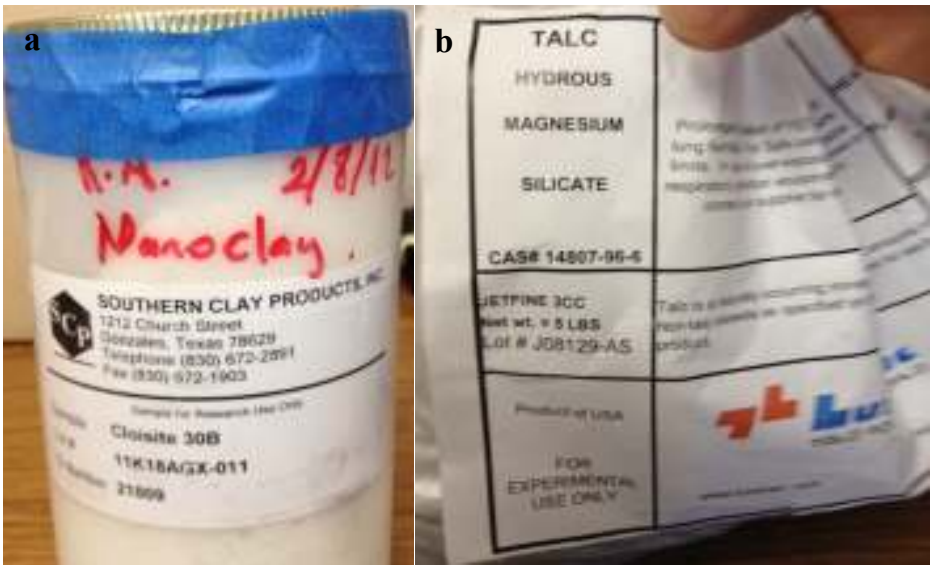

Figure 3. 2. a) Nanoclay b) Talc.

3.1.3 Nanotalc

Nanotalc (Hydrous magnesium silicate) was provided by Luzenac inc. it is a white brittle powder (Figure 3. 2. b).

3.1.4 Graphene

Graphene (N006-010-P) was purchased from Angstron Materials, Inc., Dayton, OH. It is powdered and black in color with thickness of 10 to 20 nanometers.

The nanoclay is amine functionalized while the graphene is not functionalized, and used as it is.

3.2 Methodology

3.2.1 Sample Preparation

3.2.1.1 Solution

Polyvinyl chloride was used as the main matrix and DMAC was used as solvent. The PVC was mixed with DMAC to prepare the solution with 15 wt% and 85 wt % respectively. Preparing the proper solution with proper viscosity is very important. In order to have the proper solvent, at first 85 wt % DMAC was poured in the good size glass and placed on the hot plate. The magnetic bar is needed for stirring the solution while the hot plate is running. It is very

important to choose a proper temperature below the T_g of PVC. Later, the addition of PVC was done carefully. It is important to notice that the addition of PVC must be done very slowly to prevent the agglomeration of particles. In this case, the solution will not be smooth. The glass transition temperature for PVC is 80 °C, therefore, the experiment temperature should be below the glass transition temperature. Glass transition temperature is the maximum service temperature of polymers and it is necessary to know about it to control the other parameters, otherwise the properties of materials will completely change. The different weight percentages of samples were prepared for this research: 1. 0 wt % (no nanoparticles inclusion within the solution) 2. 5 wt% nanoparticles of 15 wt% PVC samples 2. 10 wt% nanoparticles of 15 wt% PVC 3. 20 wt% nanoparticles of 15 wt% PVC (Figure 3.3.b, Figure 3.3.c). For preparing the pure PVC samples the 15 wt% of PVC was solved in 85 wt% DMAC. The solution must be on the hot plate and stirred for a certain amount of time in the proper temperature for at least 12 hours to have the uniform solution with good viscosity. For those samples which includes nanoparticles the following procedure was done: Nanoparticles was squeezed to become soft to prepare the uniform solution. The 5 wt %, 10 wt % and 20 wt% nanoparticles of 15 wt% PVC was added to 85 wt% of DMAC. The solution was sonicated for a couple of hours in order to have well dispersed solution (Figure 3.3.a).

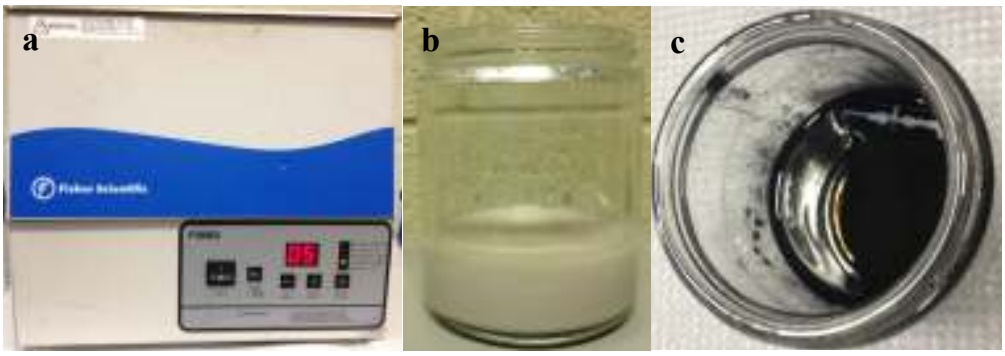

Figure 3.3. a) Sonicator b) PVC incorporated with 20 wt% nanoclay c) PVC incorporated with 20 wt% graphene.

After sonicating process the main matrix (PVC) was added to the solution by the very slow rate.. The new compound was stirred on the hot plate for the certain amount of time. It was varied from 12 hours to 36 hours continuously. It is necessary to observe the solution during the preparation of the samples frequently due to the possibility of agglomeration, magnetic bar stop stirring and unexpected accidents. The duration of the sonication, stirring on the hot plate and suitable speed depends on the percentages of dispersed nanoparticles [5, 6].

3.2.1.2 Molding/Casting

After the stirring at certain speeds continuously, the solution was cast into a specially prepared mold. Special care was taken to coat the mold with the release agent before pouring the dispersions, in order to facilitate the removal of the samples from the mold.

The melt solution was allowed to solidify at room temperature through evaporation process. Once the solvent (DMAC) had evaporated, the cast specimen was ready for the thermal test. Figure 3.4.a and 3.4.b shows the casting process of pure PVC and PVC incorporated with 20 wt% graphene nanoflake [6].

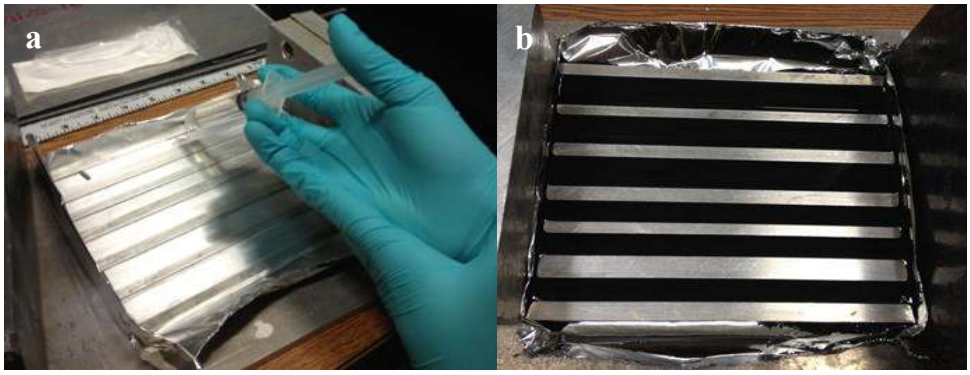

Figure 3.4. a) Casting of a) Pure PVC, and b) PVC incorporated with 20% graphene nanoflakes in the Al molds.

3.3 ASTM UL 94 V Tests

One of the most common flame tests to determine the flammability of plastic materials is called UL-94 test, which identifies the tendency of the materials either to self-extinguish or to spread the flame once the specimen has been ignited [5, 6, 31]. In this study, the vertical UL94 tests were used to determine the flame retardancy of the specimens. The specimen size must follow the standards for the flame retardancy test. During the application of the flame, it is very important to maintain a constant distance between the burner and specimen as much as possible. The specimens must be 5"x1/2" (12.7 cm x 1.7 cm) with the minimum approved thickness. The typical thicknesses are 1/16", 1/8" and 1/4". There are three major ratings (V0, V1, and V2) for the typical UL94 vertical test . V-0 is the best rating among the all three ratings [5, 44].

3.3.1 Bunsen Burner Flame

A flame is a region that combustion takes place. The flame's color depends on the substance and temperature burning. Hydrocarbon flames are either yellow or blue. Bunsen burner is used in most of the laboratories for combustion and heating purposes. The standard size of inner diameter for Bunsen burner is 3/8 inches. It is connected to a source of fuel which is propane in most of the cases. There is a gas jet at the bottom of Bunsen burner which draws air in through the air hole due to the Bernoulli effect [62].

Figure 3.5. Bunsen Burner [63].

It was invented by Robert Bunsen (German chemist). It improves the combustion efficiency by combining the flammable gases from a jet with air before ignition to produce a very hot flame. Because of the shape of the rim, the flame is conical. The amount of internal air can be controlled by opening and closing the air hole. If the air hole is closed, then the flame will be yellow. By opening the air hole, the outer cone flame color will turn to blue with colorless inner cone. The tip of the outer part of the flame is colorless which has the highest the temperature (Figure 3.5).

3.4 Scanning Electron Microscope

Scanning electron microscope captures images of a sample by scanning the materials with the help of focused electrons beams. This method was used to analyze the morphology of materials before and after the burning test.

3.5 Thermogravimetric Analysis (TGA)

Thermogravimetric is a thermal analysis to examine the mass change of a specimen as a function of time in an isothermal mode or as a function of temperature in scanning mode. TGA is an analysis method to characterize the thermal stability and decomposition of materials under various conditions and also to examine the kinetics of the processes occurs in the materials. It is

a common method to compare the behavior of neat polymer with polymers contained additives during applying heat. Figure 3.6 shows the TGA unit.

Figure 3.6. TGA Unit [64]

In TGA, the mass change of the sample is measured either relative percentage or absolute value in milligrams, and then the results will be plotted against time or temperature. The changes of mass in plastics can occur in one or more steps. M_L is the percentage loss of mass and is calculated from the m_s (initial mass before heating) and m_f (when temperature is reached at the end) by using the equation below :

$$M_L = \frac{m_s - m_f}{m_s} \times 100 \qquad [12]$$

The TGA measurement was performed from 0-1000 °C at a heating rate of 10 °C/ min.

3.6 Differential Scanning Calorimetry (DSC)

The differential scanning calorimetry (DSC) is an analysis technique to measure the energy that is necessary to establish a nearly zero temperature difference between an inert reference material and a substance as it is subjected to identical condition (temperature regime) in a controlled environment with identical rate [4, 32, 41]. Figure 3.7 shows the DSC unit.

Figure 3.7. Differential Scanning Calorimetry [65]

By the help of this analysis technique, very useful information can be extracted such as phase changes, glass transition and melts. High speed and ease of the process are the biggest advantages of DSC, which helps to observe the transitions in materials. DSC is one the most common thermal analysis technique. It uses in many analytical, quality assurance, process control and research laboratories. A heating rate was 10 °C/min and the heating scan was carried from 30 °C to 250 °C and cooled down from 250 °C to 30 °C [66].

3.7 Mechanical Properties

Five sets of samples were prepared for UL94 test and couple of samples were prepared for the tensile test. All the samples were made out of the same solution. Since the thickness of materials was not enough to use the common tensile test machine, the micro tensile test was used to perform the tensile test. The compact stress-strain apparatus was used in this experiment (Figure 3.8).

Figure 3.8. Compact stress-strain apparatus.

Stress-strain curve (Figure 3.9) characterizes the materials behavior during the tensile test. It is an important graphical measure of mechanical properties of materials. Based on the ductility and brittleness of materials the shape of the curve is different.

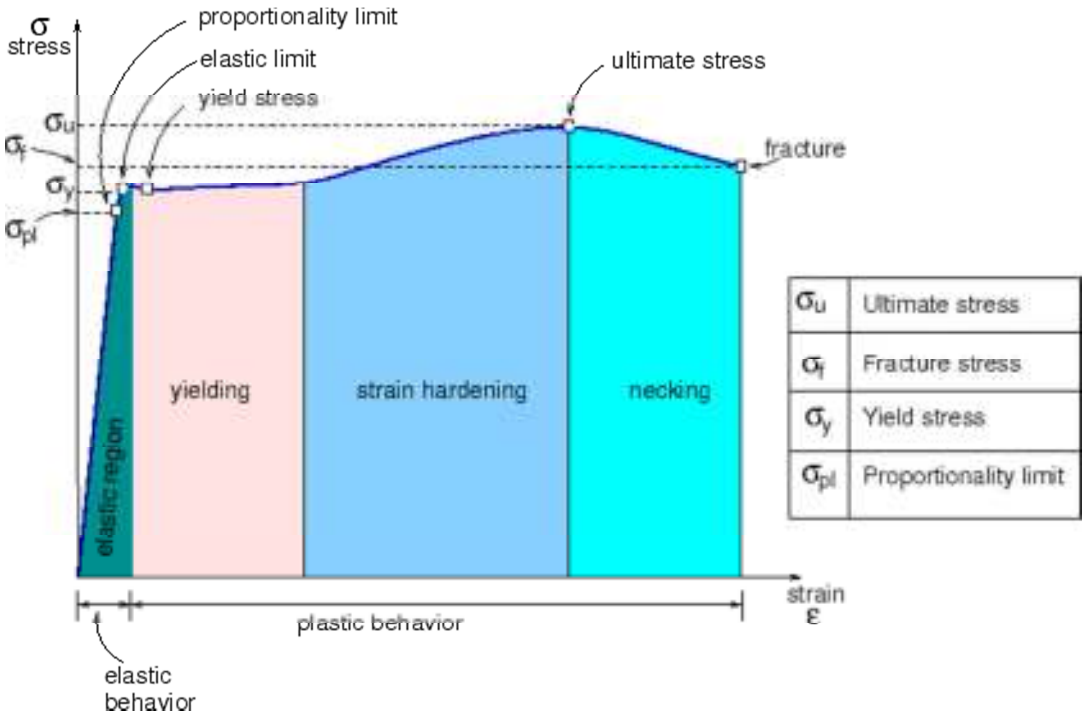

Figure 3.9. Typical stress-strain curve [67].

Chapter 4

RESULTS AND DISCUSSION

4.1 ASTM UL94 V Test

In this study, the vertical ASTM UL-94 test was used to determine the flame retardancy of the specimens. All parameters followed the standards for flame retardancy test including specimen size, the distance between the burner and the specimens. Table 4.1 shows the UL 94 classification of pure PVC and PVC with nanoparticle inclusions.

Table 4.1. UL94 V test rating for all samples.

UL-94 / Specimen	V - 2	V - 1	V- 0
PVC => Failed			
5% Nanoclay		✓	
10% Nanoclay			✓
20% Nanoclay			✓
5% NanoTalc	✓		
10% NanoTalc	✓		
20% NanoTalc			✓
5% Graphene		✓	
10% Graphene			✓
20% Graphene			✓

Based on the results, PVC with 0 wt% of the nanoparticles failed in the first 10 second period. The whole PVC sample started burning completely. Figure 4.1.a shows the PVC incorporated with 20 wt% graphene during the UL 94 test. Figure 4.1.b,c,d shows the images of residual char of the 20 wt% of nanoclays and nanotalcs and graphene after UL-94 burning test. As is seen in Table 1, the specimens containing 10 wt% of nanoclay and graphene and also 20 wt% of all nanoparticles showed the best fire resistance among all the samples. They are classified as V-0 which is the best rate. All the samples were weighed before and after the burning test. The samples containing 20% weight percentage of nanoparticles showed the best results among all the samples.

Figure 4.1. Images of a) PVC with 20 wt% graphene during the UL94V test, b) PVC with 20 wt% nanoclay, c) PVC with 20 wt% nanotalc, d) PVC with 20 wt% of graphene after the burning test.

4.2 Scanning Electron Microscope

The SEM analyses were performed on the samples before and after the flame sources on the samples with and without nanoscale inclusions.

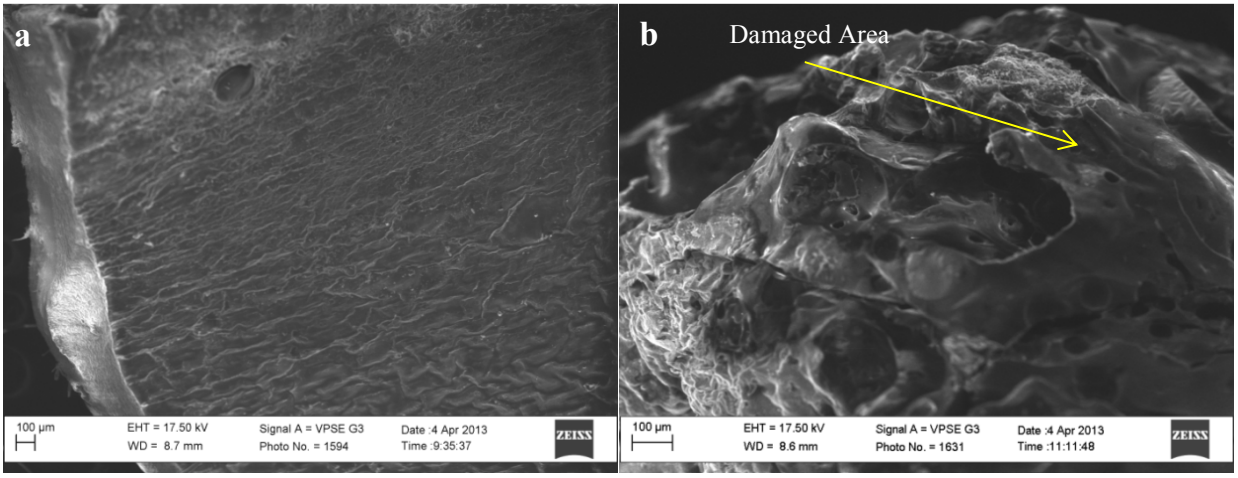

Figure 4.2. SEM images of pure PVC samples a) before the burning, and b) after the burning tests.

Figure 4.2.a shows the SEM images of the surface of unburned PVC, while Figure 4.2.b shows the surface of the burned PVC sample failed after a 10-second of the burning test. The surface of the pure PVC is completely damaged after the exposure to the open heat source, and surface morphology was immediately destroyed.

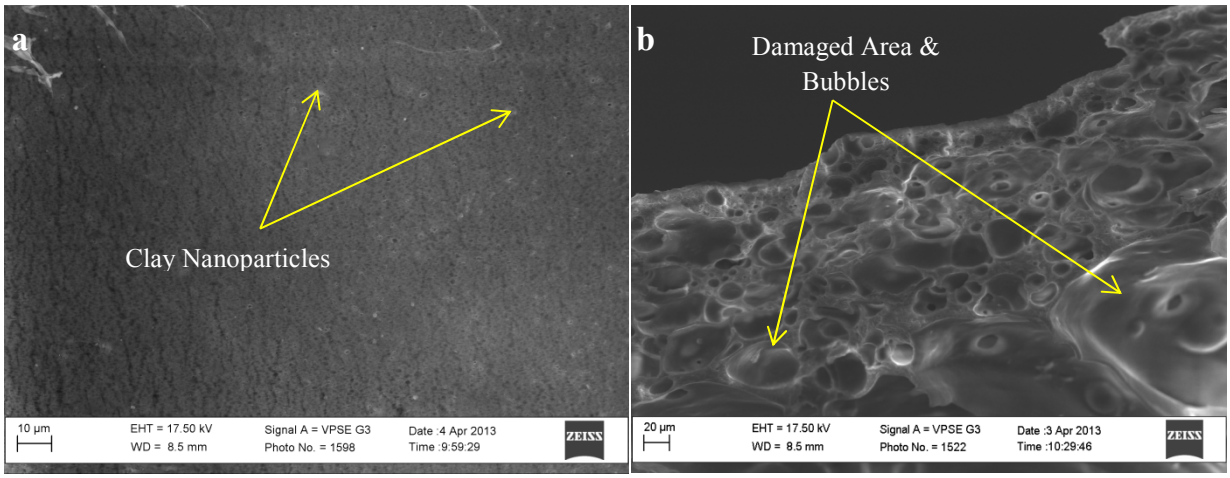

Figure 4.3. SEM images of a) the unburned PVC+5 wt% nanoclay, and b) the burned PVC+5 wt% nanoclay.

Figure 4.3.a shows the SEM images of unburned PVC+5% nanoclay, the nanoclay particles can be seen on the surface of the material before performing a thermal test. Figure 4.3.b shows the surface of the burned PVC with 5 wt% of nanoclay inclusion. As is seen in this figure, there are some bubbles but also lots of damages on the surface as well.

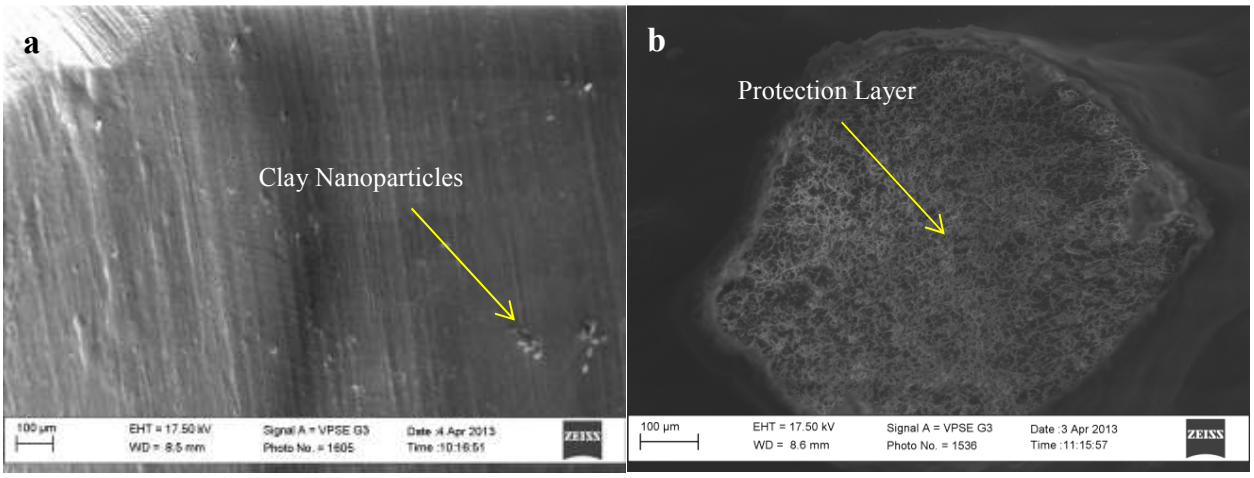

Figure 4.4. SEM images of a) the unburned PVC+10 wt% nanoclay, and b) the burned PVC+ 10 wt% nanoclay.

Figures 4.4.a and 4.4.b show the SEM images of the unburned and burned PVC samples with 10 wt% nanoclay inclusions, respectively. Before the flame test, there is a good combination between the pure PVC and PVC incorporated with nanoclay samples (Figure 4.4.a); however, the SEM surface analysis indicates the considerable swelling, holes and morphology changes after the burning tests (Figure 4.4.b). The swelling and morphological changes might be the consequence of nanoclay inclusions in the PVC structure, which act as the barrier to control the flame growth, dripping and stop further damages on the samples.

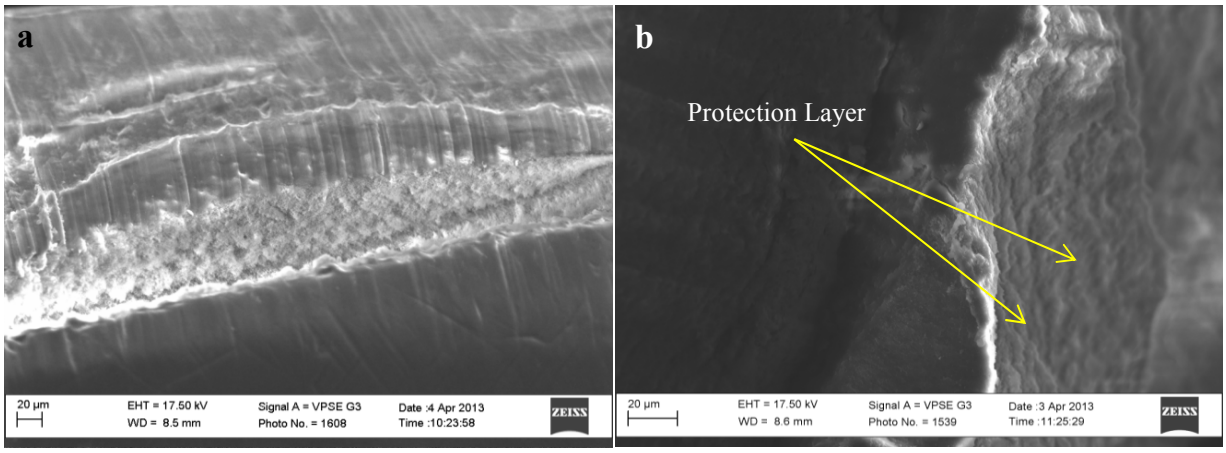

Figure 4.5. SEM images of a) the unburned PVC+20 wt% nanoclay, and b) the burned PVC+20 wt% nanoclay.

Figure 4.5.a and 4.5.b show the SEM images for the surface morphologies of the unburned and burned PVC+20wt% nanoclay, respectively. Before the flame test, there is a good correlation between polymer and inclusions. During the burning tests, nanoclay in the PVC was concentrated at the interface between the flame and PVC chains, and formed a thick layer of nanoclay inclusions. During which time, some holes, bubbles and other morphological changes were also formed at the interface. These holes are also critical in controlling the flame propagation because these holes enclose the unburned inorganic inclusions.

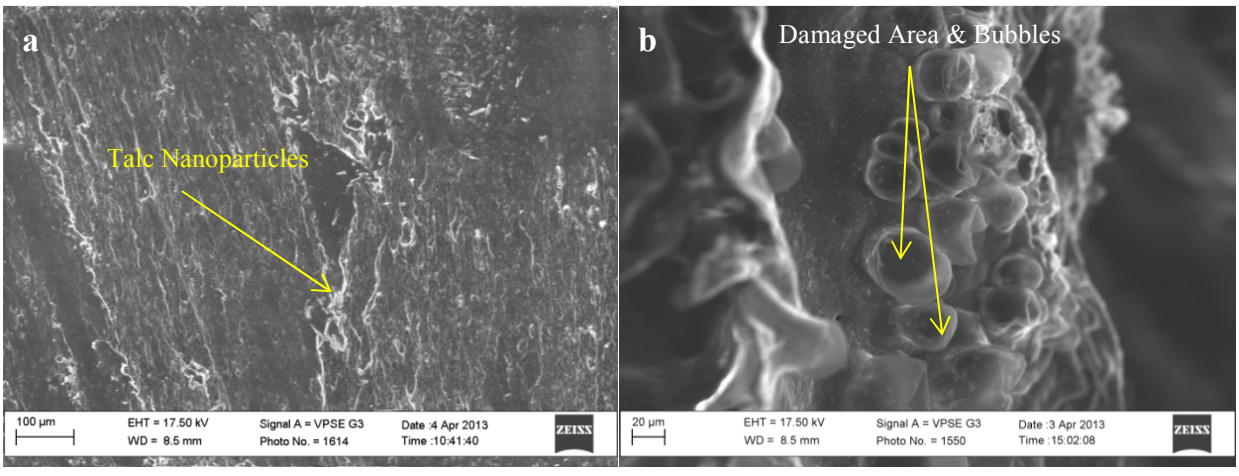

Figure 4.6. SEM images of a) the unburned PVC+5 wt% nanotalc, and b) the burned PVC+5 wt% nanotalc.

Figure 4.6.a and 4.6.b show the surface of unburned and burned PVC with 5 wt% nanotalc inclusions, respectively. The particles of nanotalc can be seen in Figure 5a and in figure 5b the formation of bobbles are obvious due to heat effect, this layer of bubbles can protect the rate of fire propagation.

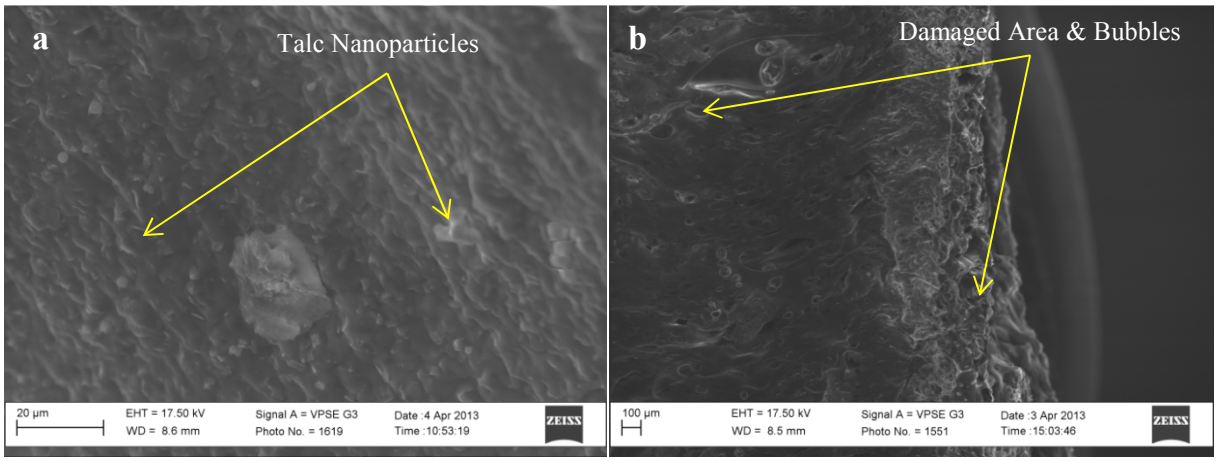

Figure 4.7. SEM images of a) the unburned PVC+10 wt% nanotalc, and b) the burned PVC+10 wt% nanotalc.

The unburned PVC containing 10 wt% nanotalc is shown in figure 4.7.a and it shows the particles of the nanotalc on the surface while the figure 4.7.b shows the burned PVC with 10 wt% nanotalc inclusions. The bubbles can be seen on the surface which helps to slow down the rate of fire and acts and protection layer on the surface.

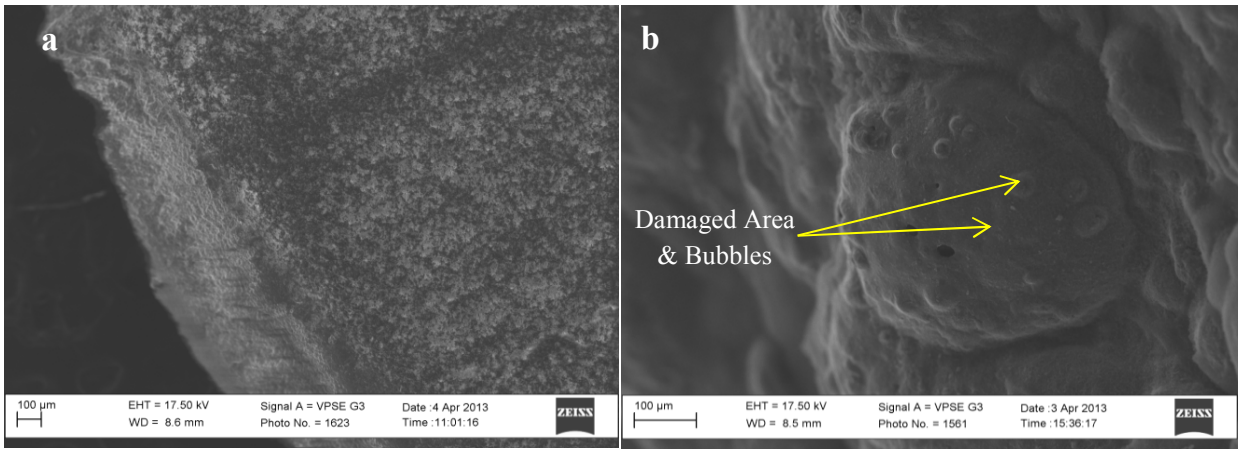

Figure 4.8. SEM images of a) the unburned PVC+20 wt% nanotalc, and b) the burned PVC+20 wt% nanotalc.

The same tests were also conducted on the PVC and nanotalc samples to find out the effects of inorganic inclusions on the flammability and fire retardancy. Figure 4.8.a and 4.8.b shows the SEM images of the unburned and burned surfaces of PVC with 20wt% nanotalc, respectively. As is seen in Figure 4.8, the similar morphological changes before and after the burning tests were observed, including swelling, bubble formations, holes and other morphological changes. This means that concentrating the nanoscale inclusions at the interface during the burning operation drastically change the flammability and fire retardancy behaviors of the samples.

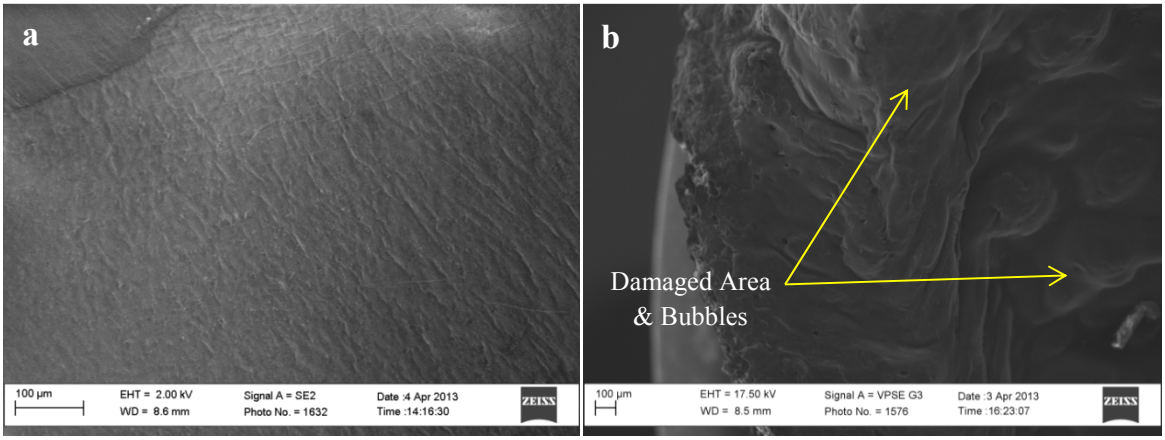

Figure 4.9. The SEM images of a) the unburned PVC+5 wt% graphene, and b) the burned PVC+5 wt% graphene nanocomposite specimen.

The same UL-94 tests were also conducted on the pure PVC and PVC with graphene inclusions. Figure 4.9 shows the SEM images of the unburned and burned surfaces of the pure PVC and PVC containing 5 wt% graphene. The unburned surface (Figure 4.9.a) shows a very smoothness and it is due to good dispersion of the initial solution. Figure 4.9.b shows burning surface after applying the UL 94 test, the surface was burned but not as severely as neat PVC, and also the bubbles are seen in the figure.

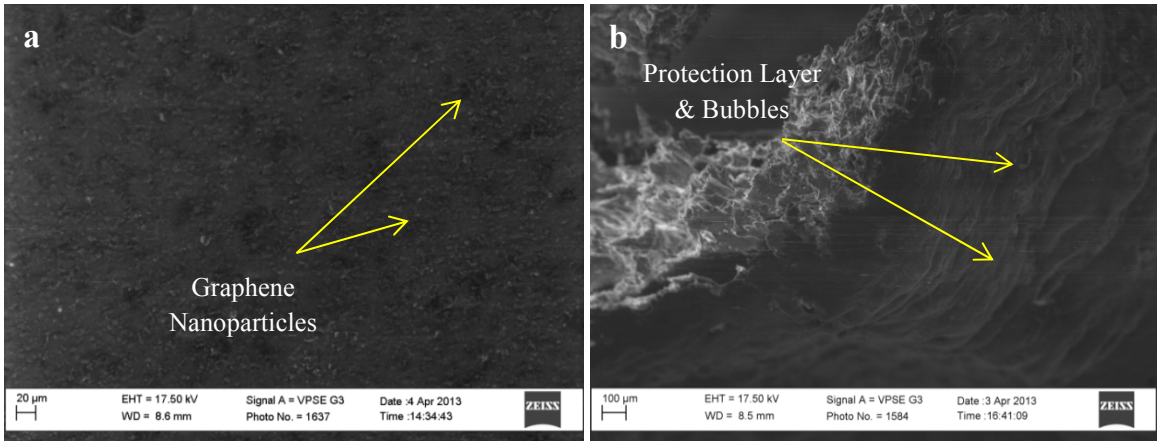

Figure 4.10. The SEM images of a) the unburned PVC+10 wt% graphene, and b) the burned PVC+10 wt% graphene nanocomposite specimen.

Figure 4.10.a and 4.10.b show the unburned and burned PVC with 10 wt% graphene inclusion. In the left figure the particles of graphene can be observed which is natural. Since the weight percentages of nanoinclusion increased the more nanoparticles on the surface will be observed. Based on the figure 10b, there is thick layer will appear on the surface due to presence of graphene.

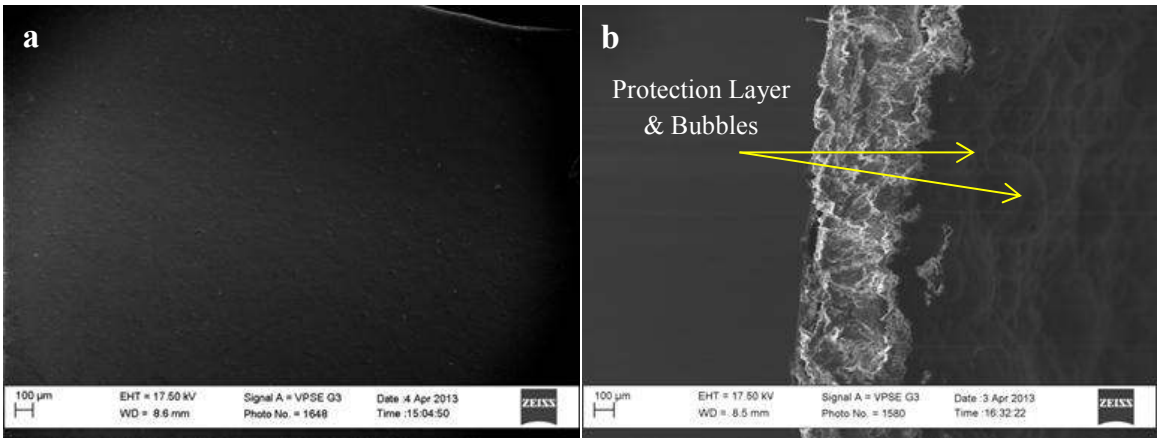

Figure 4.11. The SEM images of a) the unburned PVC+20 wt% graphene, and b) the burned PVC+20 wt% graphene nanocomposite specimen.

As is seen in Figure 4.11, the same morphological changes were observed on the burned nanocomposites, including bubbles and swelling formations. Figure 4.11.a shows a very smooth surface of PVC with 20wt% graphene prior to the heat source. The smooth surface illustrates how well the graphene was dispersed. Nevertheless, Figure 4.11.b shows the bubbles on the right

side of the image, indicating the presence of thick layer of graphene on the surface. In addition to being an inorganic substance, graphene also conducts the heat very fast and dissipate the energy. This will be the second major mechanism of saving PVC containing 20wt% graphene nanocomposites against the flame.

4.3 Thermogravimetric Analysis

Thermogravimetric analysis (TGA) is the standard weight loss test to examine any mass changes of the specimens as a function of temperature and time. In these nanocomposite samples, organic polymer and inorganic inclusions exist in the system, of which the first one burns out much earlier. In the present tests, the maximum temperature attained to 1000 °C and the temperature increase rate was 10 °C/min.

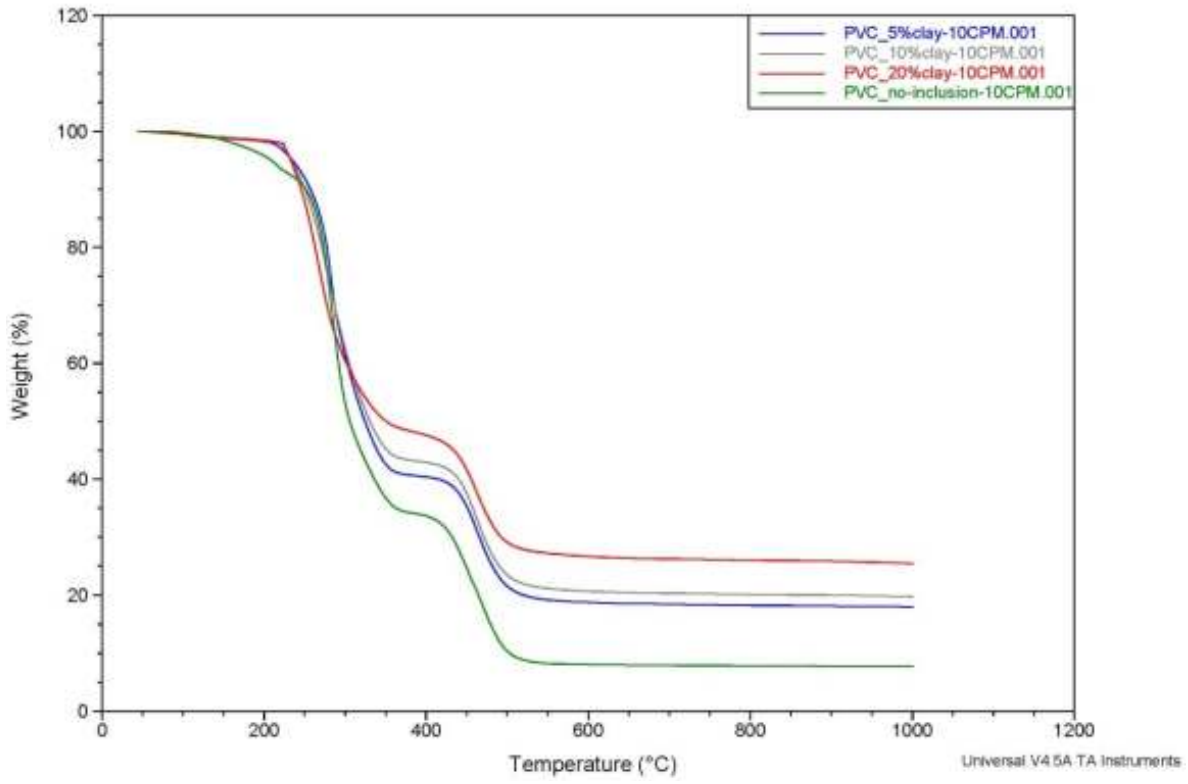

Figure 4.12. The TGA analysis of the pure PVC samples and PVC containing 5,10,20 wt% nanoclays.

The TGA curves of the neat PVC and PVC with different weight percentages of nanoinclusion are being traced in figures below. Figure 4.12 shows the weight loss versus temperature for different weight percentages of nanoclay in PVC.

According to Figure 4.13, very rapid weight loss was observed on PVC with no inclusion. PVC lost 92.25 % of the initial weight at temperature 337.51 °C while the combination of PVC with 5 wt% nanoclay lost 81.96 % weight at 340.89 °C.

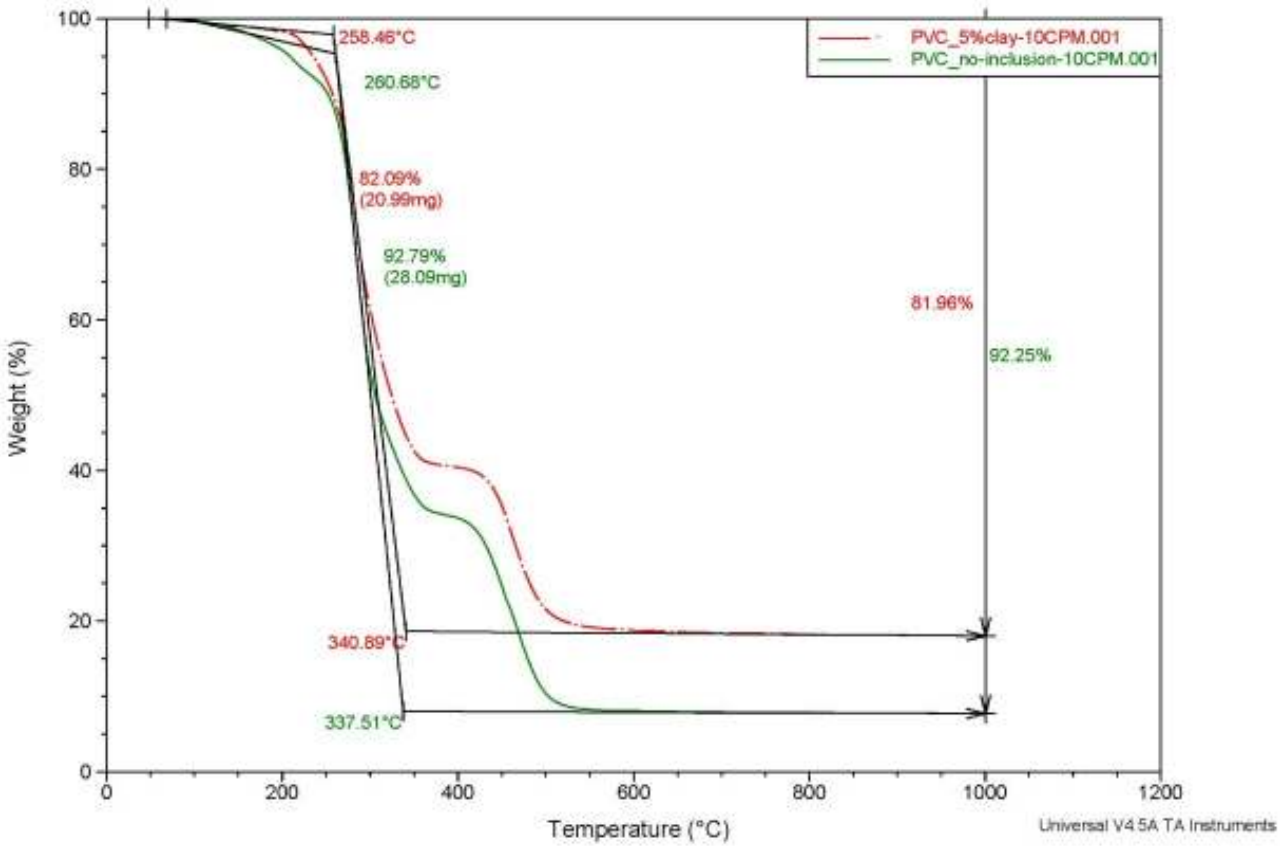

Figure 4.13. The TGA analysis of the pure PVC samples and PVC containing 5wt% nanoclays.

The same test was performed on PVC containg the 10 wt% nanoclay and higher thermal stability was observed compared to PVC with no inclusion (Figure 4.14). The PVC sample containing 10 wt% of nanoclay lost 80.24 % of the initial weight at the temperature of 364.87 °C while this number is 92.25% weight loss at the temperature 337.51 °C, which is the huge difference.

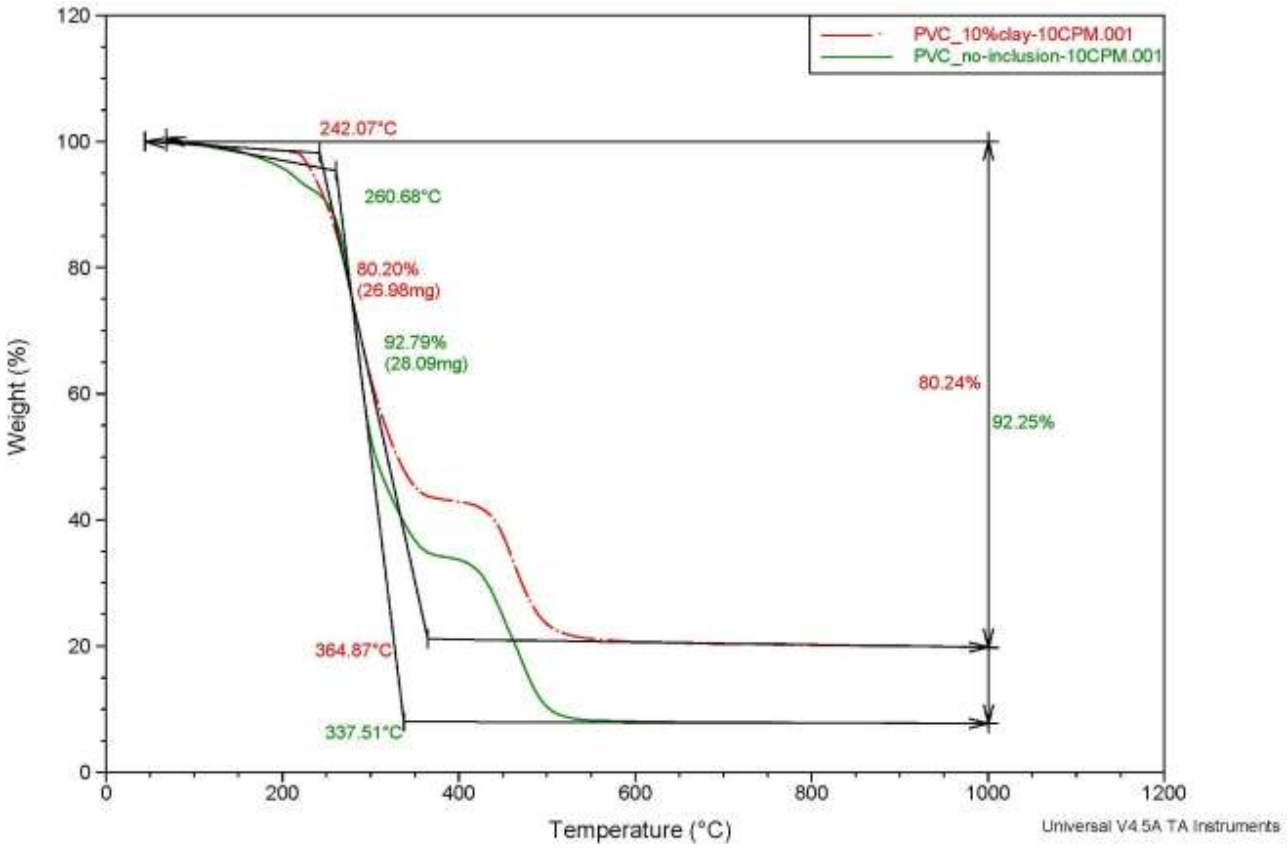

Figure 4.14. The TGA analysis of the pure PVC samples and PVC containing 10wt% nanoclays.

Figure 4.15 shows the PVC containing 20 wt% nanoclay, which shows the better thermal stability compared to 5 and 10 wt% clay. The weight loss at 338.38 °C is 74.38% of initial weight.

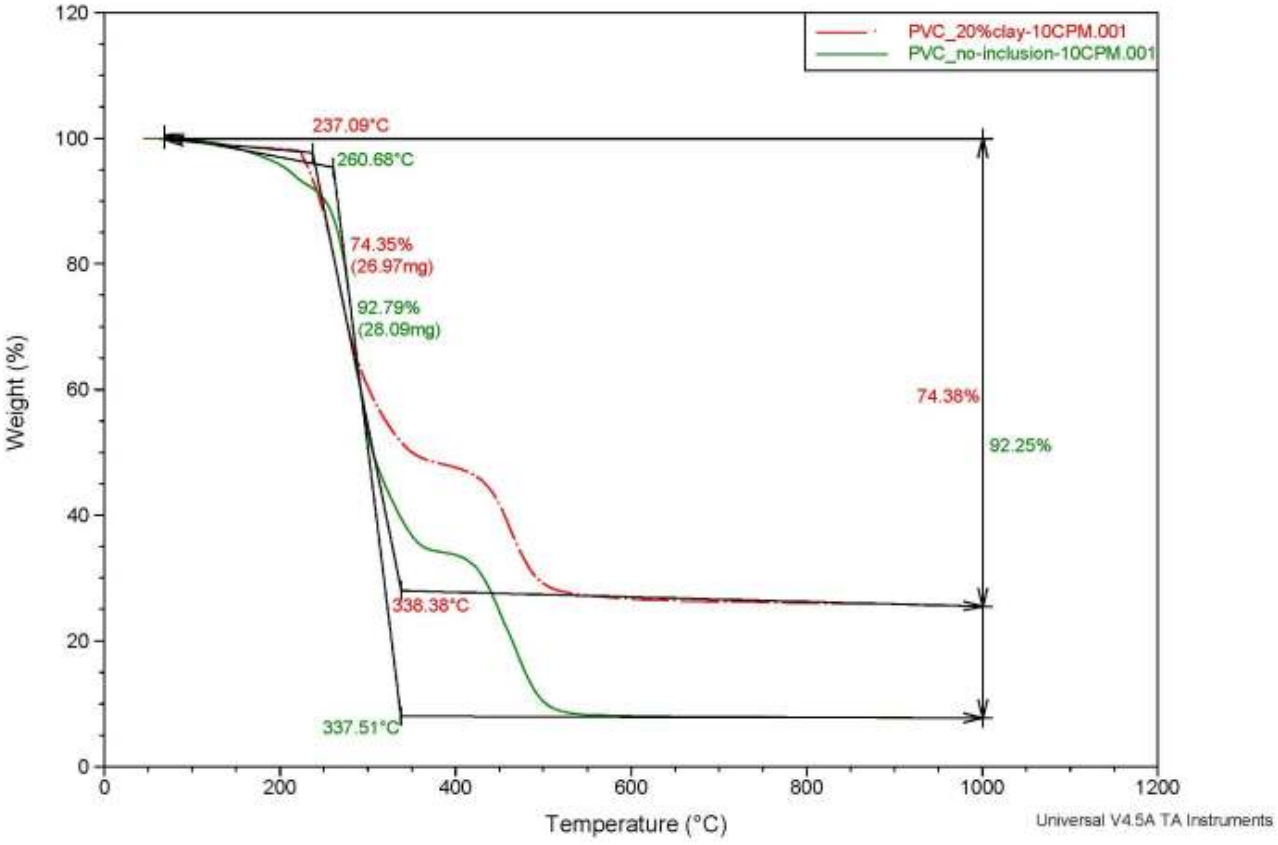

Figure 4.15. The TGA analysis of the pure PVC samples and PVC containing 10wt% nanoclays. As it was seen, the PVC with no inclusion show lower thermal stability.

The same TGA tests were also conducted on the PVC incorporated with 20wt% of nanotalc. Figure 4.16 illustrates the TGA results of the PVC with 0,5,10 and20 wt% nanotalc nanocomposite sample.

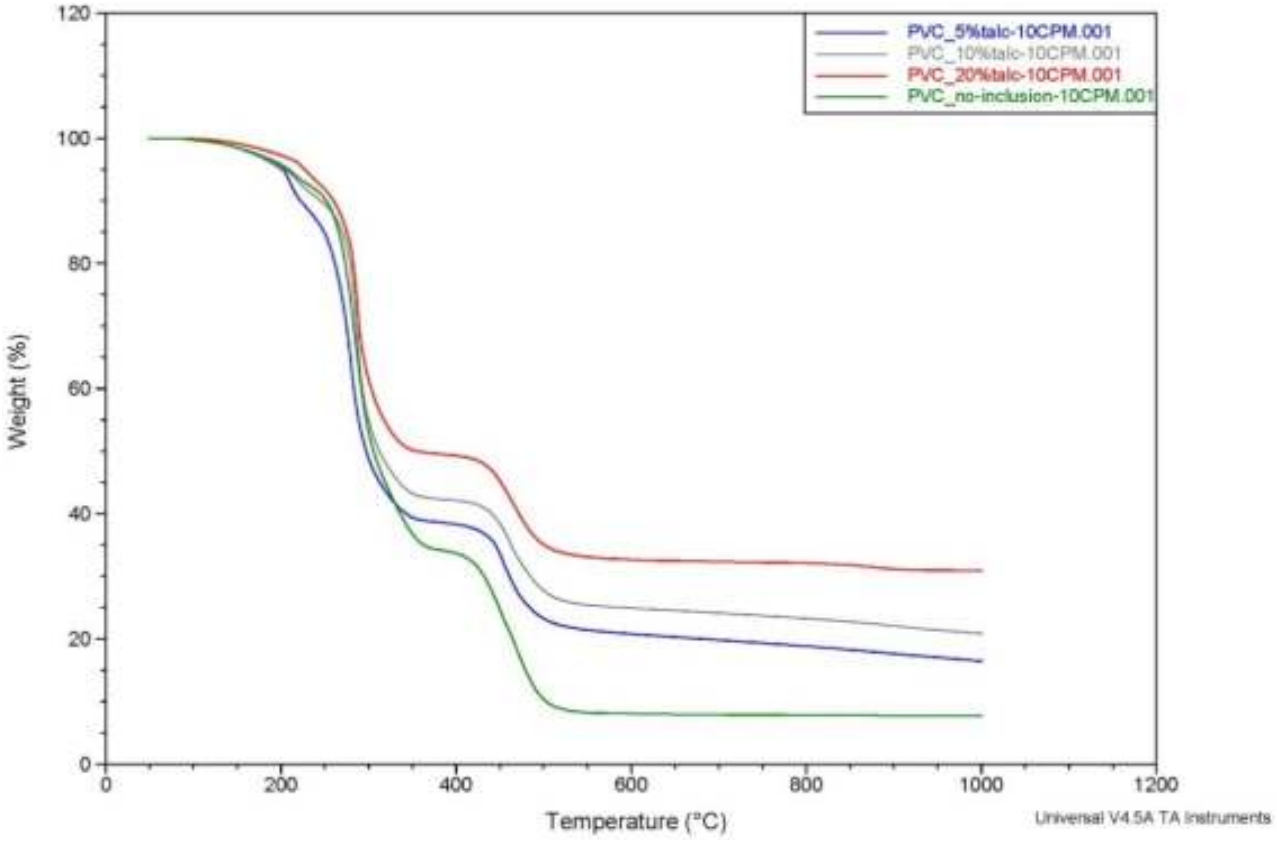

Figure 4.16. The TGA analysis of the pure PVC samples and PVC containing 5,10,20 wt% nanotalc.

As can be seen in Figure 4.17, the sample containing 5 wt% nanotalc lost the 83.54 % of its initial weight at a temperature of 314.25 °C compared to PVC with no inclusion.

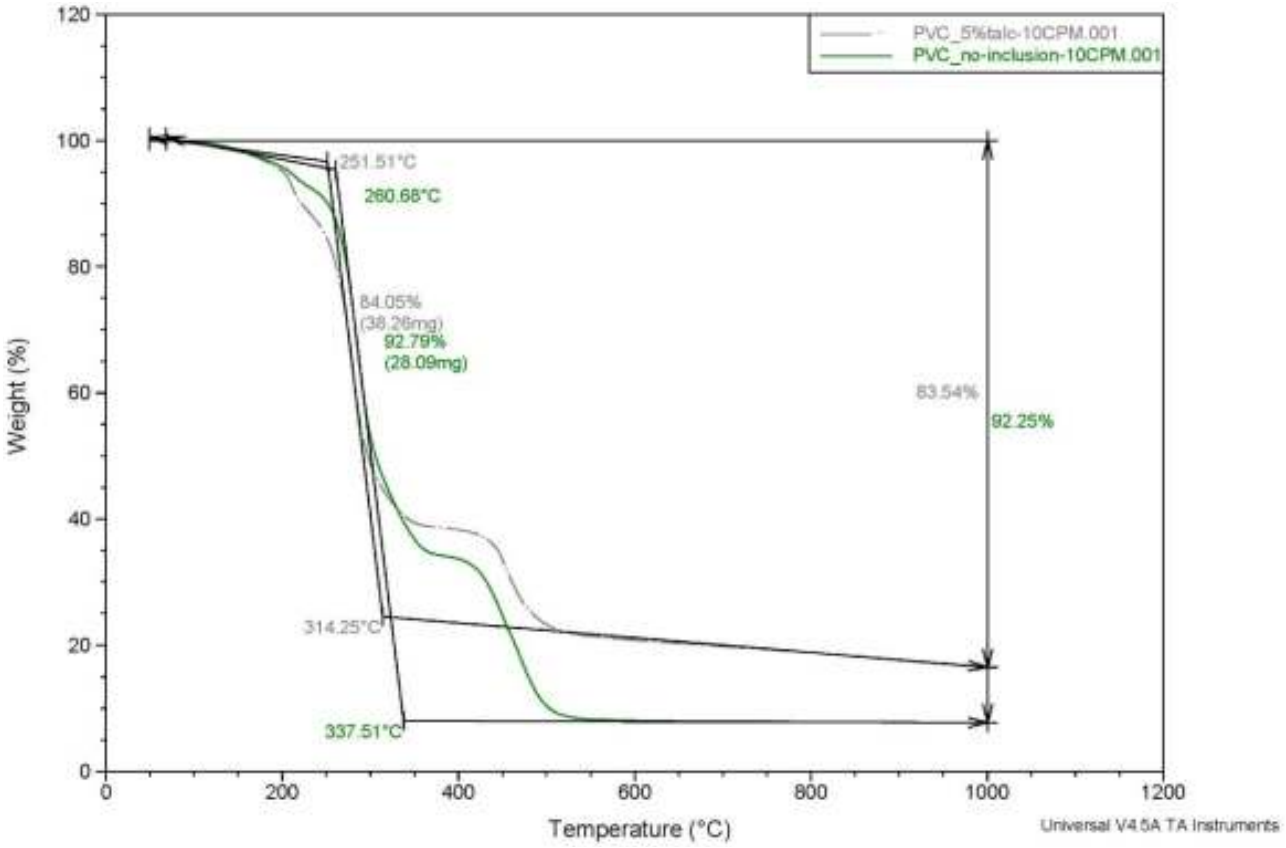

Figure 4.17. The TGA analysis of the pure PVC samples and PVC containing 5wt% nanotalc.

Figure 4.18 illustrates the TGA results of the PVC with 10 wt% nanotalc. It shows that the PVC containing 10 wt% lost 79.11 % of the initial weight at 310.40 °C while the PVC with 0% nanotalc lost 92.25 % of its initial weight.

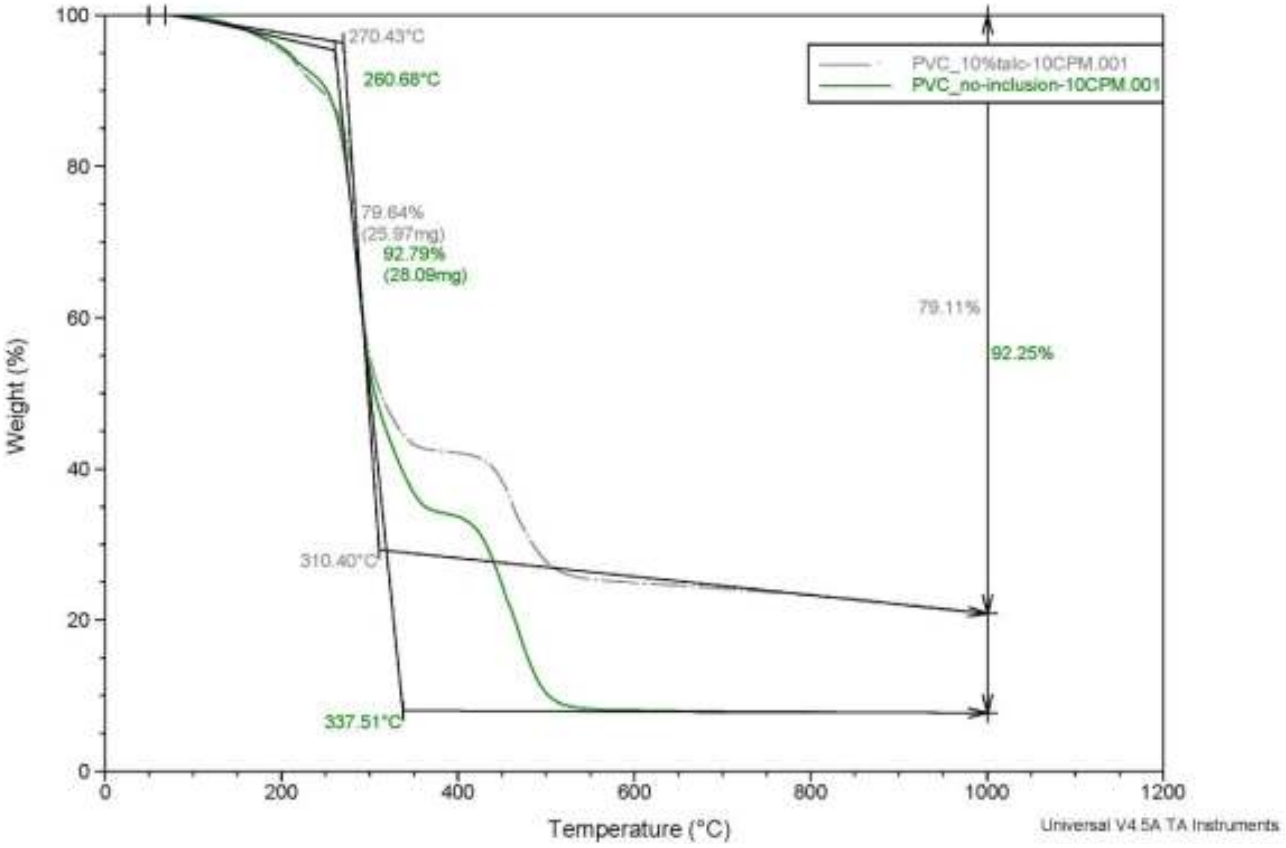

Figure 4.18. The TGA analysis of the pure PVC samples and PVC containing 10wt% nanotalc.

Figure 4.19, shows the TGA measurement of the PVC with 20 wt% nanotalc. According to figure 8, PVC containg 20 wt% nanotalc maintained more weight compared to pure PVC. It lost 69.13% of the initial weight at 314.47°C.

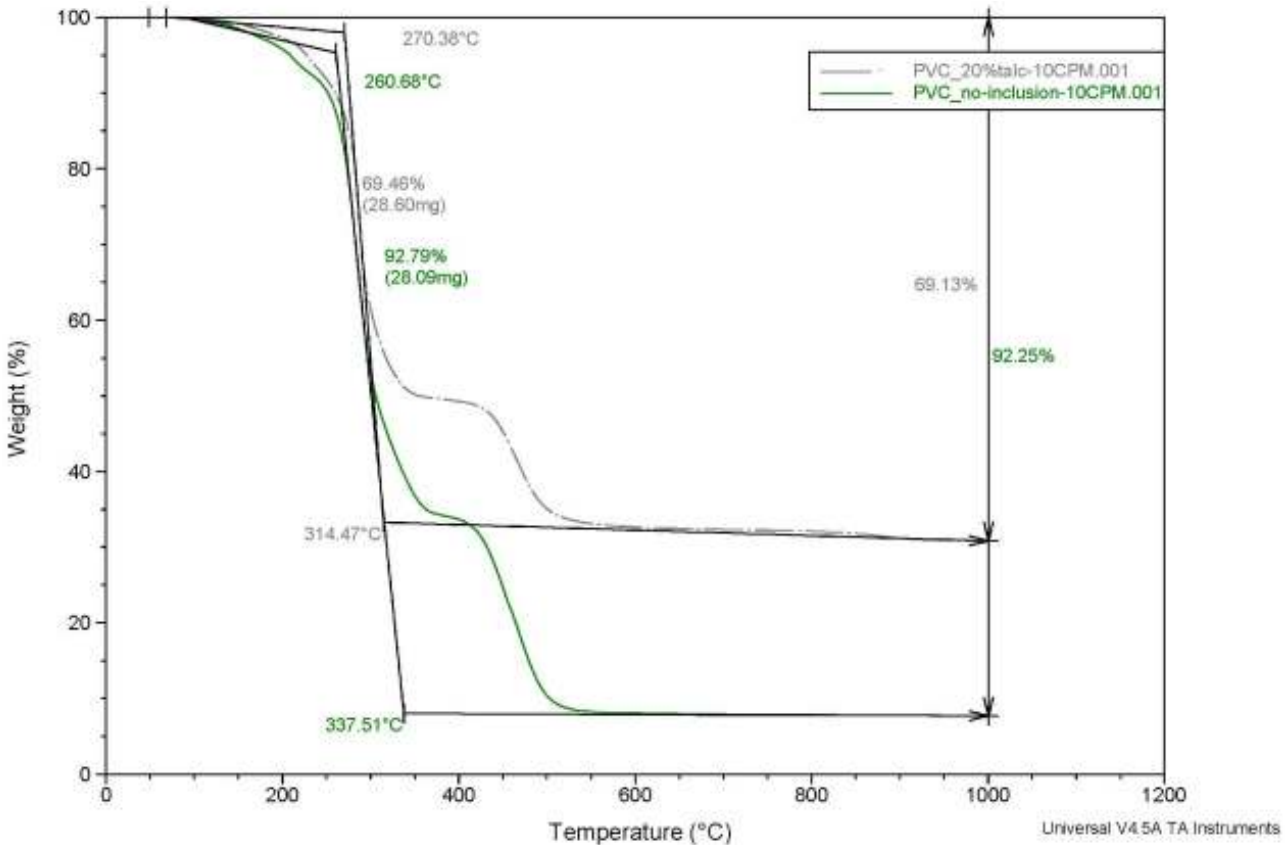

Figure 4.19. The TGA analysis of the pure PVC samples and PVC containing 20wt% nanotalc.

The same TGA tests were also conducted on the PVC incorporated with different weight percentages of graphene nanoflakes. Figure 4.20 illustrates the TGA results of the PVC with 5,10, 20wt% graphene nanocomposite sample. It shows that the combination of PVC with 20 wt% graphene nanoflake shows better thermal stability compared to 5 and 10 wt%.

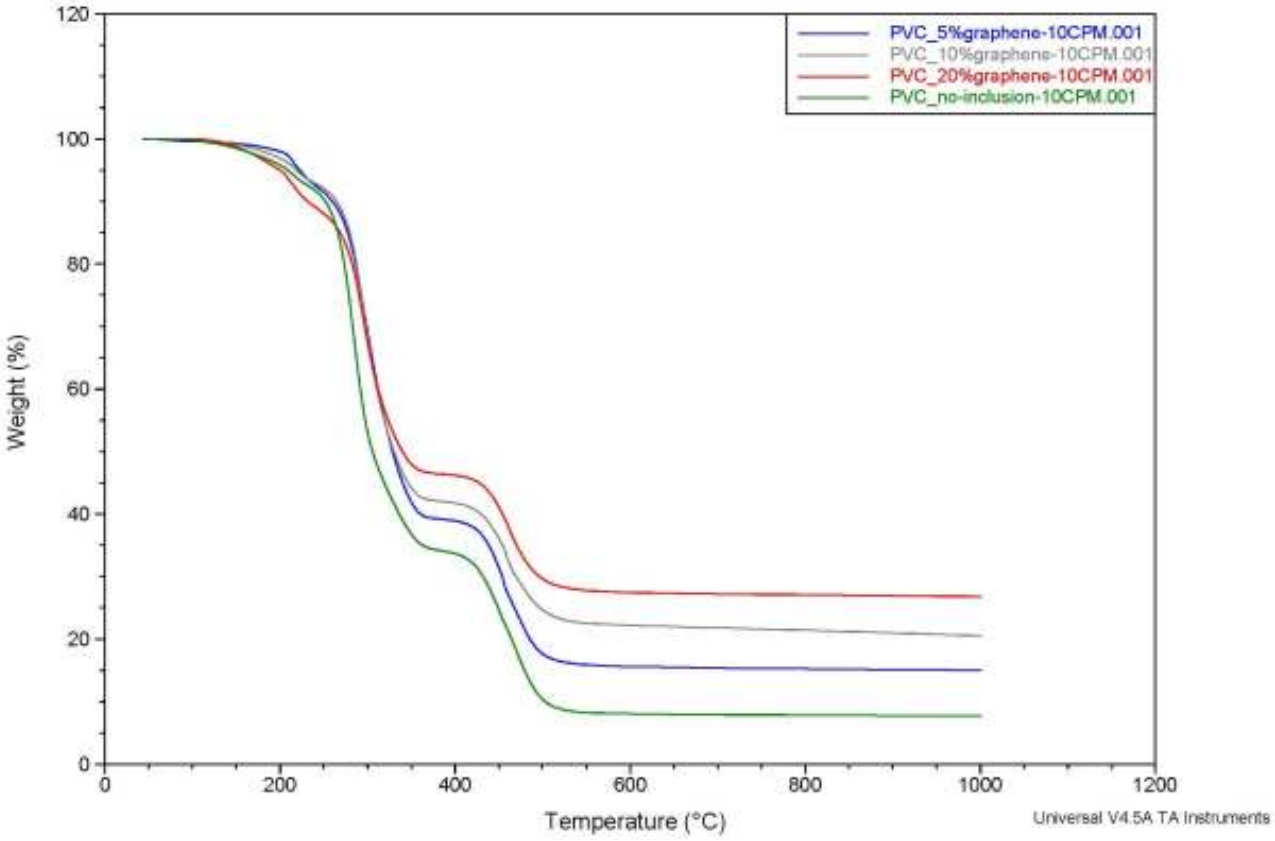

Figure 4.20. The TGA analysis of the pure PVC samples and PVC containing 5,10,20 wt% graphene nanoflake inclusions.

Figure 4.21 shows the TGA analysis of the PVC with 5 wt% of graphene inclusions. The TGA curve for the PVC-graphene sample shows that, this sample maintained more weight of the initial weight compared to PVC incorporated with no nanoinclusion. This sample lost 84.79% of the initial weight at a temperature of 366.75 °C.

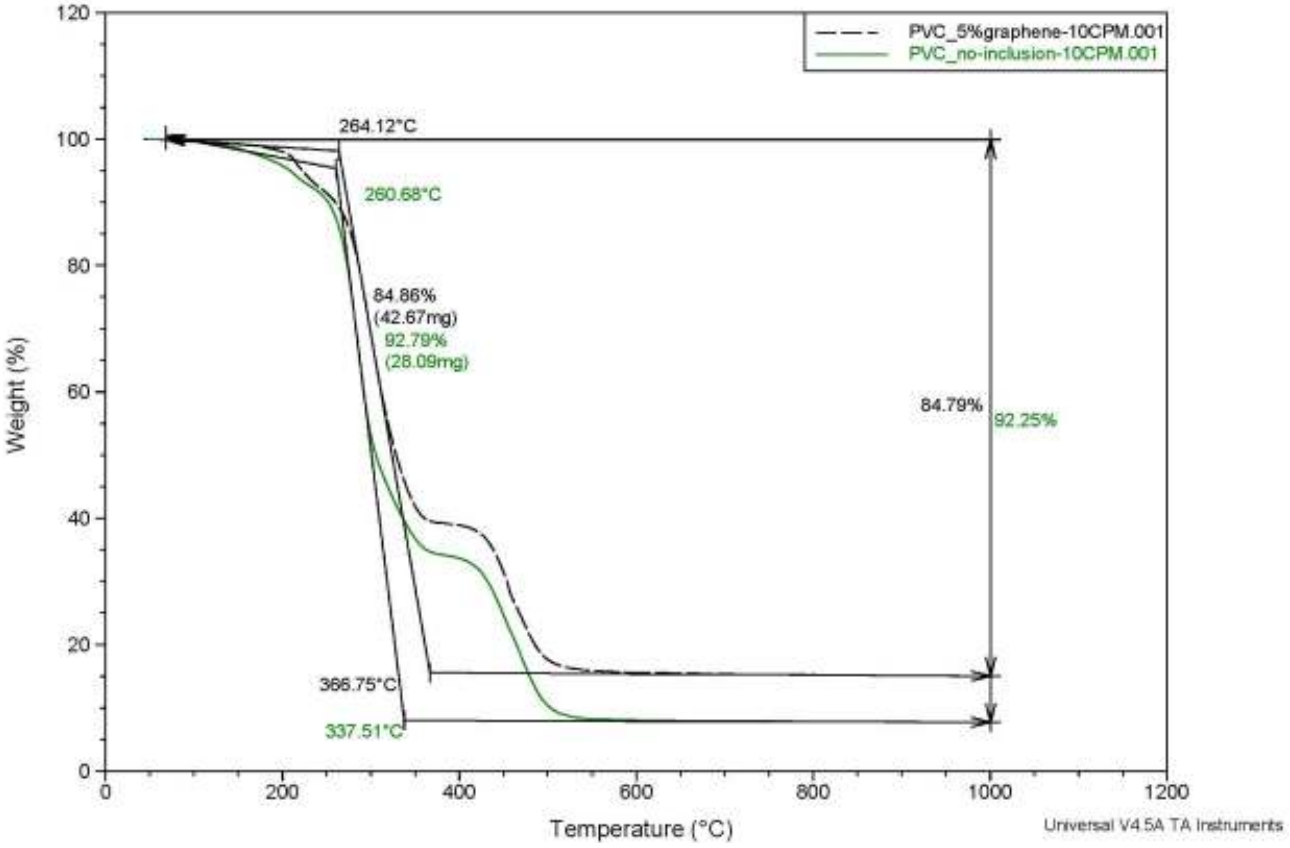

Figure 4.21. The TGA analysis of the pure PVC samples and PVC containing 5 wt% graphene nanoflake.

Figure 4.22 illustrates the TGA curve for the PVC containing 10 wt% graphene nanoflake, and based on this graph the PVC with graphene shows better thermal stability and more weight was retained compared to pure PVC. The weight loss of the PVC containing 10 wt% graphene was 79.46% of the initial weight.

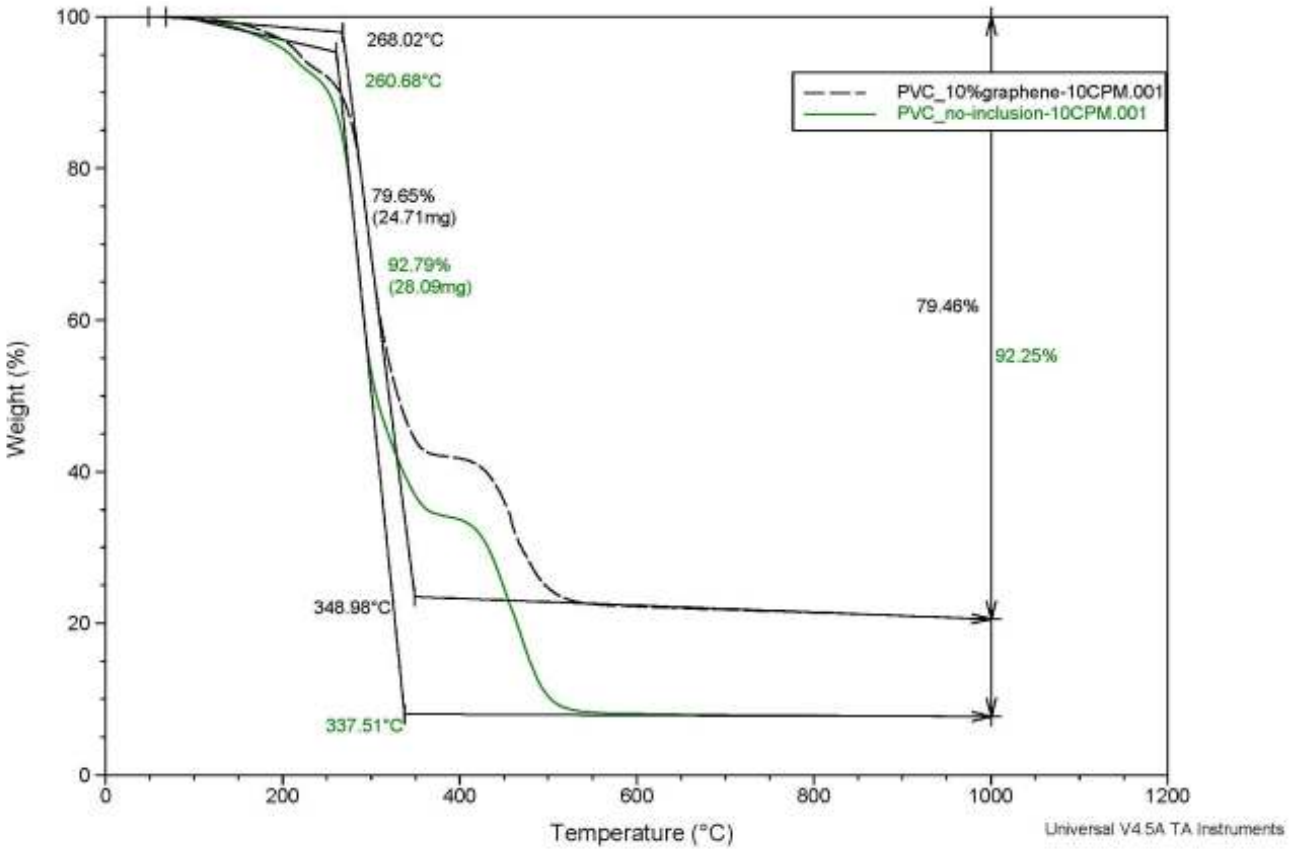

Figure 4.22. The TGA analysis of the pure PVC samples and PVC containing 10 wt% graphene nanoflake.

Figure 4.23 is the TGA analysis of PVC with 20% of graphene nanoflake. According to graph this sample shows higher thermal stability compared to 5 and 10 wt% of the same nanoinclusion. It lost 73.22 % of the initial weight at a temperature of 352.30 °C.

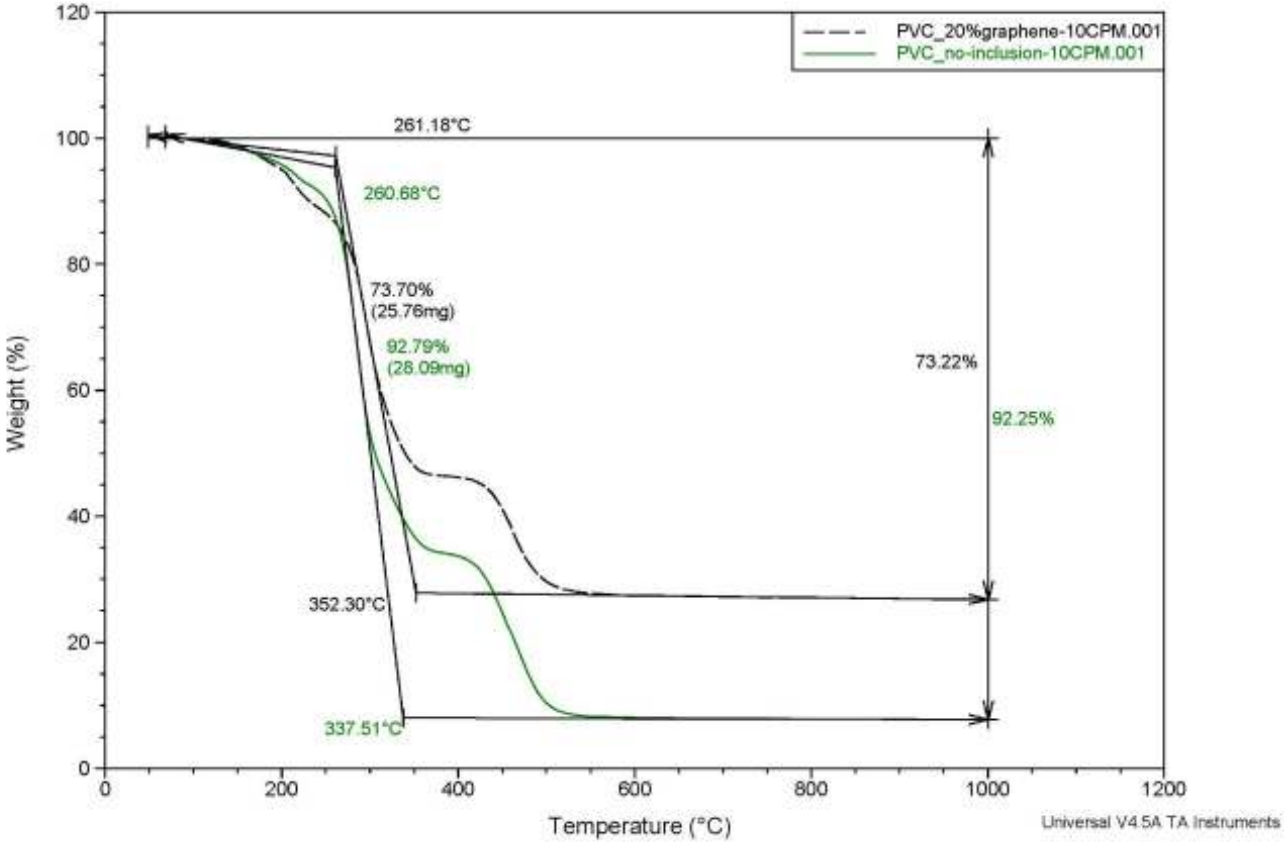

Figure 4.23. The TGA analysis of the pure PVC samples and PVC containing 20 wt% graphene nanoflake.

Evidently, the thermal decomposition of those PVC incorporated with nanoinclusion materials shift slightly up to the higher temperature range than the pure PVC and it confirms the enhancement of thermal stability of pure PVC when it incorporated with nanoinclusions.

4.4 Differential Scanning Calorimetry

The data obtained from DSC instrument, which operates in a heat flow mode. A heating scan is carried from 20 °C to 250 °C at the heating rate of 10 °C/min. It is held at 250 °C to 30 °C at a cooling rate of 10°C/min.

Figure 4.24, illustrates the DSC measurement of pure PVC and PVC incorporated with 20 wt% clay. According to this graph, pure PVC absorbed more energy compared to incorporated with nanoinclusion and the release rate of the energy in the sample with nanoclay was slightly faster compared to pure PVC. It represents the heat penetration in sample containing nanoclay was lower than pure PVC and it caused more heat resistance which showed an increase in heat flow rate.

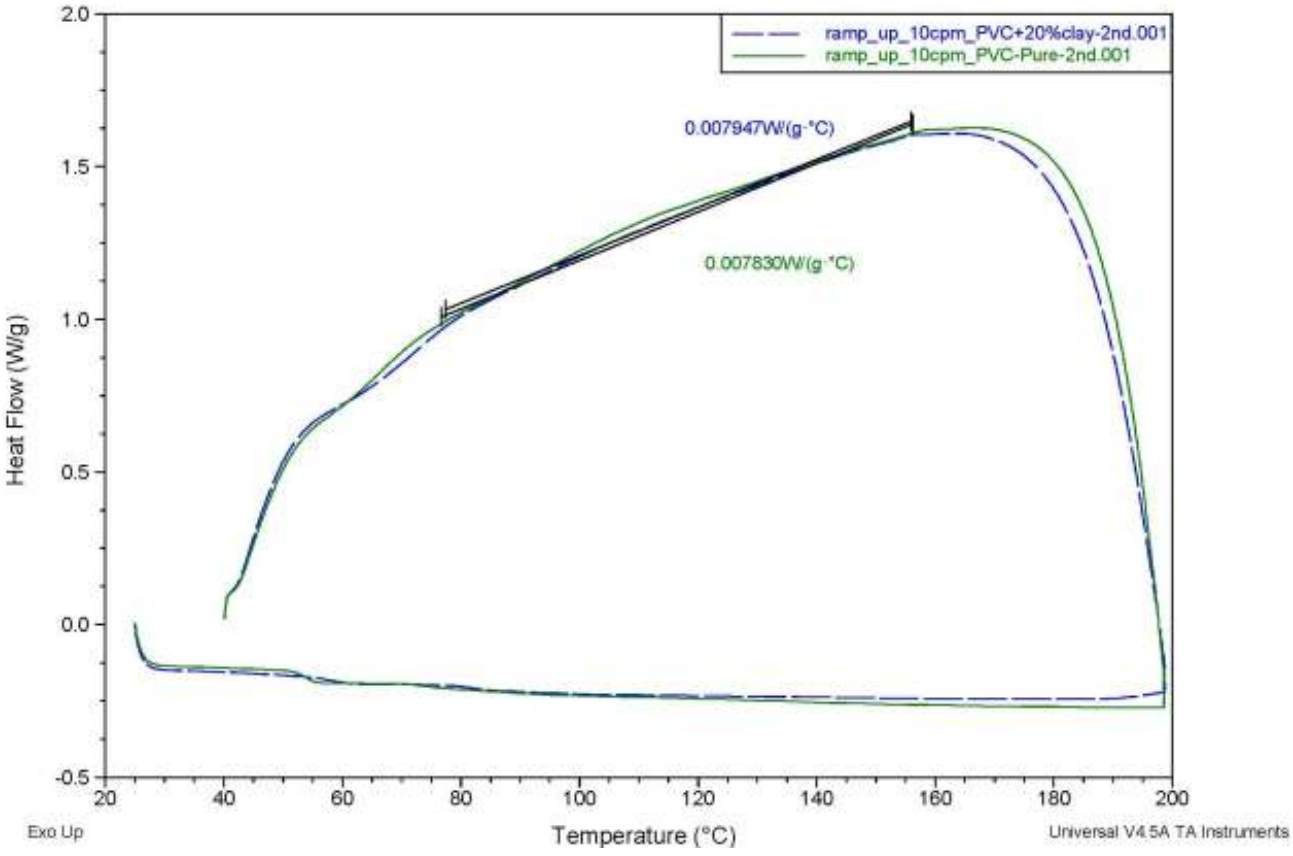

Figure 4.24. The DSC analysis of the pure PVC samples and PVC containing 20 wt% nanoclay.

Figure 4.25 shows the DSC analysis on PVC and PVC with 20 wt% nanotalc. Based on heating scan the sample containing 20 wt% talc absorbed more energy compared to PVC but the energy release rate is quicker compared to pure PVC which helps nanotalc sample to show better resistance.

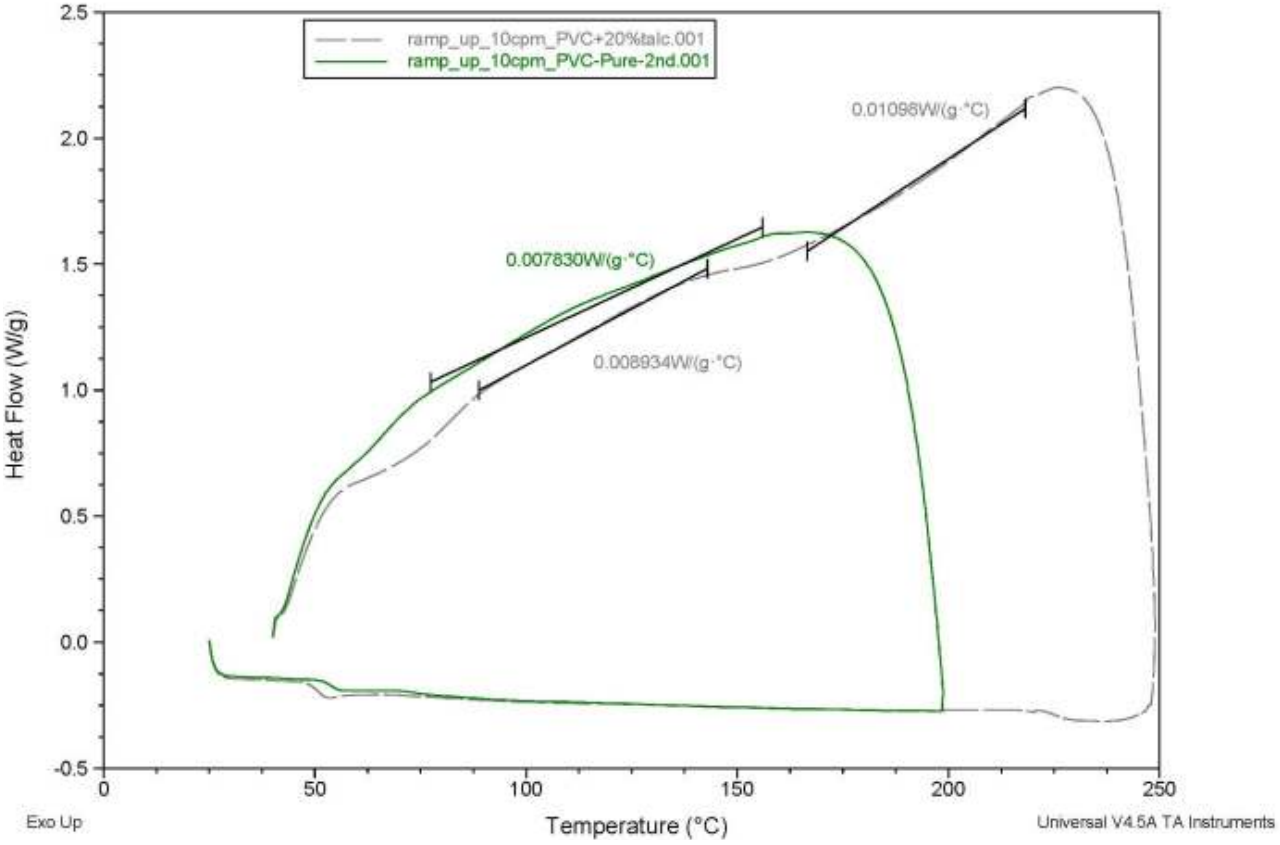

Figure 4.25. The DSC analysis of the pure PVC samples and PVC containing 20 wt% nanotalc.

Figure 4.26 illustrates the DSC results for PVC and PVC with 20 wt% of graphene. According to heating scan, graphene absorbed less energy compared to PVC but the energy release rate for both samples are very close. More information about the DSC is provided in the APPENDIX of this thesis.

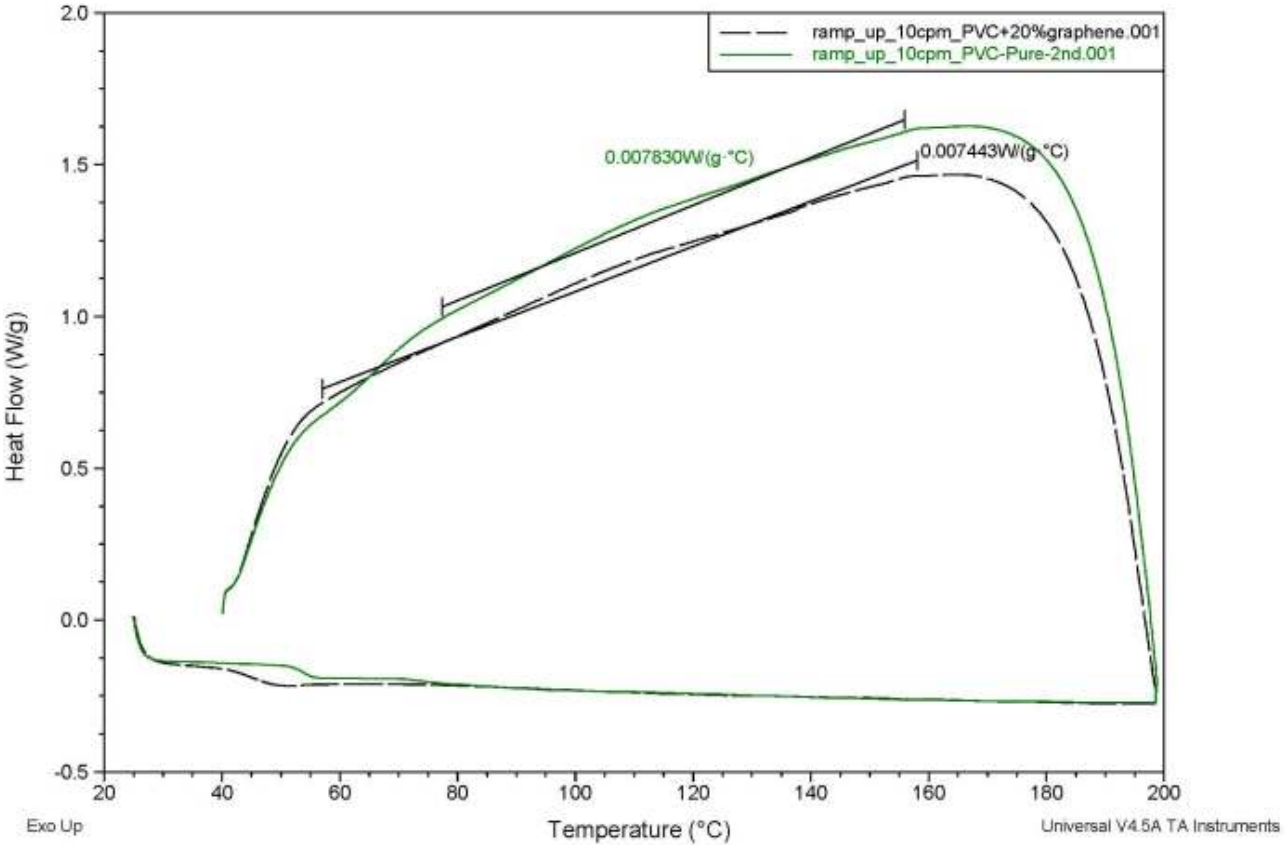

Figure 4.26. The DSC analysis of the pure PVC samples and PVC containing 20 wt% graphene nanoflake.

4.5 Mechanical Properties

The tensile test was conducted on the samples which was prepared for the UL 94 by the micro tensile test machine. All the samples followed the same dimensions as required for the UL 94 ASTM, to measure the mechanical properties of the specimens. The tensile test was conducted on all the PVC and PVC with 20 wt% nanoinclusion samples and mechanical properties was measured. The below figures are the mechanical properties of PVC with 20 wt% of all nanoinclusions which showed the best thermal stability and flame retardancy. Figure 4.27 shows the stress-strain curve for the PVC with no nanoinclusion.

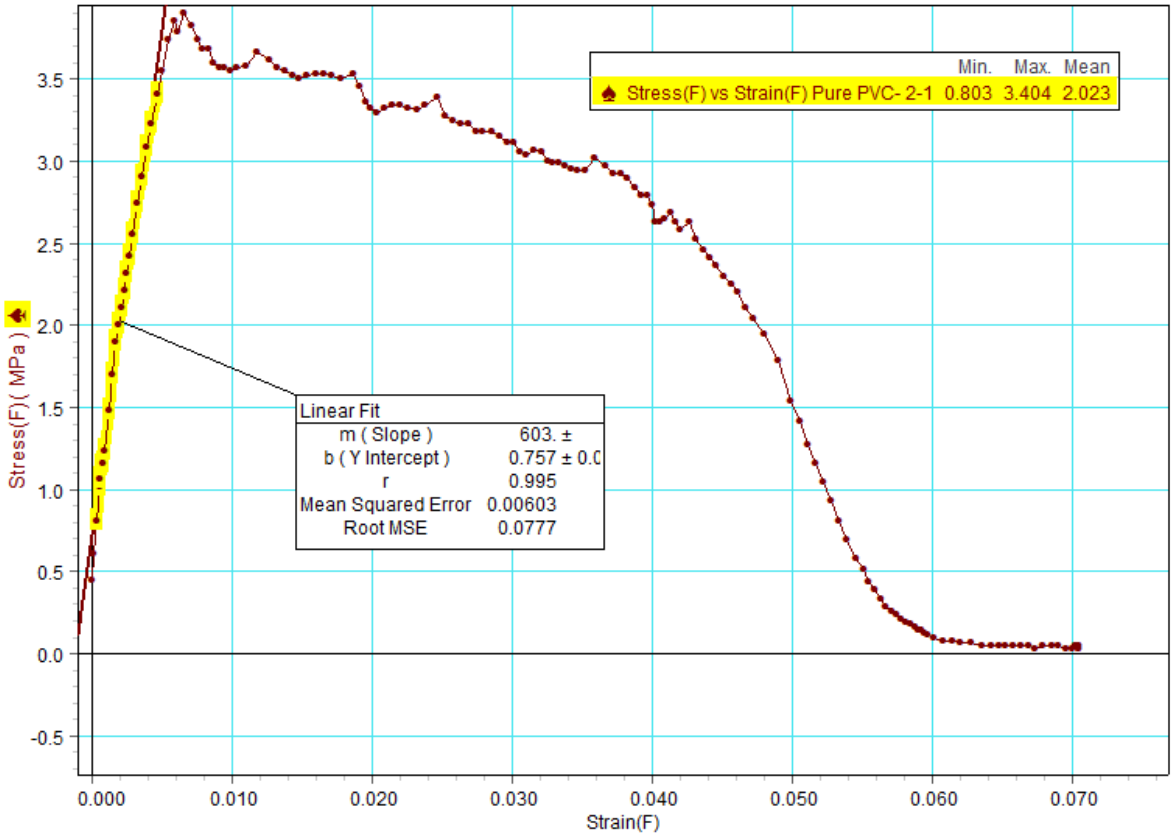

Figure 4.27. The Stress-strain curve for the pure PVC.

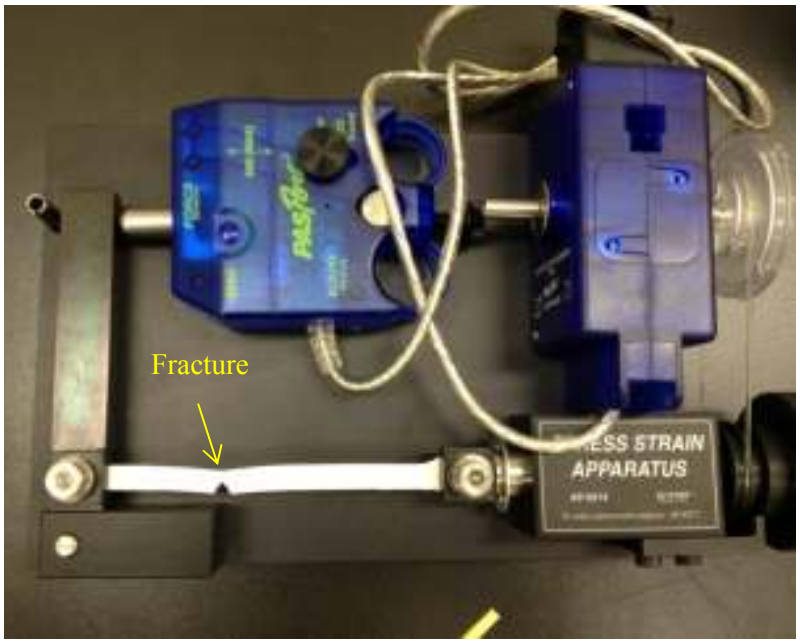

Figure 4.28. Tensile test of PVC.

According to Figure 4.27, the Young's modulus is 603 MPa in elastic limit. The Ultimate tensile strength (σ_U) is about 4 MPa and Yield strength (σ_Y) is about 3.85 Mpa and Fracture stress is about 2.5 MPa. Figure 4.28 shows the PVC in the absence of nanoinclusion under the tensile test.

Figure 4.29 illustrates the stress strain curve for the PVC with 20 wt% nanoclay. More ductility was observed in this sample. The Young's modulus is 538 MPa and the ultimate tensile strength (σ_U) is about 4.7 MPa and Yield strength (σ_Y) is about 4 MPa and fracture strength is 4.2 MPa.

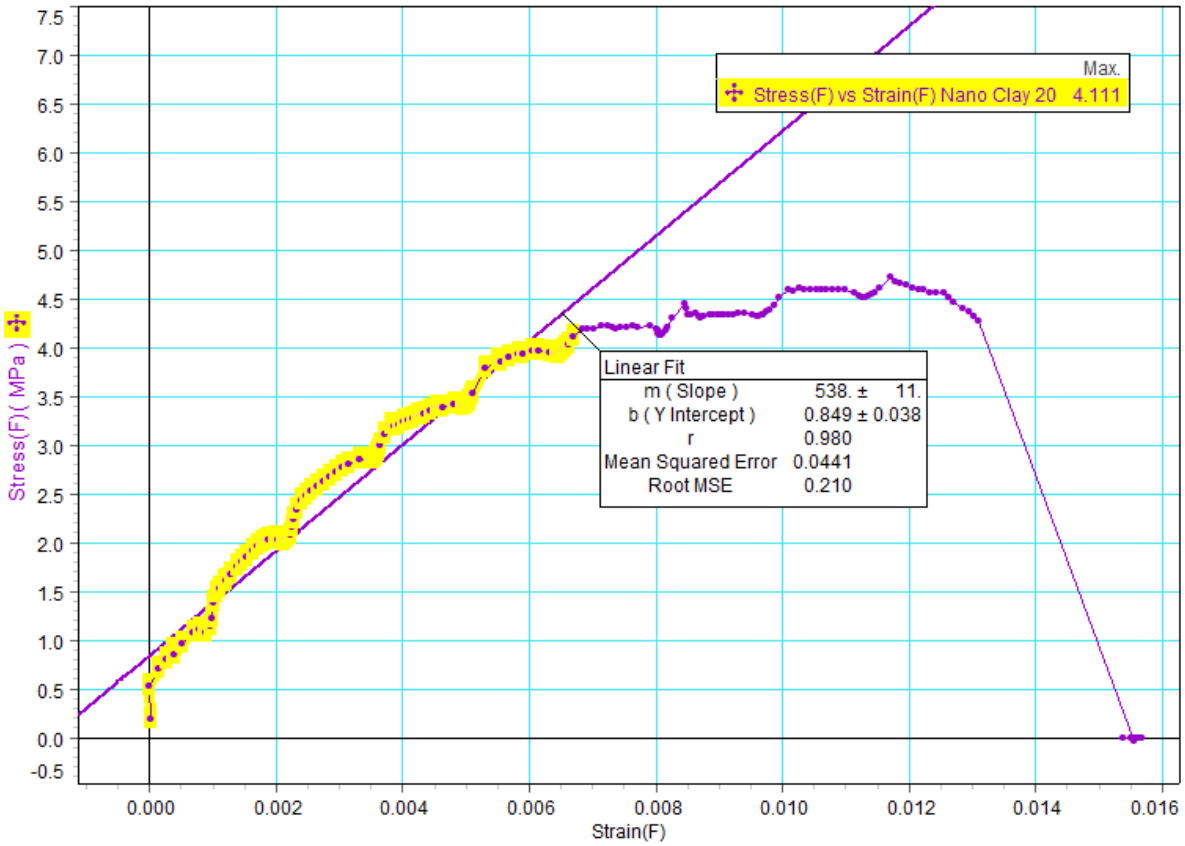

Figure 4.29. The Stress-strain curve for the PVC with 20 wt% nanoclay.

Figure 4.30 shows the mechanical properties of PVC with 20 wt% nanotalc. According to this graph more brittleness was observed compared to pure PVC. The Young's modulus is 918 MPa and the ultimate strength (σ_U) is about 5.4 MPa and Yield strength (σ_Y) is about 5.1 MPa and fracture strength is 5.3 MPa. Figure 4.31 shows the nanotalc under the tensile test.

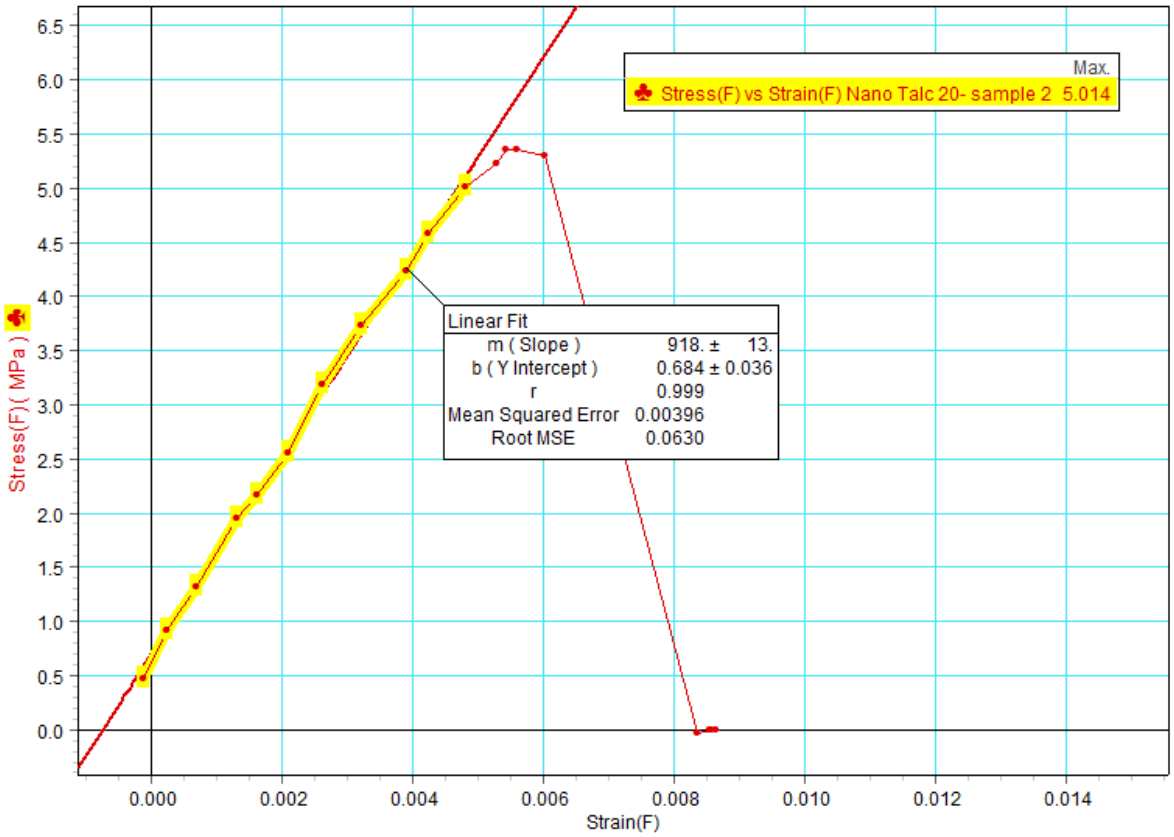

Figure 4.30. The Stress-strain curve for the PVC with 20 wt% nanotalc.

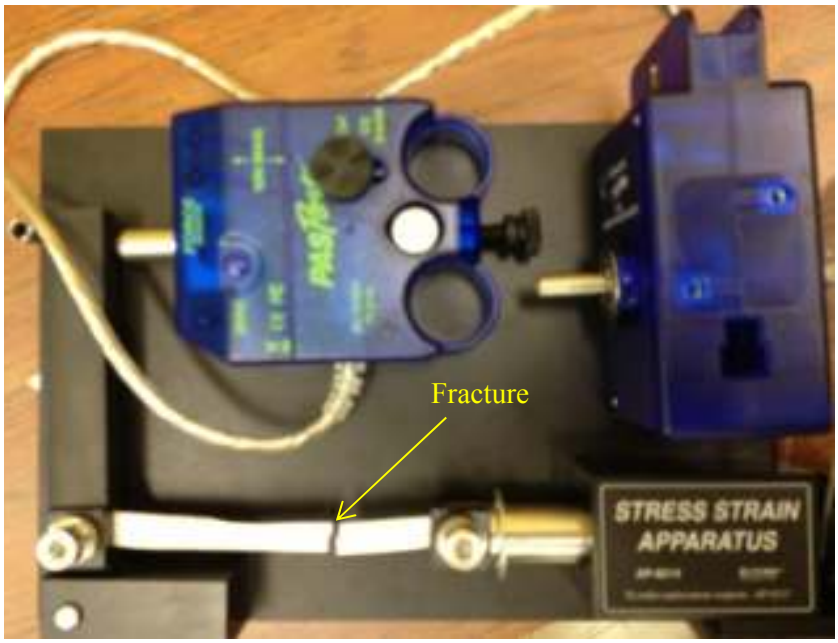

Figure 4.31 Tensile test of PVC incorporated with 20 wt% nanotalc.

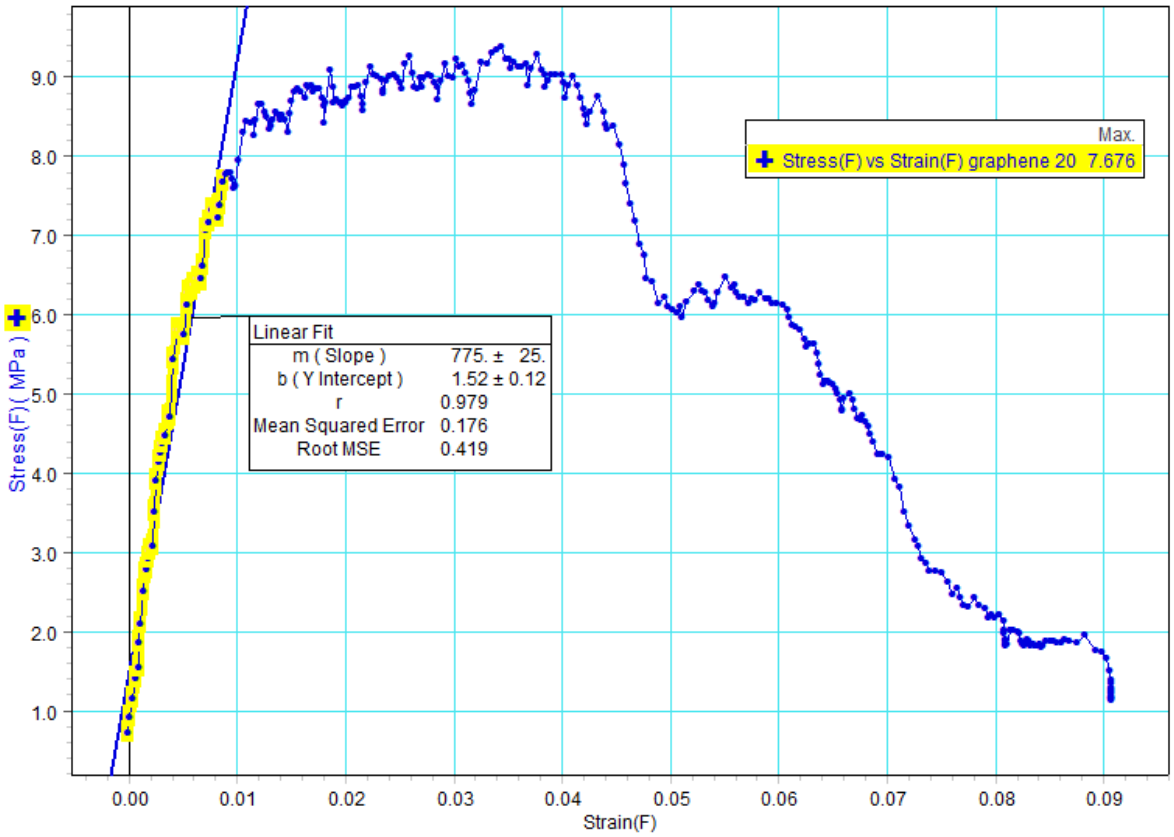

Figure 4.32. The Stress-strain curve for the PVC with 20 wt% graphene.

Figure 4.33. Tensile Test of PVC incorporated with 20 wt% graphene.

Figure 4.32 shows the mechanical properties of PVC incorporated with 20 wt% graphene. The Young modulus is 775 MPa and the yield strength (σ_Y) is 7.8 MPa and the ultimate stress strength (σ_U) is 9.3 MPa and Fracture strength is 8.5 MPa. Figure 4.33 shows the PVC with 20 wt% graphene under the tensile test. More information about the tensile tests is provided in the APPENDIX of this thesis.

4.6 Literature Studies

L. Madaleno et al. discussed the effect of clays in PVC. In this test, the two types of nanoclays, Na-MMT and OMMT, were dispersed in PVC and the following results were observed. 1, 2, 5, 10 and 25 phr of each nanoclays were dispersed in PVC. The pure tetrahydrofuran was used as a solvent. According to TGA results, all the samples containing nanoclay were more stable compared to unfilled PVC. Based on this analysis, the samples with OMMT and Na-MMt have a higher thermal stability compared to neat PVC and the enhancement of residues at very high temperatures support these results (Figure 4.34.a, Figure 4.34.b) [68].

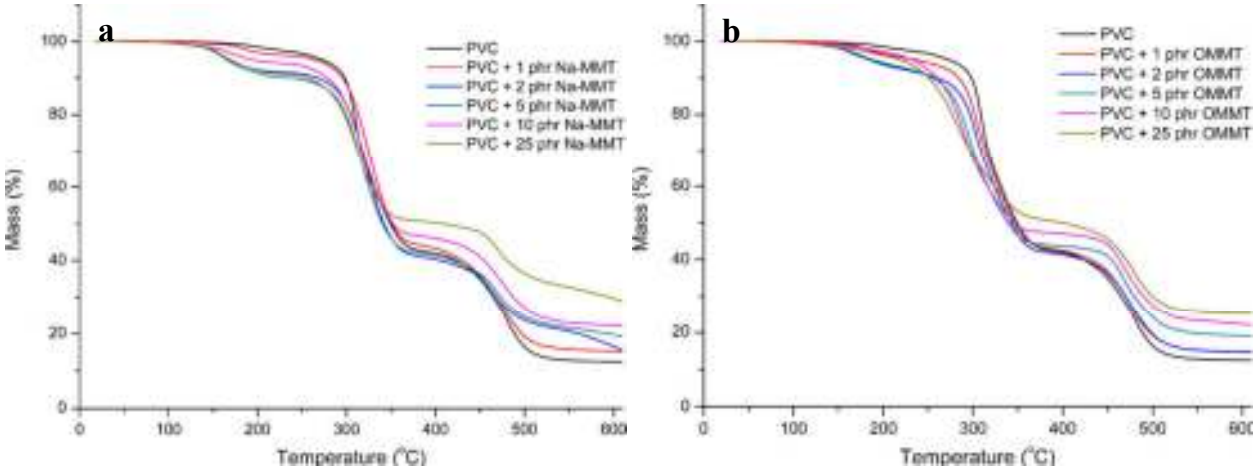

Figure 4.34. The TGA analysis of the a) PVC and PVC/Na-MMT, and b) PVC and PVC/OMMT nanocomposites [68].

In terms of tensile strength, 2 phr of PVC/Na-MMT achieved the highest value among all the samples. For the 2 phr of clay, the tensile strength was 26% higher compared to neat PVC. All the samples strengths increased with the addition of Na-MMT compared to pure PVC. The sample with 1 phr of OMMT achieved highest tensile strength among the all samples of PVC/OMMT, which was very close to neat PVC. All the PVC sample incorporated with OMMT showed a decrease of tensile strength compared to pure PVC, specifically after 5 phr of OMMT. In this study, it was explained that the tensile strength improvement could be the effect of the good interaction between the clays and PVC matrix. Also, a decrease in tensile strength is caused by clays agglomeration during the solution preparation [68].

There have been several SEM studies on the combination of PVC and clays. Many agglomerations were observed under the SEM (Figure 4.35). This is the results of poorly dispersed nanoclays during solution preparation [68].

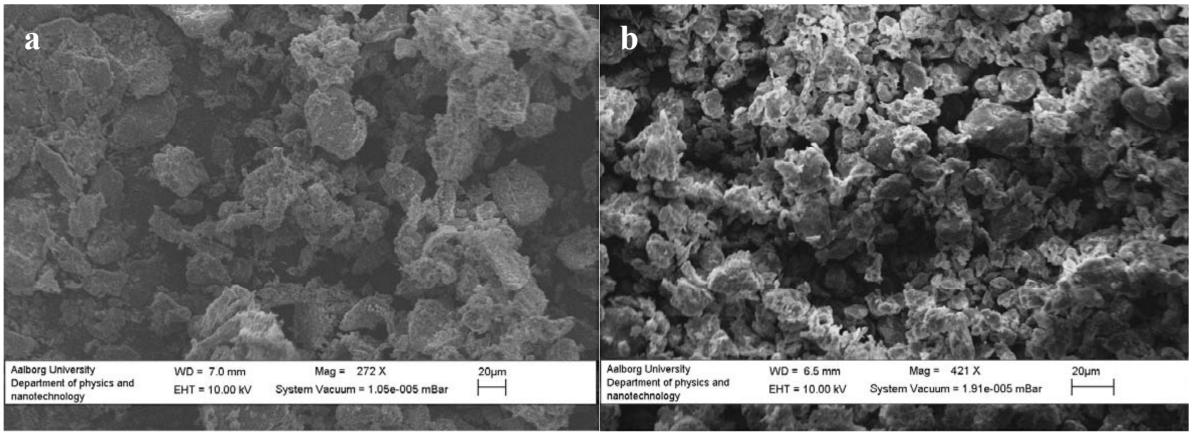

Figure 4.35. The SEM images a) PVC+Sodium montmorillonite b)PVC+ Organically modified montmorillonite [68].

In the other studies, phosphorylated multiwalled carbon nanotube (p-MWCNT) and multiwalled carbon nanotube (MWCNT) were dispersed into the PVC and the toluene was used as solvent. Based on SEM images, MWCNT and p-MWCNT were dispersed homogeneously in

the PVC matrix without agglomeration. Figure 4.36 displays the SEM studies on PVC samples incorporated with MWCNT and p-MWCNT. [69].

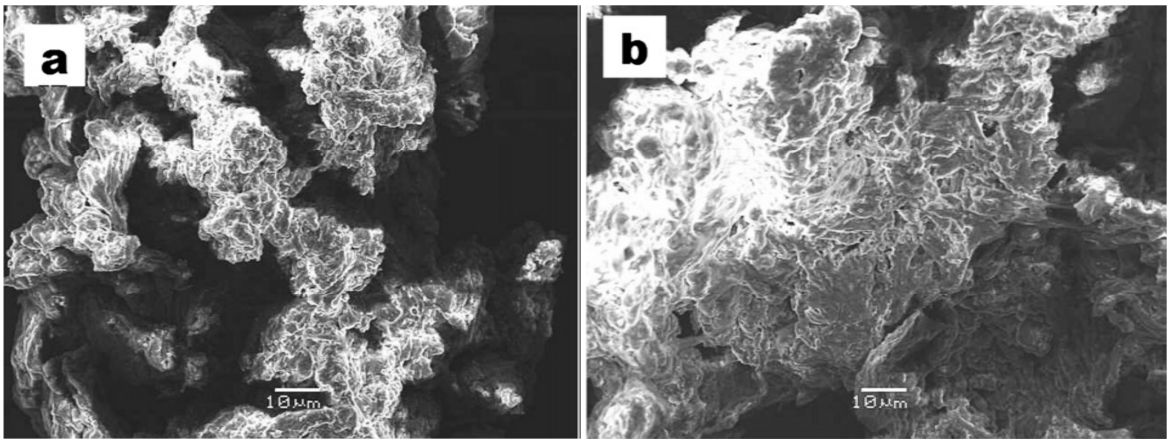

Figure 4.36. The SEM images of (a) PVC+MWCNT, (b) PVC+ p-MWCNT composites [69].

In this study the TGA analysis was done on the all samples and following results were obtained.

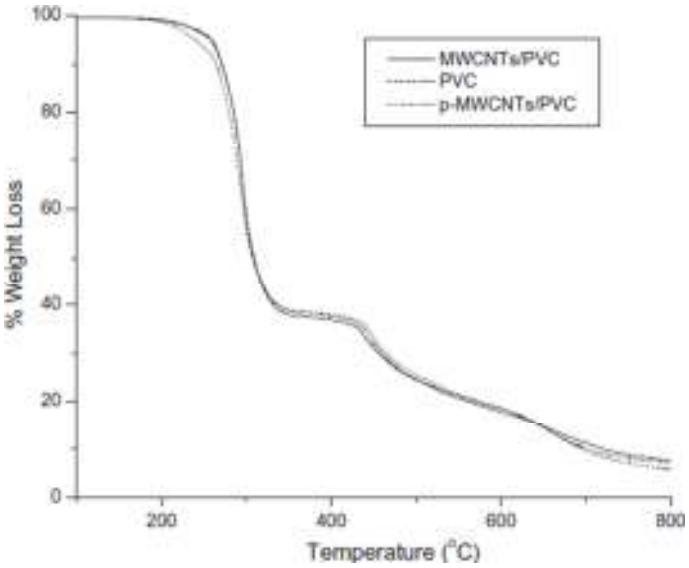

Figure 4.37. The TGA analysis of the PVC, MWCNT/PVC and p-MWCNT/PVC composites [69].

According to TGA analysis, it was observed that the PVC lost 60% of the initial weight at a temperature between 230-340 °C. The same wt% loss for PVC containing nanoscale

inclusion falls between 260-340 °C. This means the samples that were incorporated with carbon nanotubes displayed better heat resistance compared to unfilled PVC (Figure 4.37) [69].

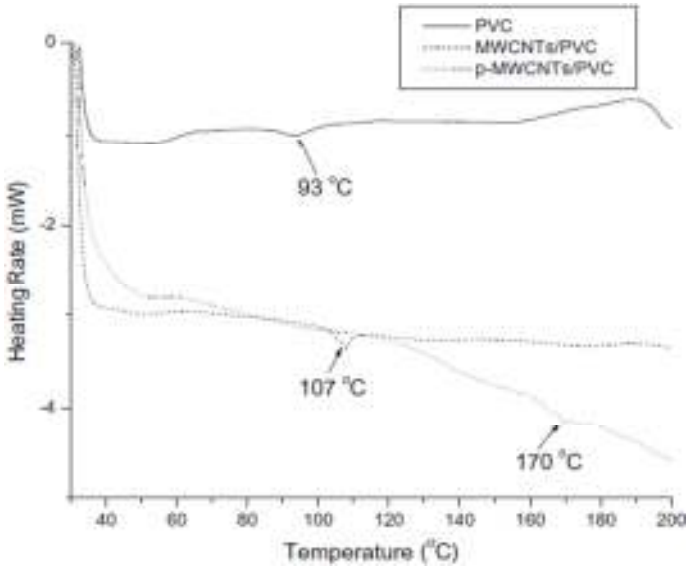

Figure 4.38. The DSC analysis of PVC, MWCNT/PVC and p-MWCNT/PVC composites [69].

The data from DSC analysis shows that the introduction of p-MWCNT within the PVC matrix displayed a higher onset temperature and glass transition temperature compared to neat PVC and MWCNT/ PVC [69].

According to the tensile strength test, there was an increase in the modulus of the PVC/MWCNT and PVC/p-MWCNT composites compared to the pure PVC. It was illustrated that this increase is the effect of covalent bonding at the interface of PVC and carbon nanotubes. PVC displayed a ultimate tensile strength (UTS) of 34.08 MPa while the UTS for MWCNT/PVC and p-MWCNT/PVC was about 32.49 MPa and 31.44 MPa respectively. This decrease is the result of an increase in modulus of elasticity. The modulus for PVC is 742.27 MPa while the modulus for MWCNT/PVC and p-MWCNT/PVC are 812.48 and 821.79 respectively. This number shows that by adding more nanotubes, the new composition becomes more brittle. This is the reason that they show less tensile strength compared to pure PVC [69].

Based on another study, single and multi-walled carbon nanotubes were dispersed in the PVC matrix. Tetrahydrofuran was used as solvent. According to SEM studies, depending on the nanocomposite composition the amount of agglomeration will change. As it is observed in the pictures below, the amount of agglomeration is increased by increasing the percentages of the nanotubes (Figure 4.39.a, Figure 4.39.b) [70].

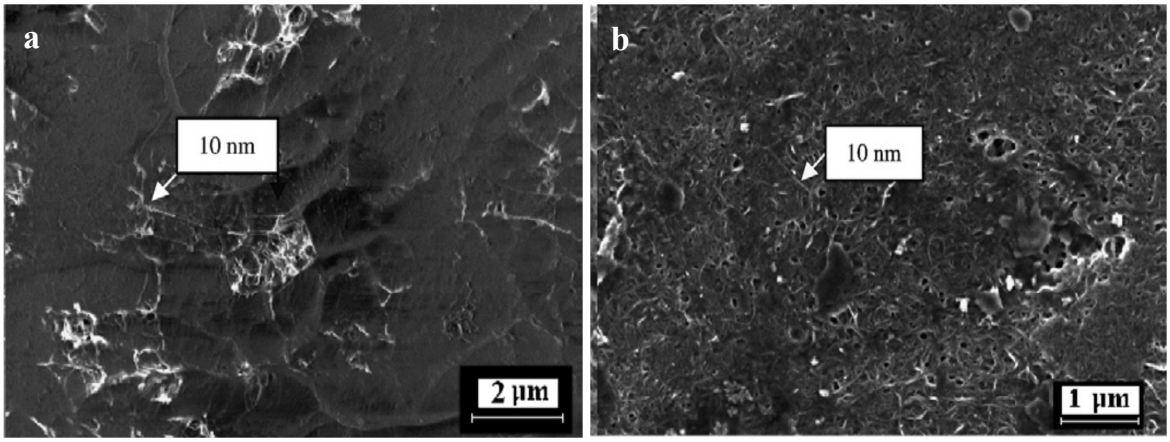

Figure 4.39. The SEM images of a) PVC+0.2 wt% SWCNT, and b) PVC+20 wt% content of MWCNT [70].

Based on the DSC results, by adding carbon nanotubes to the main matrix very slight changes in the thermal stability of composites were obtained (Figure 4.40) [70].

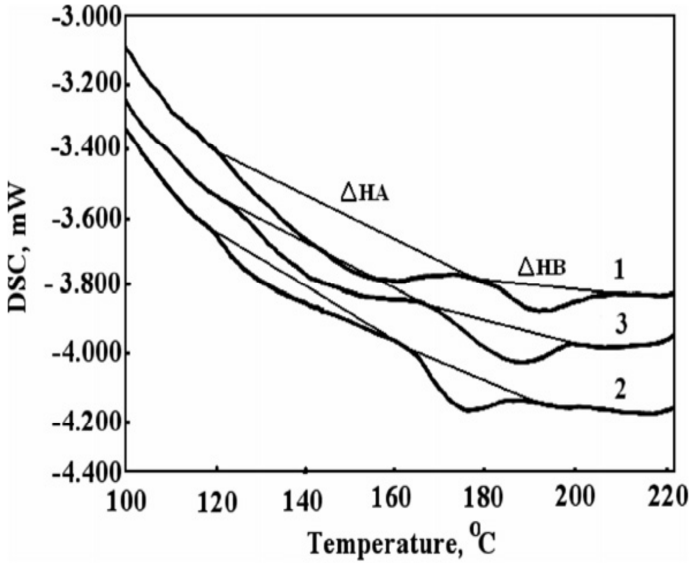

Figure 4.40. The DSC analysis of 1. PVC without CNT, 2. PVC with 0.2 wt% content of SWCNT, 3. PVC with 20 wt% content of MWCNT [70].

R. Verjado et al. discussed the possible use of the carbon nanotube as flame retardant in the elastomeric foam under the fire. The ethanol was used as solvent. CNT with different weight percentages was dispersed into the solvent and the new solution was dispersed into SiH [71].

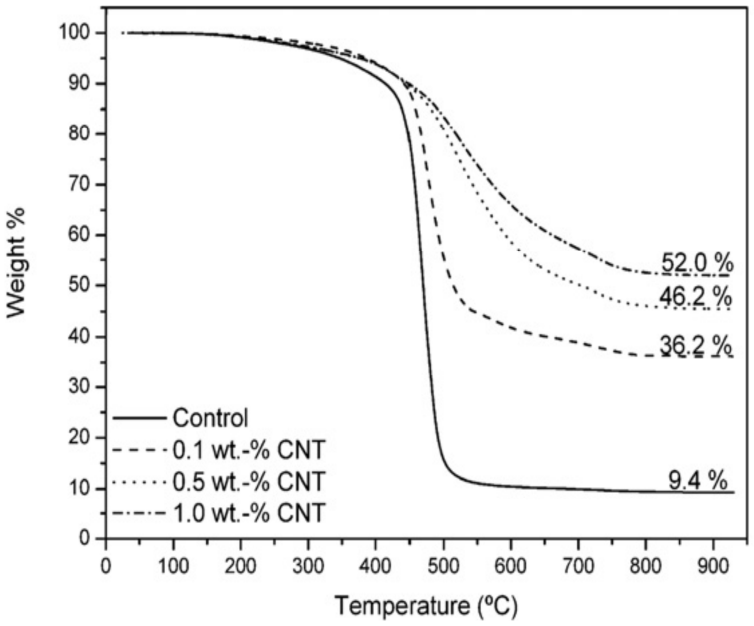

Figure 4.41. The TGA analysis of silicon based with different percentages of carbon nanotube [71]

As it can be seen from the TGA studies, it is a very sharp weight loss for the samples without nanoparticles incorporation. The weight loss of samples with nanoinclusion showed better thermal stability (Figure 4.41) [71].

According to another research study, the effect of eleven types of Nanographene platelets (NGP) with the thickness of 0.34 to 100 nm were investigated to produce polymer nanocomposites (PNCs) with unique properties. The TGA studies were performed under different rates. Figure 4.42 shows the TGA studies under the rate of 10 °C/min [72].

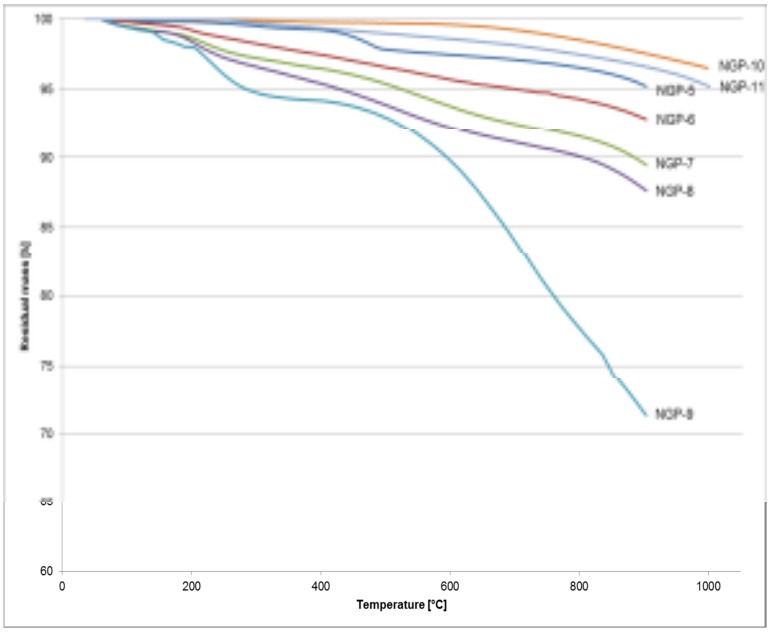

Figure 4.42. The TGA analysis of polymer with NGP-5 to NGP-11 [72].

Based on the above figure, the most thermally stable sample is, NGP-10 with more than 98 wt% residue at the heating rate of 10 °C/min [72].

T. Kuilla et al. discussed the effect of graphene as a nanofiller in different polymers such as polyaniline (PANI), polycarbonate, PET, poly(vinylidene fluoride) (PVDF), polycarbonate (PC) and polystyrene (PS). The addition of 0.38 vol% Graphite nanoplatelets (GNPs) in the polystyrene matrix provided better thermal stability compared to unfilled polystyrene [73].

According to TGA results, the sample containing Polystyrene/Functionalized Graphene composite displayed a higher thermal stability compared to PS (Figure 4.43) [73].

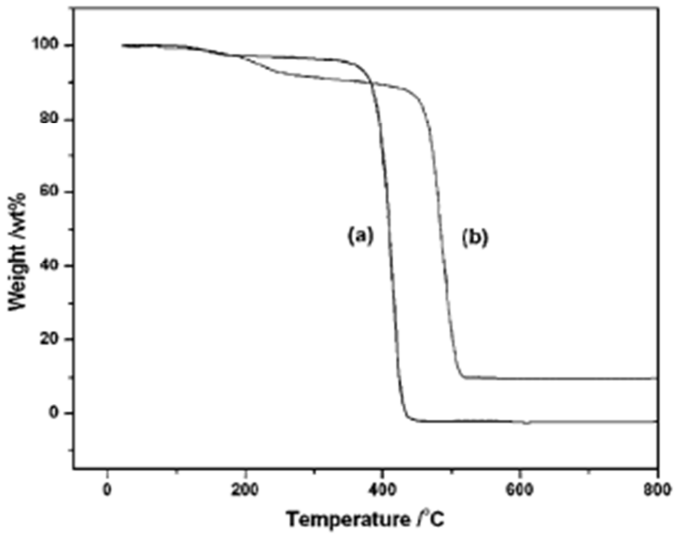

Figure 4.43. The TGA analysis (a) Polystyrene and (b) Polystyrene/Functionalized Graphene composite [73].

R. Young et al. reviewed the tensile strength of Polyurethane incorporated with different percentages of graphene.

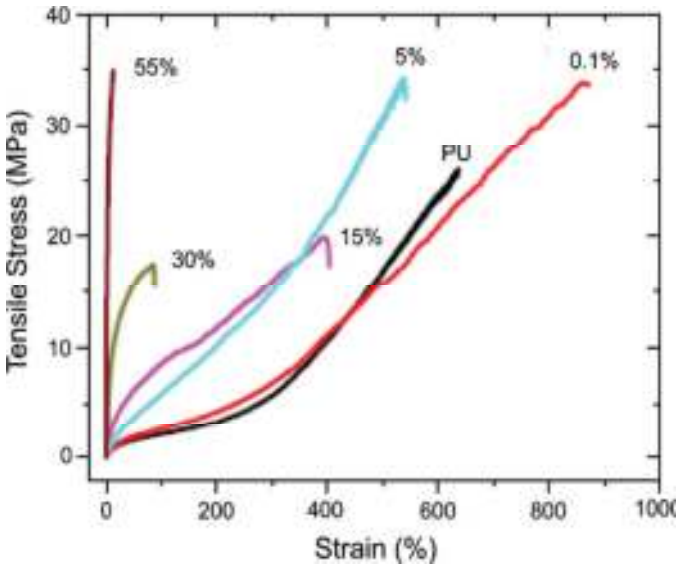

Fig 4.44. The Stress-strain curve for the polyurethane with different weight percentages of graphene [39].

It can be seen in figure 4.44, by increasing the percentages of graphene into the main matrix, a large increase in the slope of the stress strain curve was observed [39].

Based on a different study, the fire retardancy of ethylene-vinyl acetate (EVA) filled with magnesium hydroxide/Talc composites was investigated. The EVA filled with magnesium hydroxide and organomodified montmorillonite (oMMT) composition was investigated as well. The TGA test was conducted and the following results were obtained [74].

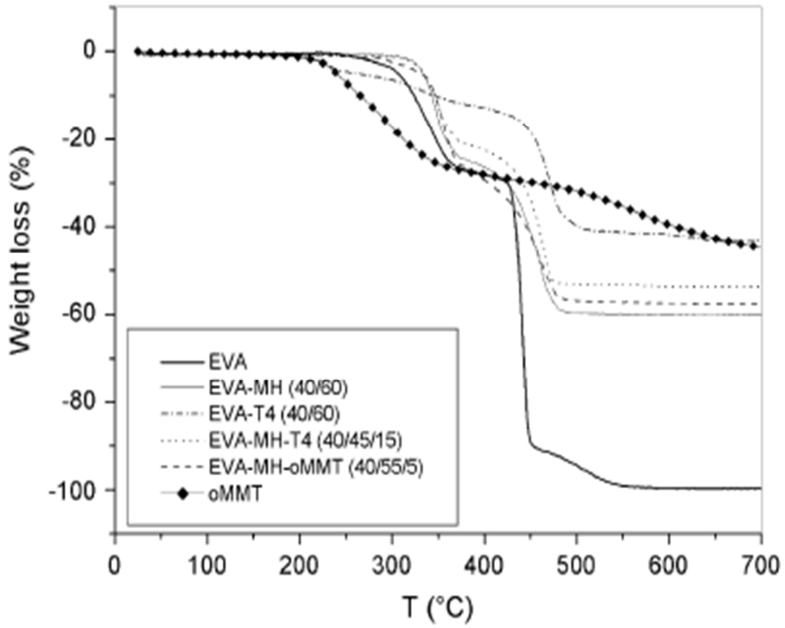

Figure 4.45. The TGA analysis of various filled EVA composites, pure EVA and pure oMMT [74].

Based on the TGA results, EVA showed the lowest thermal stability compared to the samples filled with oMMT. The samples containing EVA and 45wt% MH (Talc) and 15% T4 displayed better thermal stability (Figure 4.45) [74].

Y. Wang et al. discussed the dripping behavior of burning different polymers under the UL94 test. According to his analysis, it was discovered that by adding more talc into low-density polyethylene (LDPE), the dripping frequency was decreased. This means the LPDE incorporated with talc nanoinclusion has no V-rating under the UL 94 vertical test [75].

According to a similar study, the effect of cloisite 30B, cloisite 10A and some stabilizer in PVC were discussed. Based on the TGA results, better thermal stability for PVC with cloisite 30B was obtained compared to PVC with cloisite 10A (Figure 4.46) [76].

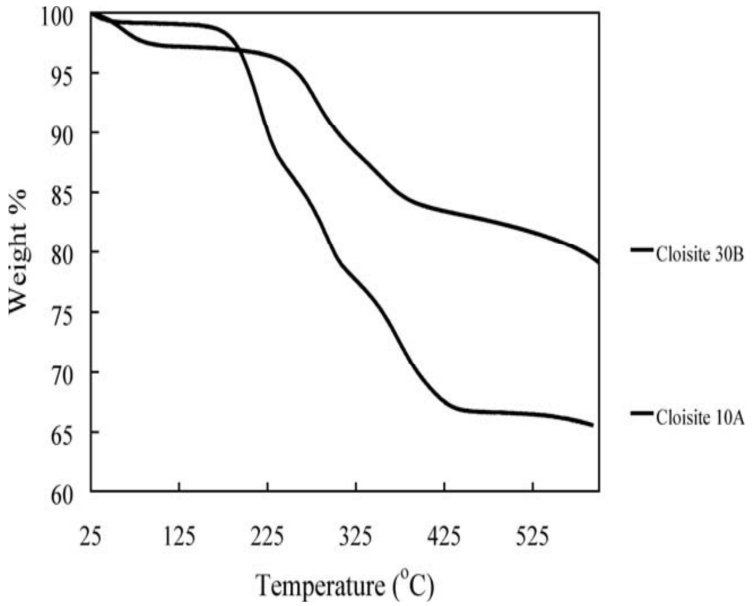

Figure 4.46. The TGA analysis of PVC incorporated with Cloisite 30B and Cloisite 10A [76].

M. Mondragon et al. discussed the mechanical properties of PVC/poly(ε-caprolactone) (PCL) with organophilic-montmorillonite (OMMT) and PVC/Polylactide (PLA) with organophilic-montmorillonite OMMT produced the following results.The combination of PVC/ PCL and OMMT nanocomposite showed highest tensile strength among all the samples (Figure 4.47) [77].

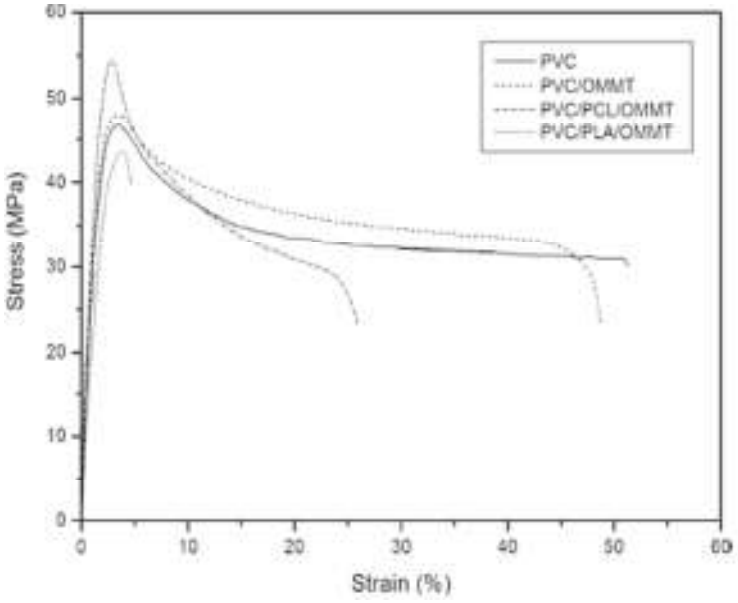

Figure 4.47. The Stress-strain curve for unfilled PVC and PVC incorporated with nanoinclusions [77]

In a similar study, the effect of cloisite 30B into Polyamide (nylon) 11 under UL94 test was discussed. The neat PA 11 samples did not pass the UL 94 ratings. The samples containing 7.5 % clay into PA 11 were classified as V-0 rating while all the PA 11 samples containing carbon nanofibers passed the requirements for UL 94 V0 [78].

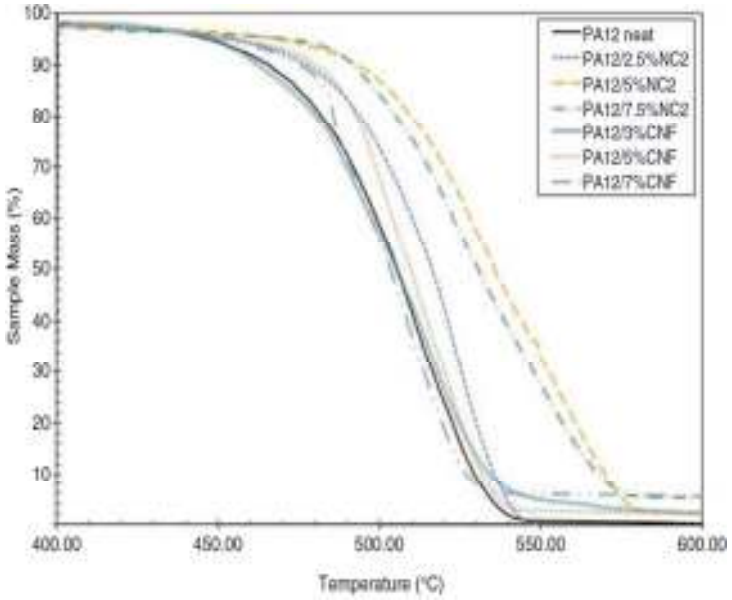

Figure 4.48. The TGA analysis of the PA12 neat and different weight percentages of nanoparticle-filled PA12 [78].

The figure shown above is the TGA studies of Polyamide (nylon) 12 (PA12) incorporated with cloisite 30B (NC2) and carbon nanofibers (CNF) (Figure 4.48). According to this graph, all the samples containing nanoinclusion displayed better thermal stability compared to neat PA 12 [78].

K. Fukushima et al. prepared the poly(lactic acid) (PLA) based nanocomposite containing 2 different nano fillers: Cloisite 30B and expanded graphite. The UL 94 vertical burning test was conducted on the prepared samples. According to the results, the PLA was classified as V-2 rating while all PLA samples containing cloisite 30B and expanded graphite did not pass the requirements of the UL 94 vertical test [79].

M. Shen et al. considered the effect of different percentages of various graphite into high density polyethylene composite (HDPE). The ozone (O_3)-hydrothermal process was used to prepare the expandable graphite (EG). Based on the TGA results the samples incorporated with different percentages of EG showed better thermal stability in contrast to pure HDPE (Figure 4.49) [80].

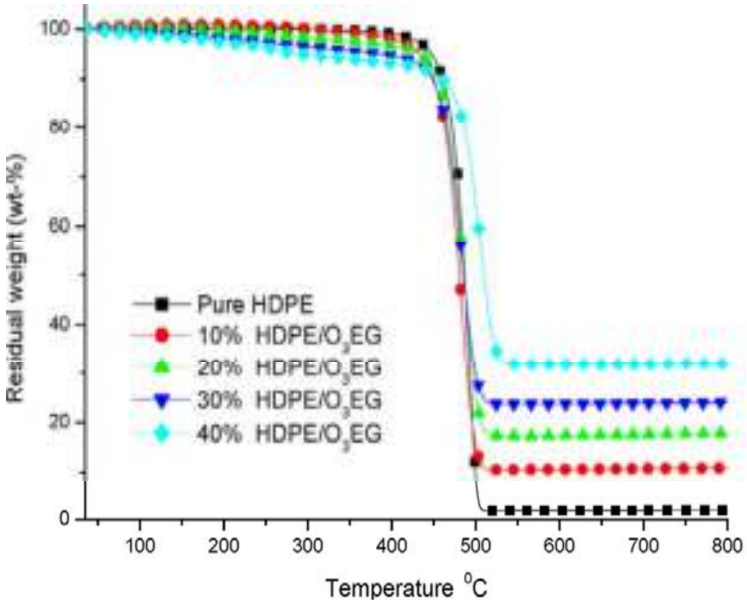

Figure 4.49. The TGA analysis of high-density polyethylene (HDPE) with different wt% of ozonehydrothermal expandable graphite (O3-EG) [80].

Also, the blends of HDPE with natural graphite, ultrasound irradiation expandable graphite and ozone-hydrothermal expandable graphite were prepared and the UL 94 vertical test was performed on all samples. All HDPE samples containing natural graphite failed under the UL 94 test. HDPE samples containing 40 wt% ultrasound irradiation expandable graphite were rated as V1 in UL 94 vertical burning test. The 10, 20 wt% hydrothermal expandable graphite into HDPE passed the V1 and V0 respectively. For HDPE composites containing 20 wt% of ozone (O_3)-hydrothermal expandable graphite (HDPE/ O_3-HEG) passed V2 in the vertical burning test. The HDPE samples containing 30 and 40 wt% O_3-HEG were classified as V0 in vertical burning test [80].

According to different investigation, different weight percentages (1, 3, 6 and 10 wt%) of clay nanoparticles were dispersed in A3-type star poly(methylmethacrylate) (PMMA). The DSC test was performed on all samples. Based on the DSC analysis, all the samples containing nanoparticles showed higher glass transition temperature than pure polymer (Figure 4.50) [81].

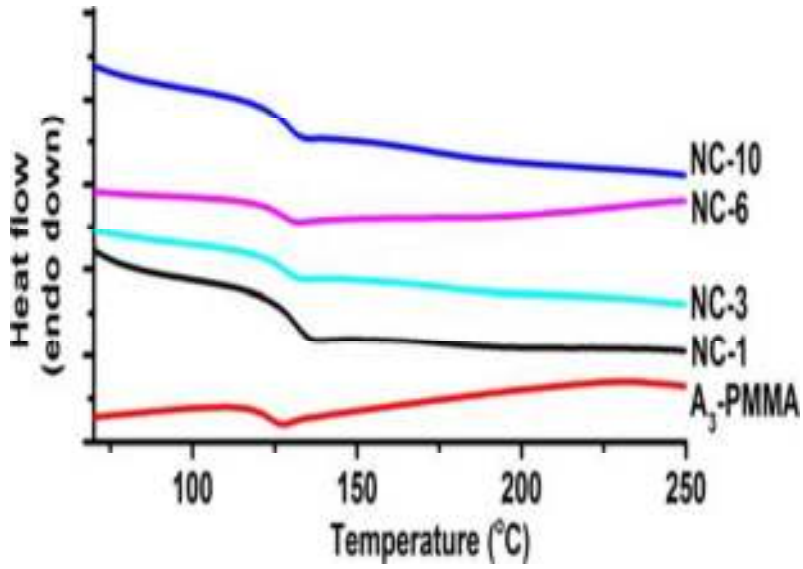

Figure 4.50. The DSC analysis of A3-PMMA star polymer (PMMA) and PMMA/ MMT nanocomposites (NC-1, 3, 6 and 10) [81].

According to another study, epoxy resin was mixed with different percentages of clays. Based on the DSC studies, the sample containing 1.5 wt% clay (organically modified montmorillonite) displayed the highest glass transition temperature among all the samples [82].

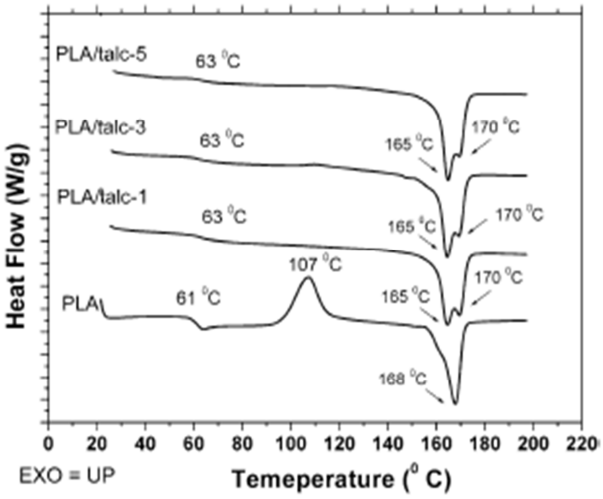

Figure 4.51. The DSC analysis of PLA and PLA/talc composites [83].

S. Jain et al. investigated the effect of talc on the properties of ploy(lactic acid) (PLA). Based on the DSC analysis, the samples containing Talc showed higher Tg. As shown in figure 4.51, the glass transition temperature of pure PLA is about 61 °C, while the temperature for the samples containing talc is about 63 °C [83].

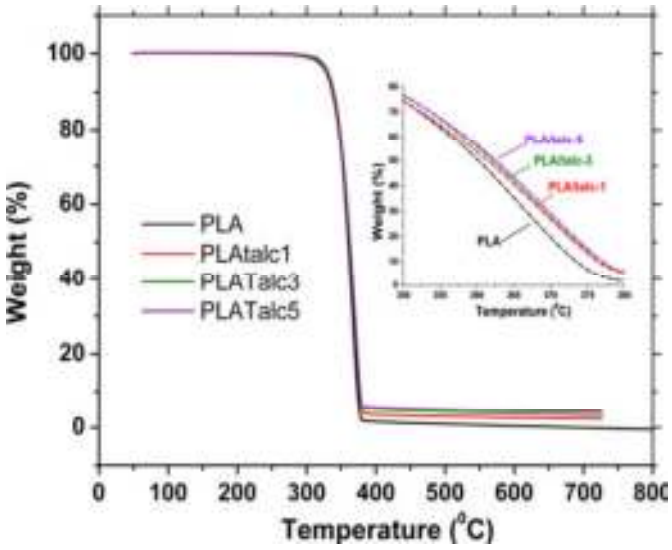

Figure 4.52. The TGA analysis of PLA and PLA incorporated with talc [83].

Based on the TGA curves, it is seen those samples incorporated with talc showed better thermal stability compared to pure PLA (Figure 4.52) [83]. According to SEM images, more agglomeration will occur by increasing the weight percentages of talc into the main matrix. Figure 4.53 shows the pure PLA and PLA with different weight percentages of talc under SEM.

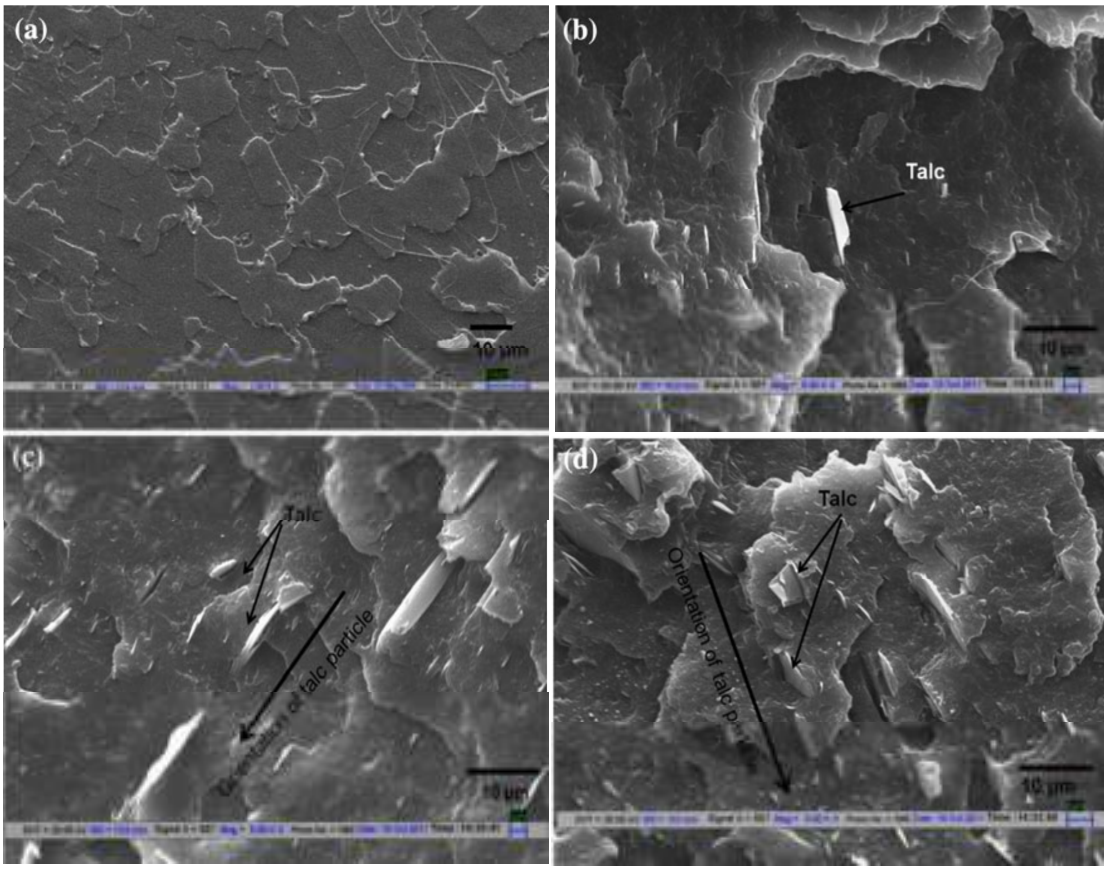

Figure 4.53. The SEM images of a) PLA, b) PLA/talc-1, c) PLA/talc-3, d) PLA/talc-5 [83].

The strain stress curve was plotted for all samples (Figure 4.54). Based on the plots, the PLA samples incorporated with talc showed higher tensile strength compared to unfilled PLA [83].

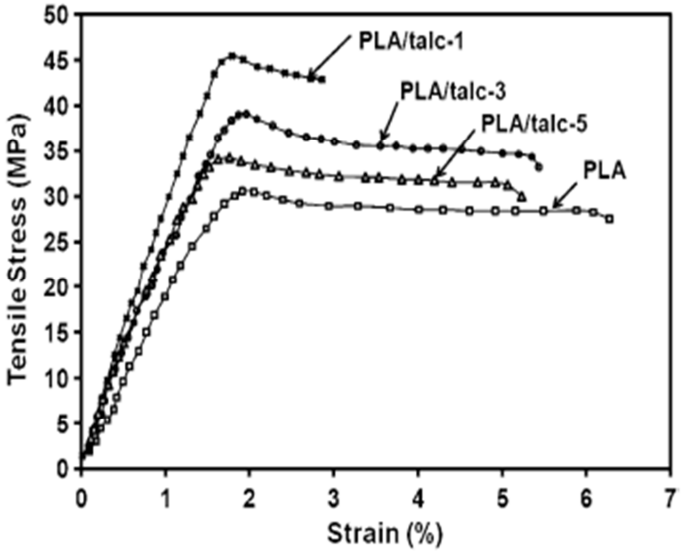

Figure 4.54. The Stress-strain curve of PLA and PLA/talc composites blown films [83].

E. Bajsic investigated the effect of talc on thermal and mechanical properties of the thermoplastic polyurethane (TPU) and polypropylene (PP) blends. According to TGA results, the addition of talc into thermoplastic polyurethane/polypropylene increased the thermal stability and final decomposition temperature of all samples except for 3 wt% talc, compared to neat thermoplastic polyurethane/polypropylene (TPU/PP) (Figure 4.55) [84].

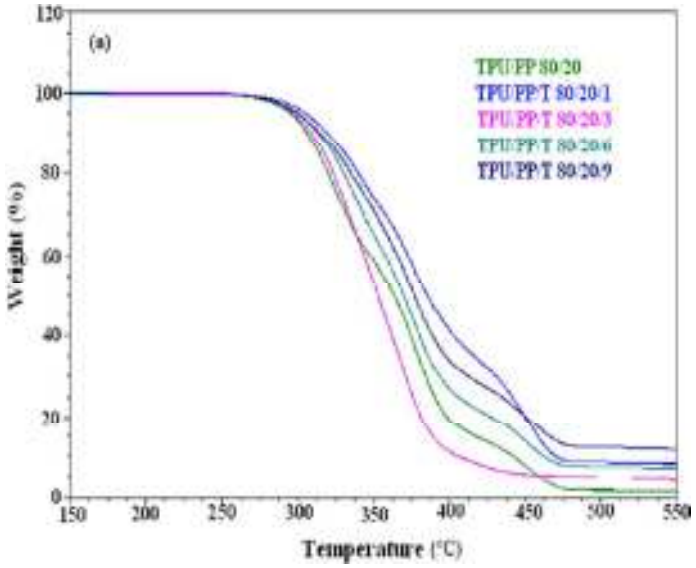

Figure 4.55. The TGA analysis of thermoplastic polyurethane/polypropylene (TPU/PP 80/20) and TPU/PP incorporated with different weight percentages of talc [84].

Based on the DSC studies, the glass transition temperature of TPU80 /PP20 blends was higher than all the samples that contained a talc inclusion (Figure 4.56) [84].

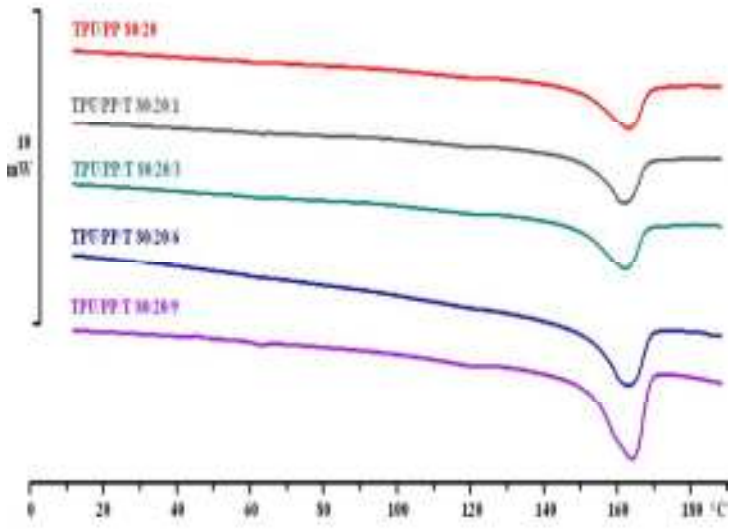

Figure 4.56. The DSC analysis of TPU/PP 80/20 and talc-filled blends [84].

Based on the tensile test results, by increasing the weight percentages of talc into TPU/PP blends, the reduction of tensile strength and Young's modulus was observed [84].

Recently, various types of nanotechnology and its products have been utilized to increase the efficiencies of the new materials and systems. However, these new developments also bring many uncertainties and risks to human health and the environment. Therefore, the future of nanotechnology depends largely on public acceptance of the risks and benefits associated with the use of nanomaterials. Further studies need to be conducted on these nanomaterials to find their nanosafety concerns [85].

CHAPTER 5

CONCLUSIONS

In this research, the effects of nanoscale inclusions on the flame retardancy of PVC specimen were investigated in detail using the various analysies techniques.

The UL 94 ASTM was conducted on all samples incorporated with different nanoparticles.The samples containing 10 wt% of nanoclay and graphene and 20 wt% of all the nanoparticles rated as V0 which is the best flame retardancy rating. Based on the TGA and DSC analysis, the addition of nanoscale inclusions increased the degradation temperatures of the PVC nanocomposites. However, nanoclay showed higher degradation temperature comparted the nanotalc, which may be because of the strong interaction and covalent bond formation between the polymer chains and nanoclay samples compared to the second option.

By comparing all the samples with percentage values, graphene showed better thermal stability among those samples of PVC incorporated with 5 wt% nanoscale inclusions. This sample lost 84.79% of the initial weight and 8% improvement was obtained compared to the pure PVC. Nanoclay represented the best thermal stability among the 10% incorporated nanoinclusions. This specimen lost 80.24% of the initial weight and about 12% improvement was obtained compared to the neat PVC. Graphene also displayed the higher degradation among the all samples of the 20 wt% inclusions. This sample lost 73.22% of the initial weight and 19% improvement was obtained compared to the pure PVC. The SEM analysis was used to study the morphological changes of the PVC samples incorporated with nanoclay, nanotalc and graphene in the presence and absence of the flames. According to the SEM images, the nanoscale inclusions created a layer of inorganic surfaces during the UL-94 test, which mainly blocked the

fire and dripping of the PVC specimens. The TGA and DSC results are mainly agreed well with the SEM analysis.

The tensile tests were conducted on the PVC and PVC with 20 wt% nanoinclusion, which was the best rated samples in the UL94 test. All the samples incorporated with nanoinclusion received higher strength compared to the neat PVC. The addition of clay and graphene nanoparticles provided more ductility in main matrix compared to the talc samples which made the PVC more brittle. By the addition of 20 wt% nanoclay to the pure PVC the ultimate tensile strength increased 17.5%. By the addition of 20 wt% nanotalc to the main matrix, the ultimate tensile strength increased 35% compared to the pure PVC. However, by the addition of 20 wt% of graphene to the pure PVC, 132.5% improvement was obtained for ultimate tensile strength.

CHAPTER 6

FUTURE WORK

The neat PVC sample without any nanoparticles was made of 85 wt% solvent and 15 wt% PVC prior to the electrospinning process. For the nanocomposite samples, the 5,10 and 20 wt% of nanoparticles were added into the main matrix. The solution was sonicated to make very smooth final solution. The rest of the solution which was made for the preparation of UL 94 test, used to produce fibers. Electrospinning is the well known method to produce micro and nano fibers. All the fibers for different weight percentages of nanoinclusion were prepared and SEM analysis for talc and clay was completed. The SEM of graphene is needed to be done as well. Figures below show the SEM images of PVC fibers with different weight percentages of nanoclay and nanotalc inclusions. (Figures 6.1 through 6.3). Flam retardancy of these nanocomposite fibers are needed in the future studies.

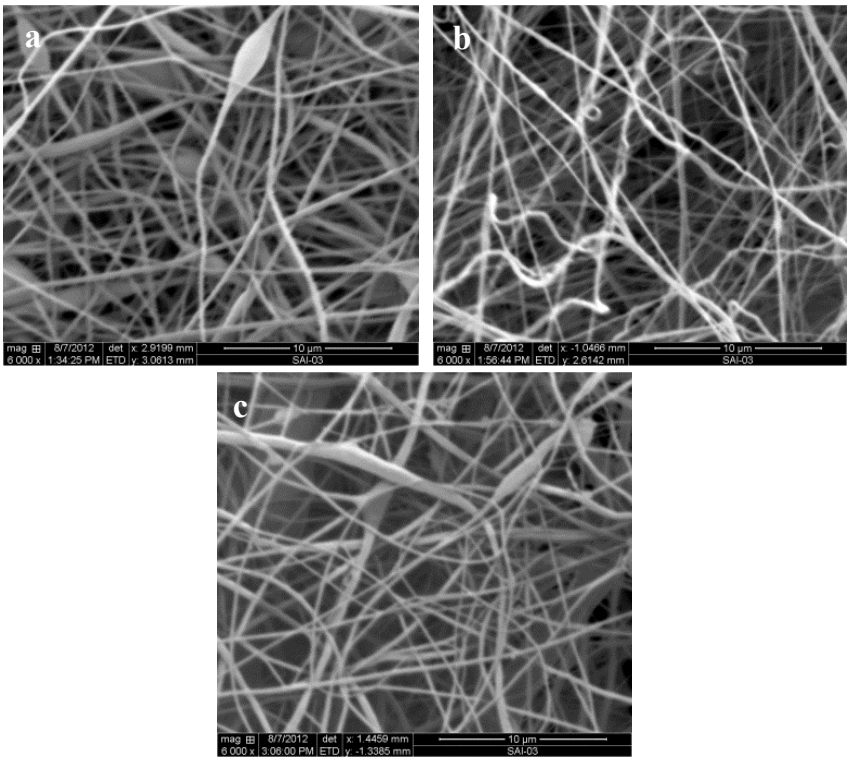

Figure 6.1. SEM images of a) Pure PVC b) PVC with 5 wt% Nanoclay b) PVC with 5 wt% Nanotalc

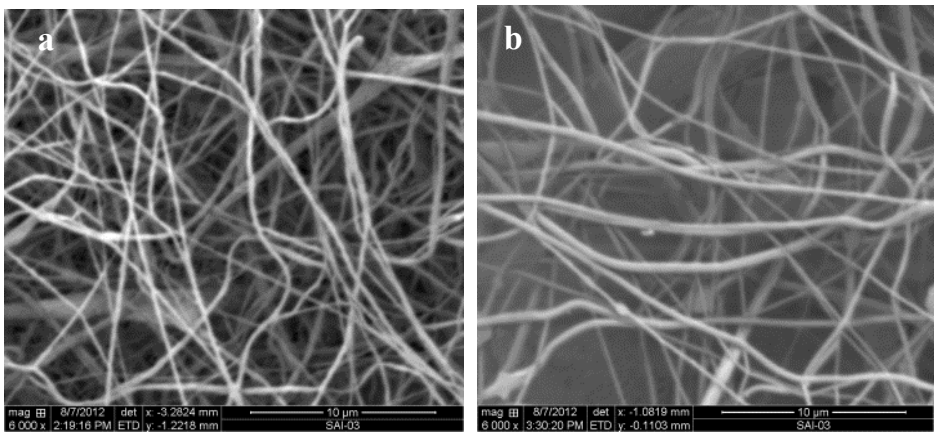

Figure 6.2. SEM images of a) PVC with 10 wt% Nanoclay b) PVC with 10 wt% Nanotalc.

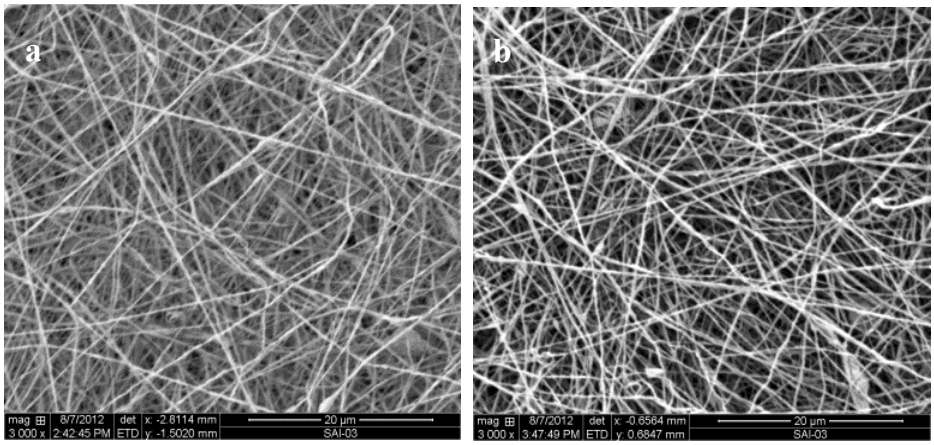

Figure 6.3. SEM images of a) PVC with 20 wt% Nanoclay b) PVC with 20 wt% Nanotalc.

Additionally, the following areas need the further studies:

- Modeling the nanocomposite structure being subjected to high temperatures
- More analysis of the fibers and more thermal tests on the fibers and compare the results with the cast nanocomposites
- More investigation on conducting the heating tests on the fibers.
- Measuring the mechanical properties of fibers

REFERENCES

REFERENCES

1. https://www.google.com/search?sa=G&q=fire+brigade&tbm=isch&tbs=simg:CAQSVRpTCxCo1NgEGgQIBQgIDAsQsIynCBoqCigIARIC5QQaIJGeRScJkJJ2tHiK9Vz4ptKkvK2OhmiHCv-Ifl1oiYqXDAsQjq7-CBoKCggIARIEFjTjAww&ei=TX5tUtapFOrK2gXBiIG4DA&ved=0CCcQwg4oAA&biw=1280&bih=880#imgdii=_. Cited November 5, 2013

2. Wilkie, C.A., and A.B. Morgan, "Fire retardancy of polymeric materials", 2010: CRC Press.

3. Leng, J. and A.K.-t. Lau, "Multifunctional polymer nanocomposites.", 2011: CRC Press.

4. Laoutid, F., L. Bonnaud, M. Alexandre, J-M. Lopez-Cuesta, and Ph. Dubois, "New prospects in flame retardant polymer materials: From fundamentals to nanocomposites.", Materials Science and Engineering: R: Reports, 2009. 63(3): p. 100-125.

5. Ghazinezami, A., A. Jabbarnia, and R. Asmatulu, "Fire retardancy of nanocomposites incorporated with nanoscale inclusions.", ASME 2013 International Mechanical Engineering Congress and Exposition, IMECE2013, 2013 (In Press).

6. Ghazinezami, A., A. Jabbarnia, Seyed A. Soltani, N. Nuraje, and R. Asmatulu, "Improving the fire retardancy of polymeric structures via addition of nanoclay and graphene nanoflakes.", New Materials And Technologies For Industry, Environment And Health Protection, 2013: p. 93-99.

7. Olad, A., "Polymer/Clay nanocomposites.", Advances in Diverse Industrial Applications of Nanocomposites. RijeKa: InTech, 2011: p. 113-38.

8. Jordan, J., K.I. Jacob, R. Tannenbaum, M.A. Sharaf, and I. Jasiuk, "Experimental trends in polymer nanocomposites—a review.", Materials Science And Engineering: A, 2005. 393(1): p. 1-11.

9. Gacitua, W., A. Ballerini, and J. Zhang, "Polymer nanocomposites: synthetic and natural fillers. A review.", Maderas Cienc Tecnol, 2005. 7: p. 159-178.

10. Hussain, F., M. Hojjati, "Review article: polymer-matrix nanocomposites, processing, manufacturing, and application: an overview.", Journal of Composite Materials, 2006. 40(17): p. 1511-1575.

11. LeBaron, P.C., Z. Wang, and T.J. Pinnavaia, "Polymer-layered silicate nanocomposites: an overview.", Applied clay science, 1999. 15(1): p. 11-29.

12. Ehrenstein, G.W., G. Riedel, and P. Trawiel, "Thermal analysis of plastics: theory and practice.", 2004: Hanser Verlag.

13. Laoutid, F., P. Gaudon, J.M. Taulemesse, J.M. Lopez-Cuesta, J.I. Velasco, and A. Piechaczyk, "Study of hydromagnesite and magnesium hydroxide based fire retardant

systems for ethylene–vinyl acetate containing organo-modified montmorillonite.", Polymer degradation and stability, 2006. 91(12): p. 3074-3082.

14. Pandey, J.K., K.R. Reddy, and A. Kumar, R.P. Singh, "An overview on the degradability of polymer nanocomposites.", Polymer degradation and stability, 2005. 88(2): p. 234-250.

15. Duquesne, S., M.L. Bras, C. Jama, E.D. Weil, and L. Gengembre, "X-ray photoelectron spectroscopy investigation of fire retarded polymeric materials: application to the study of an intumescent system.", Polymer degradation and stability, 2002. 77(2): p. 203-211.

16. Bourbigot, S., M.L. Bras, S. Duquense, and M. Rochery, "Recent advances for intumescent polymers.", Macromolecular Materials and Engineering, 2004. 289(6): p. 499-511.

17. Kashiwagi, T., and J.W. Gilman, "Silicon-based flame retardants. Fire retardancy of polymeric materials.", CRC Press 2000: p. 353-389.

18. Finnigan, B., D. Martin, P. Halley, R. Truss, and K. Campbell, "Morphology and properties of thermoplastic polyurethane nanocomposites incorporating hydrophilic layered silicates.", Polymer, 2004. 45(7): p. 2249-2260.

19. Armentano, I., M. Dottori, E. Fortunati, S. Mattioli, and J.M. Kenny, "Biodegradable polymer matrix nanocomposites for tissue engineering: a review.", Polymer degradation and stability, 2010. 95(11): p. 2126-2146.

20. Hamdani, S., C. Longuet, D. Perrin, J.M Lopez-Cuesta and F. Ganachaud, "Flame retardancy of silicone-based materials.", Polymer Degradation and Stability, 2009. 94(4): p. 465-495.

21. Song, R., Z. Wang, X. Meng, B. Zhang, and T. Tang, "Influences of catalysis and dispersion of organically modified montmorillonite on flame retardancy of polypropylene nanocomposites.", Journal of Applied Polymer Science, 2007. 106(5): p. 3488-3494.

22. Pastore, H.O., A. Frache, E. Boccaleri, L. Marchese, and G. Camino, "Heat Induced Structure Modifications in Polymer-Layered Silicate Nanocomposites.", Macromolecular Materials and Engineering, 2004. 289(9): p. 783-786.

23. Awad, W.H., G. Beyer, D. Benderly, W.L. Ijdo, P. Songtipya, M.D.M Jimenez-Gasco, E. Manias, and C.A. Wilkie, "Material properties of nanoclay PVC composites.", Polymer, 2009. 50(8): p. 1857-1867.

24. Yao, K., M. Song, D.J. Hourston, and D.Z. Luo, "Polymer/layered clay nanocomposites: 2 polyurethane nanocomposites.", Polymer, 2002. 43(3): p. 1017-1020.

25. Osman, M.A., J.E. Rupp, and U.W. Suter, "Tensile properties of polyethylene-layered silicate nanocomposites.", Polymer, 2005. 46(5): p. 1653-1660.

26. Mittal, V., “Mechanical and gas permeation properties of compatibilized polypropylene–layered silicate nanocomposites.”, Journal of Applied Polymer Science, 2008. 107(2): p. 1350-1361.

27. Krikorian, V. and D.J. Pochan, “Poly (L-lactic acid)/layered silicate nanocomposite: fabrication, characterization, and properties.”, Chemistry of materials, 2003. 15(22): p. 4317-4324.

28. Theng, B.K.G., “Formation and properties of clay-polymer complexes.”, Vol. 4. 2012: Access Online via Elsevier.

29. Fornes, T. and D. Paul, “Modeling properties of nylon 6/clay nanocomposites using composite theories.”, Polymer, 2003. 44(17): p. 4993-5013.

30. Mittal, V., “Polypropylene-layered silicate nanocomposites: filler matrix interactions and mechanical properties. Journal of Thermoplastic Composite Materials.”, 2007. 20(6): p. 575-599.

31. Alexandre, M. and P. Dubois, “Polymer-layered silicate nanocomposites: preparation, properties and uses of a new class of materials.”, Materials Science and Engineering: R: Reports, 2000. 28(1): p. 1-63.

32. Nam, P.H., P. Maiti, M. Okamoto, T. Kotaka, N. Hasegawa, and A. Usuki, “A hierarchical structure and properties of intercalated polypropylene/clay nanocomposites.”, Polymer, 2001. 42(23): p. 9633-9640.

33. http://www.imerystalc.com/content/corporate/About-talc/Talc_the_mineral/A_unique_mineral/. Cited November 5, 2013

34. http://www.imerystalc.com/content/luzenac/Plastics/Functions/Electrical_insulation_-_Fire_resistance/america.php. Cited November 5, 2013

35. Geim, A.K. and K.S. Novoselov, “The rise of graphene.”, Nature materials, 2007. 6(3): p. 183-191.

36. Novoselov, K.S. “Graphene: materials in the Flatland.”, In Microwave Conference (EuMC), 2011, 41st European. 2011. IEEE.

37. Novoselov, K.S., A.K. Geim, S.V. Morozov,D. Jiang, Y. Zhang, S.V. Dubonos, I.V. Grigorieva, and A.A. Firsov, “Electric field effect in atomically thin carbon films.”, Science, 2004. 306(5696): p. 666-669.

38. Lee, C., X. Wei, J.W. Kysar, and J. Hone, “Measurement of the elastic properties and intrinsic strength of monolayer graphene.”, Science, 2008. 321(5887): p. 385-388.

39. Young, R.J., I.A. Kinloch, L. Gong, and K.S. Novoselov, “The mechanics of graphene nanocomposites: A review.”, Composites Science and Technology, 2012. 72(12): p. 1459-1476.

40. Geim, A.K., “Nobel lecture: random walk to graphene.”, Reviews of Modern Physics, 2011. 83(3): p. 851.

41. Verdejo, R., M.M. Bernal, L.J. Romasanta, and M.A. Lopez-Manchado, “Graphene filled polymer nanocomposites.”, Journal of Materials Chemistry, 2011. 21(10): p. 3301-3310.

42. Kim, K.S., Y. Zhao, H. Jang, S.Y. Lee, J.M. Kim, K.S. Kim, J. Ahn, P. Kim, J. Choi, and B.H. Hong, “Large-scale pattern growth of graphene films for stretchable transparent electrodes.”, Nature, 2009. 457(7230): p. 706-710.

43. Kuan, H.-C., C.M. Ma, W. Chang, S. Yuen, H. Wu, and T. Lee, “Synthesis, thermal, mechanical and rheological properties of multiwall carbon nanotube/waterborne polyurethane nanocomposite.”, Composites Science and Technology, 2005. 65(11): p. 1703-1710.

44. Cipiriano, B.H., T. Kashiwagi, S.R. Raghavan, Y. Yang, E.A. Grulke, K. Yamamoto, J.R. Sheilds, J.F. Douglas, “Effects of aspect ratio of MWNT on the flammability properties of polymer nanocomposites.”, Polymer, 2007. 48(20): p. 6086-6096.

45. Kashiwagi, T., F. Du, J.F. Douglas, K.I. Winey, R.H. Harris, “Nanoparticle networks reduce the flammability of polymer nanocomposites.”, Nature Materials, 2005. 4(12): p. 928-933.

46. http://itech.dickinson.edu/chemistry/?tag=richard-hendrickson. Cited November 5, 2013

47. Peeterbroeck, S., F. Laoutid, J. Taulemesse, F. Monteverde, J.M. Lopez-cuesta, J.B. Nagy, M. Alexandre, and P. Dubois, “Mechanical Properties and Flame-Retardant Behavior of Ethylene Vinyl Acetate/High-Density Polyethylene Coated Carbon Nanotube Nanocomposites.”, Advanced Functional Materials, 2007. 17(15): p. 2787-2791.

48. Nguyen, D.A., Y.R. Lee, A.V. Raghu, H.M. Jeong, C.M. Shin, and B.K. Kim, “ Morphological and physical properties of a thermoplastic polyurethane reinforced with functionalized graphene sheet.”, Polymer International, 2009. 58(4): p. 412-417.

49. Kurahatti, R., A.O. Surendranathan, S.A. Kori, N. Singh, A.V.R. Kumar, and S. Sirvastava, “Defence Applications of Polymer Nanocomposites.”, Defence Science Journal, 2010. 60(5): p. 551-563.

50. Ansari, S. and E.P. Giannelis, “Functionalized graphene sheet—Poly (vinylidene fluoride) conductive nanocomposites.”, Journal of Polymer Science Part B: Polymer Physics, 2009. 47(9): p. 888-897.

51. Jiang, L., Y.C. Lam, K.C. Tam, T.H. Chua, G.W. Sim, L.S. Ang, “Strengthening acrylonitrile-butadiene-styrene (ABS) with nano-sized and micron-sized calcium carbonate.”, Polymer, 2005. 46(1): p. 243-252.

52. Wintterlin, J. and M.-L. Bocquet, “Graphene on metal surfaces.”, Surface Science, 2009. 603(10): p. 1841-1852.

53. Rafiee, M.A., J. Rafiee, I. Srivastava, Z. Wang, H. Song, Z. Yu, and N.Koratkar, " Fracture and fatigue in graphene nanocomposites.", Small, 2010. 6(2): p. 179-183.

54. Li, X., W. Cai, J. An, S. Kim, J. Nah, D. Yang, R. Piner, A. Velamakanni, I. Jung, E. Tutuc, S.K. Banerjee, L. Colombo, R.S. Ruoff, "Large-area synthesis of high-quality and uniform graphene films on copper foils.", Science, 2009. 324(5932): p. 1312-1314.

55. Suk, J.W., A. Kitt, C.W. Magnuson, Y. Hao, S. Ahmed, J. An, A.K. Swan, B.B. Goldberg, and R.S. Ruoff, "Transfer of CVD-grown monolayer graphene onto arbitrary substrates.", ACS nano, 2011. 5(9): p. 6916-6924.

56. Bae, S., H. Kim, Y. ee, X. Xu, J. Park, Y. Zheng, J. Balakrishnan, T. Lei, H.R. Kim, Y. Song, Y. Kim, K.S. Kim, B. Ozyilmaz, J. Ahn, B.H. Hong, and S. Lijima, "Roll-to-roll production of 30-inch graphene films for transparent electrodes.", Nature nanotechnology, 2010. 5(8): p. 574-578.

57. http://www.worldoftest.com/loi.htm. Cited November 5, 2013

58. http://www.rtpcompany.com/products/flame/ratings.htm. Cited November 5, 2013

59. http://hkdowellltd.en.ecplaza.net/ul94-horizontal-vertical-flammability-tester--270938-2436311.html. Cited November 5, 2013

60. Zanetti, M., et al., Cone calorimeter combustion and gasification studies of polymer layered silicate nanocomposites. Chemistry of Materials, 2002. 14(2): p. 881-887.

61. http://www.tutorgigpedia.com/ed/Cone_calorimeter. Cited November 5, 2013

62. http://www.uq.edu.au/_School_Science_Lessons/UNPh22.html#22.6.0H. Cited November 5, 2013

63. http://www.rsc.org/chemistryworld/Issues/2007/October/ClassicKitBunsenBurner.asp. Cited November 5, 2013

64. http://www.tainstruments.com/pdf/brochure/2011%20TGA%20Brochure.pdf. Cited November 5, 2013

65. http://sirius.mtm.kuleuven.be/Research/Equipment/Physical/Diff-scan.html. Cited November 5, 2013

66. http://www.perkinelmer.com/CMSResources/Images/44-74542GDE_DSCBeginnersGuide.pdf. Cited November 5, 2013

67. http://dolbow.cee.duke.edu/TENSILE/tutorial/node4.html. Cited November 5, 2013

68. Madaleno, L., J. Schjodt-Thomsen, and J.C. Pinto, "Morphology, thermal and mechanical properties of PVC/MMT nanocomposites prepared by solution blending and solution

blending+ melt compounding.", Composites Science and Technology, 2010. 70(5): p. 804-814.

69. Mkhabela, V., A. Mishra, and X. Mbianda, "Thermal and mechanical properties of phosphorylated multiwalled carbon nanotube/polyvinyl chloride composites.", Carbon, 2011. 49(2): p. 610-617.

70. Broza, G., K. Piszczek, K. Schulte, T. Sterzynski, "Nanocomposites of poly (vinyl chloride) with carbon nanotubes (CNT).", Composites science and technology, 2007. 67(5): p. 890-894.

71. Verdejo, R., M.M. Bernal, L.J. Romasanta, and A. Lopez-Manchado, "Graphene filled polymer nanocomposites.", Journal of Materials Chemistry, 2011. 21(10): p. 3301-3310.

72. Koo, J.H., D. Pinero, A. Hao, S.C. Lao, B. Johnson, and M.G. Baek, "Methodology for Assessment of Morphological and Thermal Characteristics of Nanographene Platelets.", AIAA, 2013, 1548: p.1-35

73. Kuilla, T., S. Bhadra, D. Yao, N.H. Kim, S. Bose, J.H. Lee, "Recent advances in graphene based polymer composites.", Progress in Polymer Science, 2010. 35(11): p. 1350-1375.

74. Duquesne, S., F. Samyn, S. Bourbigot, P. Amigouet, F. Jouffret, and K. Shen, "Influence of talc on the fire retardant properties of highly filled intumescent polypropylene composites.", Polymers for Advanced Technologies, 2008. 19(6): p. 620-627.

75. Wang, Y., J. Jow, K. Su, and J. Zhang, "Dripping behavior of burning polymers under UL94 vertical test conditions.", Journal of Fire Sciences, 2012. 30(6): p. 477-501.

76. Zheng, X. and M. Gilbert, "An investigation into the thermal stability of PVC/montmorillonite composites.", Journal of Vinyl and Additive Technology, 2011. 17(2): p. 77-84.

77. Mondragón, M., S. Sanchez-Valdez, M.E. Sanchez-Espindola, J.E. Rivera-Lopez, "Morphology, mechanical properties, and thermal stability of rigid PVC/clay nanocomposites.", Polymer Engineering & Science, 2011. 51(4): p. 641-646.

78. Lao, S.C., C. Wu, T.J. Moon, J.H. Koo, A. Morgan, L. Pilato, and G. Wissler, "Flame-retardant polyamide 11 and 12 nanocomposites: thermal and flammability properties.", Journal of composite materials, 2009. 43(17): p. 1803-1818.

79. Fukushima, K., M. Murariu, G. Camino, and P. Dubois, "Effect of expanded graphite/layered-silicate clay on thermal, mechanical and fire retardant properties of poly (lactic acid).", Polymer Degradation and Stability, 2010. 95(6): p. 1063-1076.

80. Shen, M.-Y., K. Li, C. Kuan, H. Kuan, C. Chen, M. Yip, H. Chou, and C. Chiang, " Preparation of expandable graphite via ozone-hydrothermal process and flame-retardant properties of high-density polyethylene composites.", High Performance Polymers, 2013.

81. Aydin, M., M.A. Tasdelen, T. Uyar, and Y. Yagci, “In situ synthesis of A3-type star polymer/clay nanocomposites by atom transfer radical polymerization.”, Journal of Polymer Science Part A: Polymer Chemistry, 2013.

82. Nigam, V., H. Soni, M. Saroop, G.L. Verma, A.S. Bhattacharya, and D.K. Setua Thermal, morphological, and X-ray study of polymer-clay nanocomposites. Journal of Applied Polymer Science, 2012. 124(4): p. 3236-3244.

83. Jain, S., M. Misra, A.K. Mohanty, and A.K. Ghosh, “Thermal, Mechanical and Rheological Behavior of Poly (lactic acid)/Talc Composites.”, Journal of Polymers and the Environment, 2012. 20(4): p. 1027-1037.

84. Bajsic, E.G., V. Rek, and B.O. Pavic, “The influence of talc content on the thermal and mechanical properties of thermoplastic polyurethane/polypropylene blends.”, Journal of Elastomers and Plastics, 2012.

85. Asmatulu, R., “Nanotechnology Safety.”, Elsevier, Amsterdam, The Nederland, August, 2013.

APPENDIXES

APPENDIX 1

A comparison of DSC results for different weight percentages of nanoclay, nanotalc and nanographene.

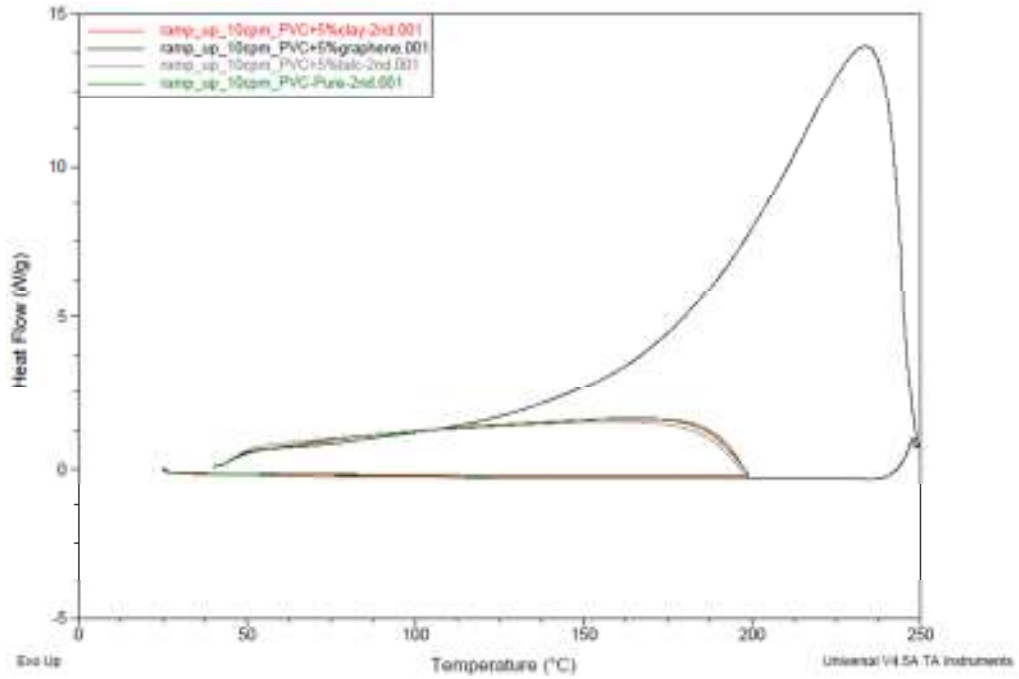

Figure 1. The DSC analysis for PVC incorporated with 5 wt% of different nanoinclusion.

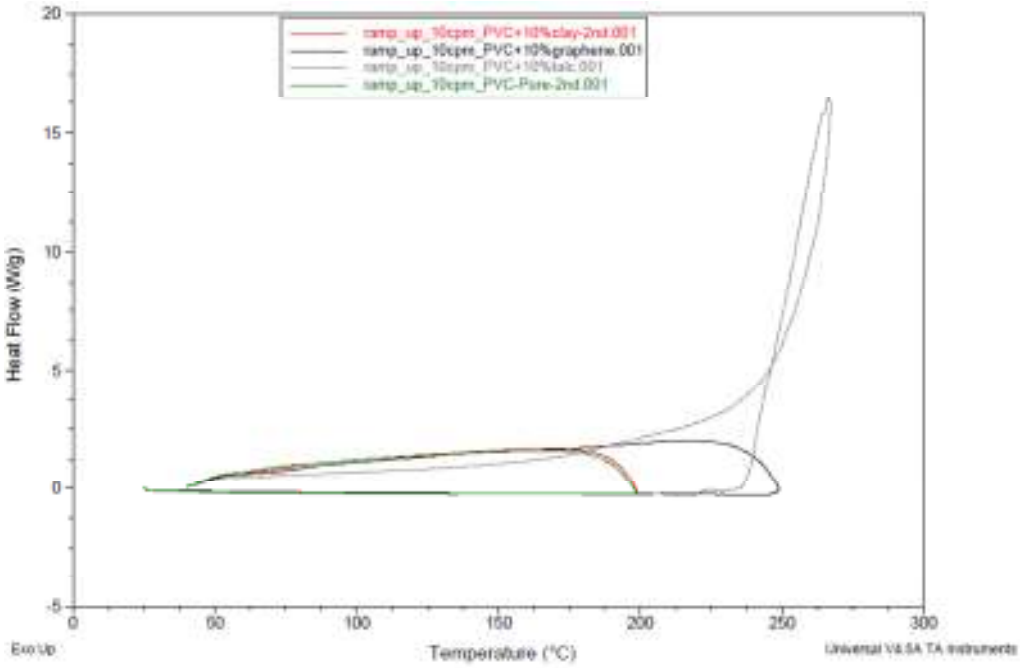

Figure 2. The DSC analysis for PVC incorporated with 10 wt% of different nanoinclusion.

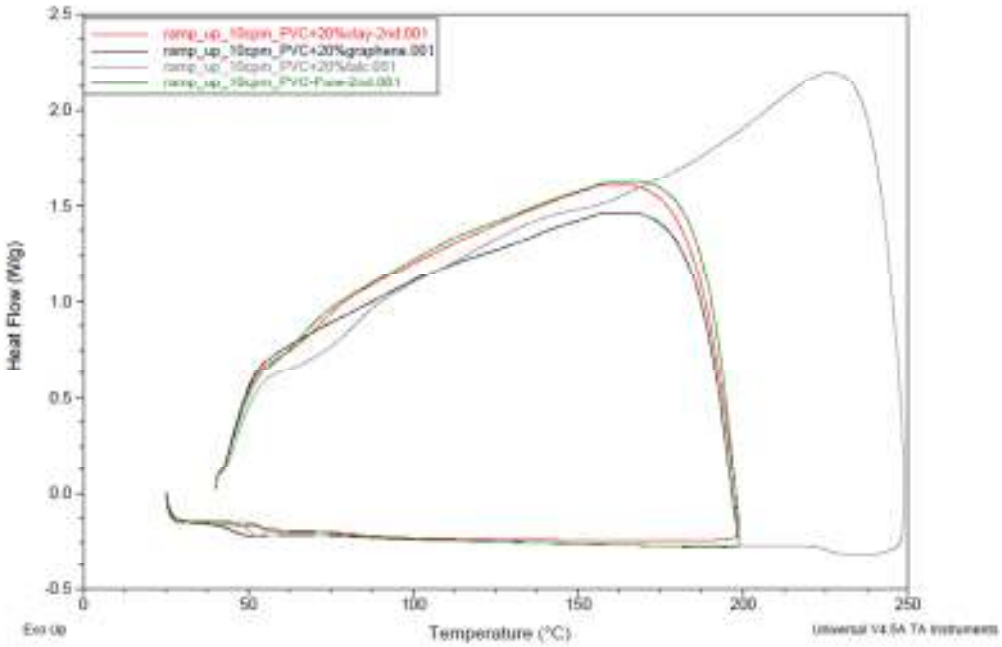

Figure 3. The DSC analysis for PVC incorporated with 10 wt% of different nanoinclusion.

APPENDIX 2

A comparison of stress strain curves for different weight percentages of nanoclay, nanotalc and nanographen.

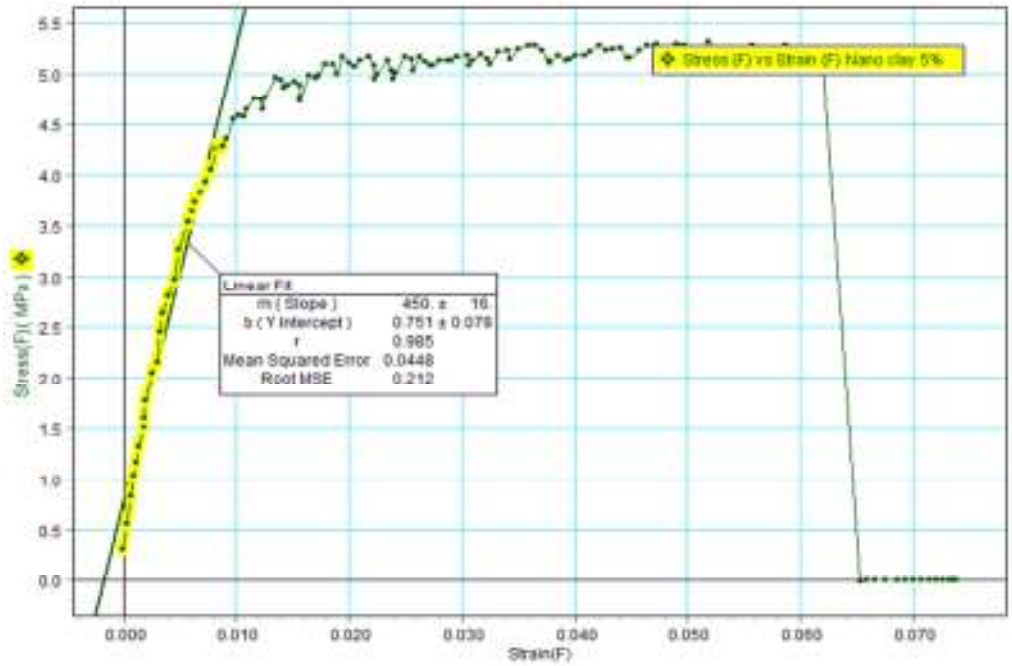

Figure 4. The stress strain curve for the PVC with 5 wt% nanoclay

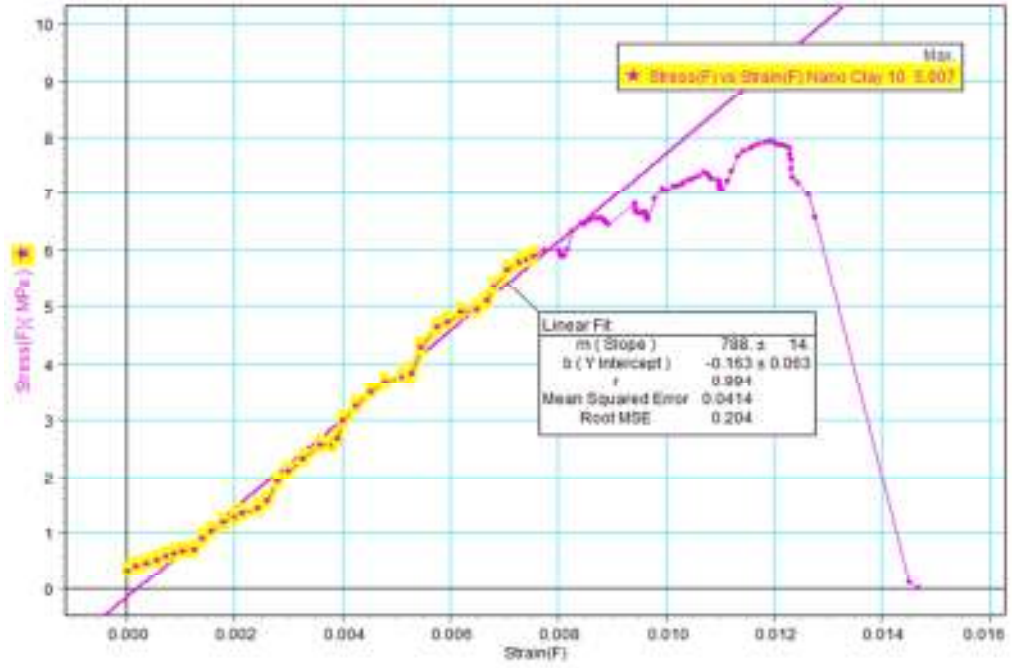

Figure 5. The stress strain curve for the PVC with 10 wt% nanoclay

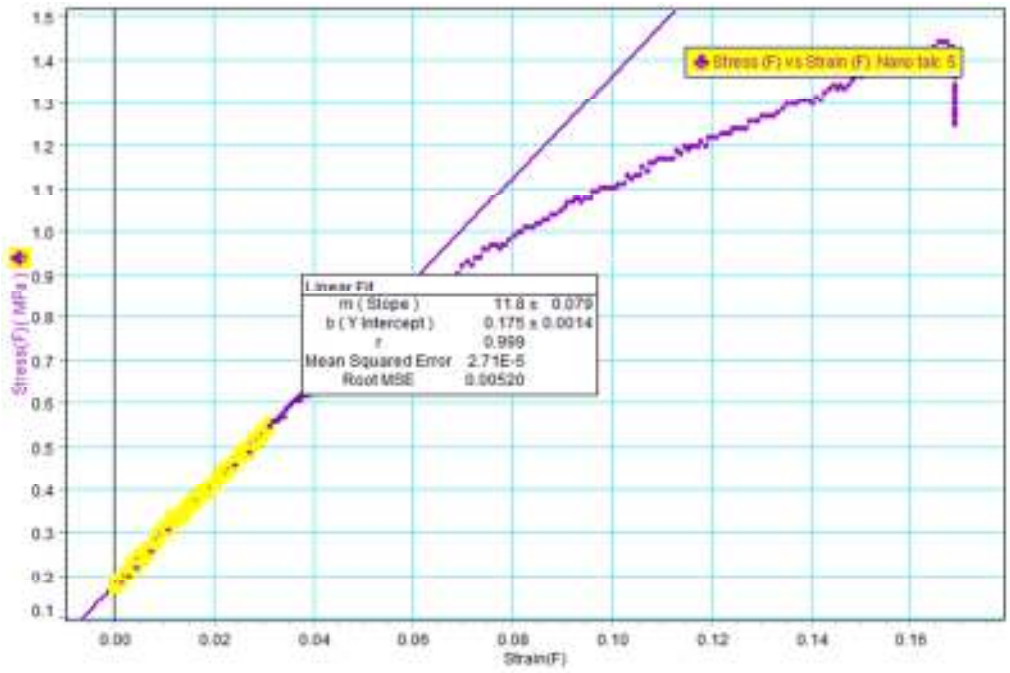

Figure 6. The stress strain curve for the PVC with 5 wt% nanotalc

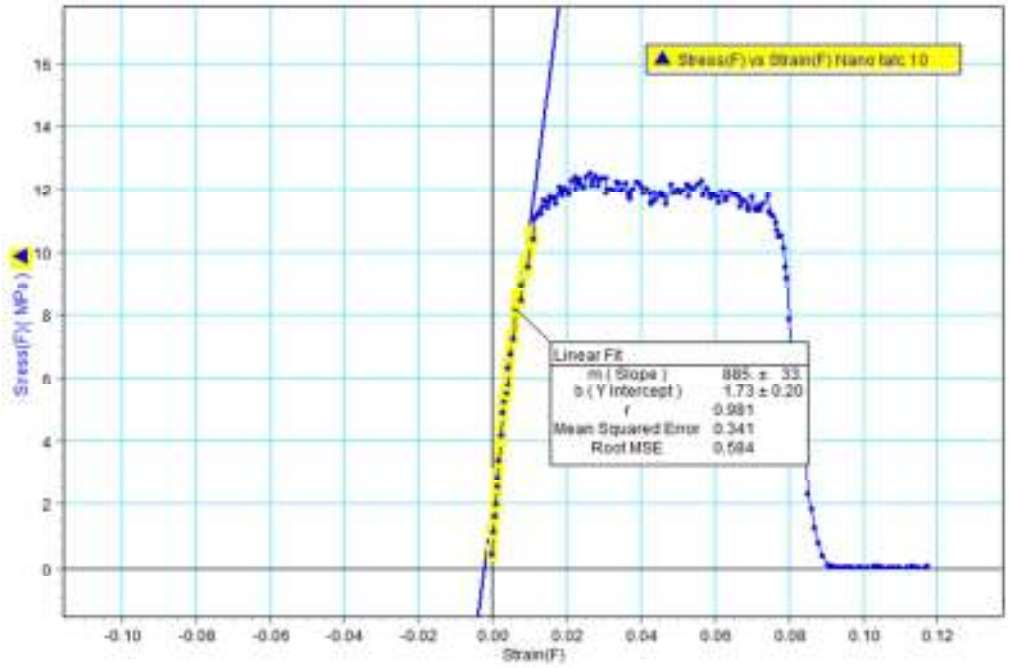

Figure 7. The stress strain curve for the PVC with 10 wt% nanotalc

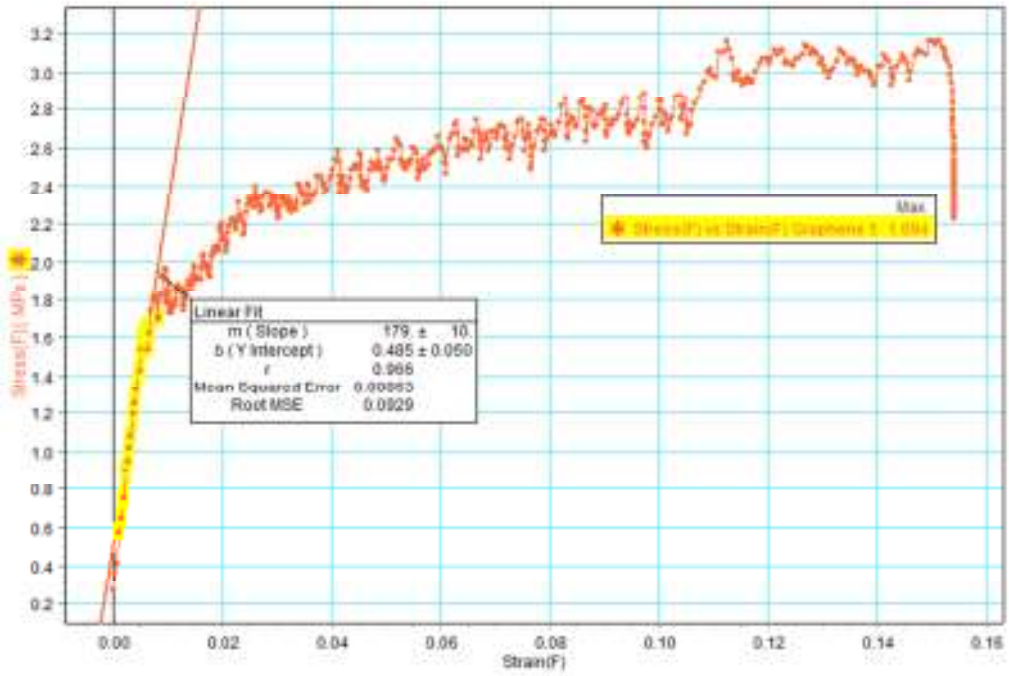

Figure 8. The stress strain curve for the PVC with 5 wt% graphene

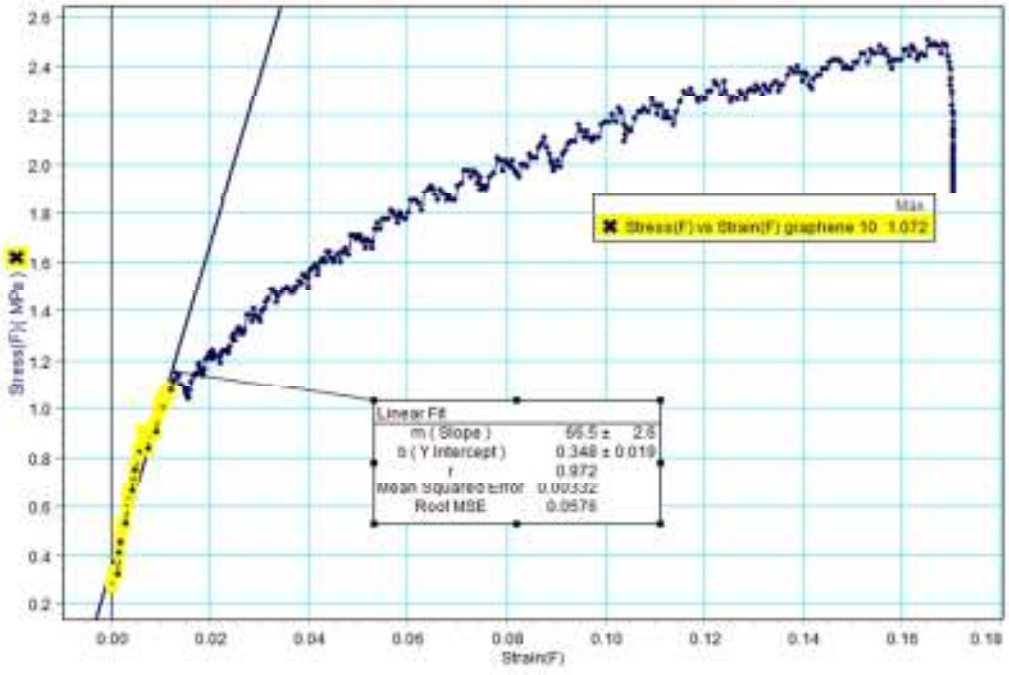

Figure 9. The stress strain curve for the PVC with 10 wt% graphene